Title
Longitudinal growth in patients with untreated hemifacial microsomia

Author
Good, Phoebe

Publication Date
2007

Peer reviewed|Thesis/dissertation

Longitudinal Growth in Patients with Untreated Hemifacial Microsomia

by

Phoebe Good, D.M.D.

THESIS

Submitted in partial satisfaction of the requirements for the degree of

MASTERS OF SCIENCE

in

ORAL AND CRANIOFACIAL SCIENCES

in the

GRADUATE DIVISION

of the

UNIVERSITY OF CALIFORNIA

San Francisco

[redacted]

Date University Librarian

DEDICATION

I would like to dedicate this work to my family, my mother Paula, my sister Chloe, my sister Lenore, and my late father Jay. It is with their support, love, and encouragement that I have completed not only this program, but accomplished all of my educational and life goals.

I would also like to express my sincerest appreciation for the day-to-day support and motivation of my classmates Monica Chmiel, Margarita Lachica, Greg Miller, and Natalie Miller. It is their camaraderie that has made completing this process fun, enjoyable, and inspirational.

Lastly, I am grateful for my dearest Mike Petersen, who provides me with the emotional support and love to endure the final steps in completing my education.

I thank all of you.

ACKNOWLEDGEMENTS

I am sincerely appreciative to Mindy Robles and Tiffany Louie for their invaluable assistance at the beginning of this project. As dental students, they helped me gather all of the patient records. Their attention to detail and genuine work ethic did not go unnoticed.

I am deeply grateful to Dr. Janice Lee for being my mentor and for her guidance and constant support not only on this project, but also for her friendship throughout my residency. This thesis would not have been possible without her encouragement and innovative ideas.

I am sincerely thankful to Dr. Karin Vargervik for also being my mentor and allowing me to use the UCSF Craniofacial Center records. She has provided guidance and invaluable input to help bring this project to completion. I appreciate her unending dedication to leading the Orthodontic program.

I would also like to thank Dr. John Huang for being a supportive committee member and for his dedication to improving the education in our Orthodontic residency.

I was privileged to have the guidance of Dr. Stuart Gansky in developing and applying the various statistic analyses for this project. His intuition made examining this project's results possible.

I would also like to express by deepest gratitude to Dr. Art Miller for his continued support and encouragement throughout our research endeavors. His enthusiasm and positive attitude towards our thesis projects has made this experience enjoyable and meaningful.

ABSTRACT

Longitudinal Growth in Patients with Untreated Hemifacial Microsomia

Phoebe Good, D.M.D.

Controversy exists over whether or not individuals with hemifacial microsomia (HFM) demonstrate progression of facial asymmetry. It is unclear whether there is continued growth of the affected side which continues at the same rate as the unaffected side.[1-6] The other possibility is that the affected side lags behind the unaffected side, and the patient demonstrates progressive facial asymmetry over time.[7-11] Previous studies evaluating this controversy were based on either large samples of grouped (by mandibular type) cross-sectional data[9] or small samples of ungrouped longitudinal data[1-6].

PURPOSE: The goal of this study is to (1) determine and characterize the growth in the affected side of patients with untreated HFM using longitudinal data and (2) ascertain if severity of the mandibular deformity influences the occurrence of deficient and asymmetric mandibular growth.

METHODS: Retrospective longitudinal posteroanterior (PA) cephalograms of growing, untreated, and nonsyndromic HFM patients were included in this study (n = 47). Each subject was categorized according to the type of mandibular deformity using the Pruzansky-Kaban schema of type I, IIa, IIb, and III. We documented gender, mandibular type, and age at each radiographic time point. Using a novel approach to determine growth and displacement in individuals with

HFM, we analyzed seven measurements on each PA cephalogram for each subject (a minimum of two time points at least one year apart for each subject).

RESULTS: Mixed model linear regression analyses, adjusting for random subject effects and fixed mandibular group effects, were used to evaluate PA cephalogram measurements by mandibular type. Several measurements demonstrated that subjects with type IIb mandibular deformity were significantly more asymmetric. Analysis of the rate of change for each measurement over time did not show statistically significant differences between mandibular types, and did have a large variance.

CONCLUSION: Type IIb demonstrates the most severe asymmetry for subjects included in this study. The rate of change of asymmetry is highly variable among HFM patients and is not predictable based on the severity of the mandibular deformity.

TABLE OF CONTENTS

List of Tables

List of Figures

Introduction

Hemifacial microsomia (HFM) is the most common congenital craniofacial anomaly, after cleft lip and/or palate, occurring in 1 out of every 4000 to 5600 live births.[12,13] This congenital condition involves the structures of the first and second branchial arches, with variable clinical dysplasias of both skeletal and soft tissues. The five major craniofacial manifestations of hemifacial microsomia include: ear (most commonly involved soft tissue), mandible (most commonly involved skeletal structure), orbit, cranial nerves (especially CN VII), and facial soft tissues (including masticatory muscles) on the affected side. HFM is frequently unilateral, however, bilateral involvement may also occur.[14,15]

The etiology and pathogenesis of hemifacial microsomia is unknown. The condition is believed to be sporadic, although there are documented examples of familial transmission.[16] The two proposed etiopathogenic theories include hematoma occurrence at the first and second branchial arches during fetal development [13,17], and abnormal neural crest development and migration [13,14,18]. Both models explain the variable and asymmetric nature of this condition.[9]

Many classification systems have been used to describe the varying degrees of deformity associated with hemifacial microsomia.[14,19,20] These often use the mandible as the cornerstone of the classification, since it is frequently affected, and its treatment is typically inevitable. The classification system at UCSF is an amalgamation of the classifications described by various authors.[8,20-24] It is based on discrete findings of the presence or absence of critical elements of the mandible and temporomandibular joints (TMJs), and consists of, in order of severity, types I, IIa, IIb, and III. Patients with a type I deformity have a hypoplastic mandible and glenoid fossa with a short ramus, but a functional temporomandibular joint in a close to normal location. Patients with Types IIa and IIb have a mandibular ramus that is short and abnormally shaped, but in type IIa, the condyle is in an acceptable location, while in type IIb, the condyle is inferiorly, medially, and anteriorly displaced. HFM patients with a type III mandible have complete absence of the affected ramus (no condyle or coronoid process), glenoid fossa, and TMJ.[25] Figure 1, adopted from Kaban et al.[26], diagrammatically demonstrates the variations in mandibular deformity.

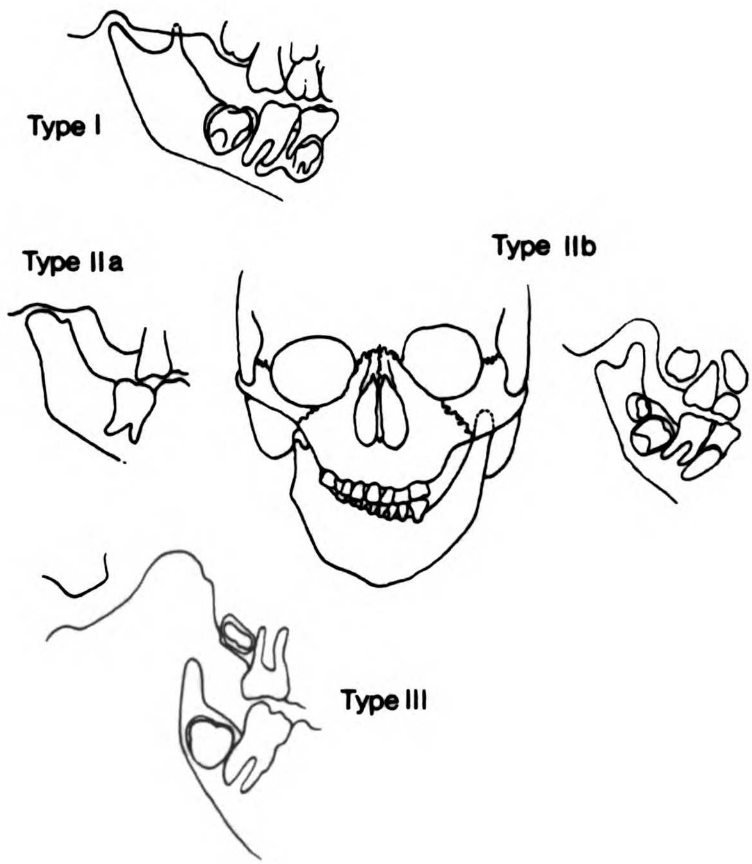

Figure 1: Radiograph tracings of hemifacial microsomia mandibular types I, IIa, IIb, and III (modified from Kaban & Troulis, 2004[26]). Note the medial and inferior displacement of the ramus and TMJ in type IIb.

Mandibular Growth

Normal Mandibular Growth

During embryogenesis, the mandibular bone forms in association with Meckel's cartilage and around the developing tooth buds. These osseous structures expand and then consolidate to form the mandibular body. Meckel's cartilage functions to carry the developing mandibular bone forward during the beginning stages, until it loses its significance as the advancing force. Other prerequisites for osteogenesis are the neurovascular and vascular networks, which are present before bone formation starts. As the bone develops, several muscle masses become attached to and included in the mandible. The muscles extending from the temporal region provide the environment to support the ramus with the condylar and coronoid processes, which are developing under genetic control.[27,28] As mandibular growth continues, the condylar process and the temporomandibular joint link together with the lateral pterygoid muscle to become the propulsive mechanism, which was previously provided by Meckel's cartilage.[25,29-31] The developing condyle not only depends on the superior and inferior heads of the lateral pterygoid for translation, but also on the suprahyoid muscles that can cause rotation of the condyle.[32] In addition, the masseter and temporalis muscles alter loading on the condyle and continually provide some of the reaction forces which the condyle needs to maintain its normal shape.[33-35]

These advancing mechanisms function as a sensorimotor feedback system which loads the condyle throughout the growth period in postnatal development.[36] The condyle needs normal loading, as experimental animals with soft diets demonstrate subtle but significant changes to the condylar shape and size of its different cartilaginous zones.[37-39] During growth, the periodic proliferation of condylar cartilage toward the joint space appears to elicit activity in the lateral pterygoid muscle, which advances the condyle and maintains joint space. Bone apposition at the interface between condylar cartilage and the mandibular bone produces a longer mandible, while various areas of the mandible remodel as the jaw is brought forward relative to its muscle attachments and other structures. It appears that bone formation at the interface between condylar cartilage and mandibular bone only occurs when the cartilage is proliferating.[40] The growth of the condyle depends upon cells dividing in the proliferative zone of condylar cartilage, which partially depends on forces developed in that region, as well as specific hormones and growth factors, and also the hypertrophic changes followed by ossification in the condyle.[41-51] Therefore, condylar cartilage is a controlling factor during growth, and developmental irregularities can affect this growth mechanism, as in hemifacial microsomia.[25,31]

Asymmetric Mandibular Growth in Hemifacial Microsomia

Individuals with HFM invariably demonstrate deviant growth, because the very structures that are responsible for mandibular growth are affected. There is a wide variation in how growth is affected in these subjects, depending on the type and severity of the structural deformity. The deficiency in the affected side of the mandible can range from missing condylar cartilage and disc to complete developmental failure of the condylar process.[31]

In type I mandibular deformities, part or all of the condylar cartilage and disc could be missing. In this instance the shape of the condylar head is normal but smaller than the unaffected side and joint movements may be decreased. The joint sensorimotor interaction with the lateral pterygoid muscle appears normal, and the mandible grows but not as much as the contralateral side because the growth attributed to the condylar cartilage may not occur as readily.

On the other end of the spectrum, patients with type III mandibular deformity, where the entire ramus is missing, the length of the mandibular body increases depending on the presence of teeth and development of the masseter, medial pterygoid, and suprahyoid muscles. Even though the advancing forces of the condylar cartilage and lateral pterygoid are missing in these individuals, the mandible is often brought forward to a small degree by the presence and function of the tongue and neck muscles.[25,31]

In general, the muscular hypoplasia correlates with the degree of the bony deficiency.[52] If the coronoid process is missing, then the temporalis muscle demonstrates severe hypoplasia and abnormal muscle recruitment; the same relationship holds true between the masseter muscle and gonial angle.[53] It is also evident that electromyographic studies of patients with HFM indicate that muscles alter bilaterally in their recruitment patterns to move the mandible. Therefore, patients with more severe bony changes of the mandible will have some muscles, particularly on the intact side, become much more active in moving the mandible. The most extreme HFM patients would suffer from not functioning on the weak side and using the intact side with more muscle recruitment in the temporalis, masseter, and medial pterygoid.[53] The coactivation pattern changes in HFM patients, and changes more with the more severe cases. This suggests that the muscle function will need to adapt with treatment of the craniofacial skeleton to provide, particularly through the dentition, more opportunities for loading the affected side to enhance and change the form, shape, and cortical mineralization of the mandible.

If an individual with HFM demonstrates restricted movement of the temporomandibular joint, where movement only consists of a hinge motion, then the jaw will grow very slowly. This joint ankylosis disengages the sensorimotor feedback mechanism, and prevents the mandible from taking a more advanced position, thus not allowing bone remodeling and apposition.[31] It is evident that the condyle's loading changes with its anterior position to the articular eminence.[54] It has also been shown that if the condyle is not functional in the fetal stage, it will have an altered shape and size.[27,28,55,56]

In all HFM subjects, the unilateral growth impairment causes deviation of the mandibular skeletal midline towards the affected side.[22] Because the mandible is short, retrusive, and narrow, downward growth of the maxilla is restricted on the abnormal side. This results in a vertically short maxilla and an occlusal plane that tilts upward on the affected side.[52]

PA Cephalometric Analysis of Craniofacial Asymmetries

The frontal cephalogram is a valuable tool in the study of asymmetry of craniofacial structures. In this projection, the right and left structures are at approximately equal distances from the film and x-ray source. This results in minimization of unequal enlargement by diverging rays, which occurs in a lateral cephalogram. The frontal cephalogram allows accurate comparison between sides since the midline skeletal and dental structures are easily identified.[57] In order to qualitatively and quantitatively evaluate the extent of the asymmetry, a method of analysis must be used. As in lateral cephalometrics, there have been several analyses developed each using a different horizontal reference plane.

Optimal Reference Plane in the Posteroanterior (PA) Cephalogram

Review of the literature on analysis of frontal cephalograms demonstrates general agreement to use crista galli as the midline reference.[58] It is routine to divide the right and left sides of the face by dropping a perpendicular from crista galli to a horizontal reference line. However, there has been disagreement about which horizontal reference plane to use.

Harvold [59] found that the zygomatico-frontal sutures and crista galli are relatively symmetrical structures, and he recommended construction of a horizontal line through the lateral limit of the zygomatico-frontal sutures for use as the horizontal axis. Ishiguro et al. [60] used the line connecting the medial point of the zygomatico-frontal suture as the horizontal reference line. Ricketts used a line through the nasal septum or crista galli perpendicular to a line connecting the centers of the zygomatic arches.[61] Svanholt and Solow [62] used a perpendicular line through crista galli to the line connecting the intersection points of the lateral orbital contour with the innominate lines.

Until 1997, no empirical data had been presented in the literature to support the use of one reference plane over any other. Lee [58] studied several reference lines in an attempt to define the most stable horizontal reference line through time. This study reported longitudinal frontal cephalometric data on the postnatal development of the bony orbit in a sample of twenty normal children with implant markers of the Björk type. The optimal reference line was defined as the one with the least oscillation over time in its perpendicular line through crista galli relative to the center of gravity of the maxillary implant markers. The reference line connecting the intersection point of the orbital cavity and the innominate lines was found to be the most stable and least variable through time. However, the endpoints of this line represent the superimposition of two distinct anatomical structures that are located in different anterior-posterior planes, which makes their location dependent on the subject's rotational head position. Lee also found the reference lines connecting the external points and internal points of the zygomatico-frontal suture, an anatomically distinct structure, demonstrated reasonable reliability. In the present study, the horizontal reference line was identified by connecting the medial points of the right and left zygomatico-frontal sutures.

Treatment of Hemifacial Microsomia

The asymmetric nature of HFM makes the treatment extremely difficult. Multidisciplinary treatment is required for an ideal outcome.[25] As mentioned before, the mandible is often the focus of treatment, and the severity of mandibular deformity determines the treatment needed. Up until recently, protocols of diagnosis and treatment include thorough clinical assessment and radiographs such as the panorex, lateral, and posteroanterior (PA) cephalograms. The combined orthopedic, surgical, and orthodontic treatment decisions are made based on the patient's clinical findings and 2-dimensional (2-D) radiographs.[2,52,63,64] Computed tomography (CT) with 3-D reconstruction is being used currently to clearly delineate the asymmetry in HFM patients. These images not only demonstrate the asymmetry of the facial bones, but also the extent of cranial base asymmetries and soft tissue deficiencies. Because HFM affects all three dimensions, CT generated 3-D images can provide clinicians with a useful tool for analysis and treatment.[65-69]

Multidisciplinary treatment of patients with HFM usually consists of a series of treatment phases that target correction of the mandibulo-maxillary asymmetry. Particular goals of treatment include: (1) to increase the size of the malformed and underdeveloped mandible and soft tissues; (2) to create an articulation between the mandible and the temporal bone; (3) to correct the secondary deformities of the maxilla; and (4) to establish a functional occlusion and optimal facial symmetry.[52,63,70] These goals are accomplished by following these treatment phases: presurgical orthopedic treatment, mandibular surgery, postsurgical bone induction, maxillary correction, final orthodontic treatment, and soft tissue augmentation.[8,25,63,64,70] Surgical treatment of types I, IIa, and some IIb mandibular deformities includes osteotomy or distraction osteogenesis. Treatment of most type IIb and all type III deformities requires total construction of a functional ramus-condyle unit, and sometimes even the glenoid fossa.[52]

One particular area of interest that influences treatment timing is the craniofacial growth of patients with HFM. Controversy exists over whether or not patients with HFM demonstrate progression of facial asymmetry. It is unclear whether there is continued growth of the affected side which continues at the same rate as the unaffected side.[1-3,5,6] The other possibility is that the affected side lags behind the unaffected side, and the patient demonstrates progressive facial asymmetry over time.[8-11,71] This area of controversy has an impact on treatment of HFM patients. Surgeons and proponents of the first theory recommend treatment of the facial asymmetry after growth is complete, which is the standard protocol for orthognathic surgical treatment of patients without HFM. The proponents of the second theory favor early treatment of HFM patients, while they are still growing, in order to improve facial and mandibular growth, reduce secondary deformities, especially in the maxilla, and enhance body image development.

Kearns et al. [9] performed a retrospective cross-sectional analysis of 67 patients with untreated hemifacial microsomia, categorized by severity. Using posteroanterior cephalograms for analysis in the vertical and horizontal planes, they concluded that facial asymmetry is progressive with age, and that increasing asymmetry correlates with the severity of the mandibular deformity. However, the sample used was a cross-section of HFM patients, each at one time point, so each patient's age group and deformity was compared to different patients' groups which most likely varied in severity of deformity.

In a series of studies presenting an opposing view, Rune et al. utilized metallic implants and roentgen stereophotogrammetry to study growth in 21 patients with hemifacial microsomia, 16 unoperated, 5 operated.[3,5,6] The most recent study was a continuation of the first two publications. Their results did not support the two claims that the asymmetry of the jaws invariably increases in time because of the growth disparity between affected and unaffected sides, or that the degree of asymmetry increases most in children with the most severe deformity.[3] This series of publications analyzed each patient longitudinally (at multiple times), and reported that there was no interindividual pattern of displacement of the jaws, suggesting that the relevance of general statements about articular growth in HFM may be questioned. However, although the sample was small, the investigators used precise and accurate longitudinal recordings of each patient. Polley and coworkers[1] studied longitudinal mandibular growth in 26 unoperated patients with HFM (categorized by mandibular deformity) over 13 years, using posteroanterior cephalometric analysis in both the vertical and horizontal planes. They found that growth of the affected side in HFM patients was similar to that of the unaffected side, such that mandibular asymmetry remained relatively constant throughout craniofacial growth.[1]

Purpose

The purpose of this study is to determine and characterize growth and displacement of the mandible in the affected side of individuals with untreated HFM using longitudinal (serial or multiple) radiographs. Further evaluation of growth in patients with HFM is warranted in order to control for the following parameters: (1) using longitudinal data of growing patients instead of cross-sectional (single time point) analysis; (2) using a larger sample size in each category of mandibular deformity; and (3) separating the samples by mandibular types. In addition, a novel approach to posteroanterior (PA) cephalometric analysis is used to determine mandibular growth and positional changes in individuals with HFM.

Specific Aim and Hypothesis

The specific aim of this project is to ascertain if severity of the mandibular deformity influences the occurrence of deficient and asymmetric mandibular growth. Our hypothesis is that subjects will demonstrate a combination of abnormal/diminished growth and normal growth in the affected side of the mandible depending on severity of the affected side (i.e. deformity type).

MATERIALS AND METHODS

This is a retrospective cohort study on growth characteristics and positional changes of the mandible of untreated HFM patients.

Subjects

Forty-seven subjects were identified from the University of California San Francisco Craniofacial Center records. Inclusion criteria for each subject were based on having:

1. at least two radiographic surveys (posteroanterior (PA) cephalogram and panogram) with at least one year between each time point during the subject's growth period;
2. a diagnosis of hemifacial microsomia without other anomalies, syndromes, or restricted joint movement;
3. no surgical correction or orthodontic treatment prior to the radiographic surveys used.

The following data were recorded for each subject:

1. type of mandibular deformity using an amalgamation of the classifications described by Pruzansky, Kaban et al., Harvold et al., and Vargervik and Kaban (type I, IIa, IIb, and III)[21-24]
2. gender
3. age at each radiographic survey
4. race/ethnicity

5. family history of craniofacial defects.

Clinic notes, clinical photographs, and radiographs (PA cephalograms and panograms) were used to collect all data. Panoramic radiographs aided in the categorization of mandibular types, while longitudinal PA cephalograms were analyzed for growth rate comparison of the affected side to the unaffected side. All radiographs were taken between the time period of 1976-2004 at the UCSF Craniofacial Center, during which time the same cephalostat and panorex machines were used. All radiographs were taken in natural head position by the same radiology technician. An x-ray tube generated a beam of 120 kV at 100 mA with the focal spot 60-in from the cephalostat, aligned so that the central beam passed exactly through the center of the ear rods.[72]

Subjects were divided into four groups based on their mandibular deformity. The four groups (Table 1) were designated based on the severity of hypoplasia of the affected ramus/condyle: type I, type IIa, type IIb, and type III. Type I subjects have a small mandible and glenoid fossa with a short ramus, but a functional temporomandibular joint in a close to normal location. Subjects with types IIa and IIb have a mandibular ramus that is short and abnormally shaped, but, in type IIa, the condyle is in an acceptable location, while, in type IIb, the condyle is inferiorly, medially, and anteriorly displaced. Type III subjects have complete absence of the affected ramus with no condyle or coronoid process, glenoid fossa, or TMJ.

Human subjects approval for this medical records study was obtained through the institutional review board at the University of California at San Francisco.

Table 1: Description of Groups

Type	Description
I	small mandible and glenoid fossa with a short ramus, but a functional temporomandibular joint in a close to normal location
IIa	mandibular ramus that is short and abnormally shaped; condyle is in an acceptable location
IIb	mandibular ramus that is short and abnormally shaped; condyle is inferiorly, medially, and anteriorly displaced
III	complete absence of the affected ramus, glenoid fossa, and TMJ

TRACING OF PA CEPHALOGRAMS

All PA cephalograms were hand traced by one investigator (PMG) in a controlled, dimly lit setting, using a light box, acetate paper, and a soft lead pencil. Two other investigators (JSL and KV) reviewed the tracings and measurements to verify the methodology. The structures and landmarks which were identified and traced are demonstrated in Figure 1, and include: the orbital rims, crista galli, innominate lines, right and left zygomatico-frontal sutures, nasal septum, right and left piriform apertures, mandibular border, maxillary first molars, mandibular second molar buds or crowns, maxillary central incisors, and mandibular central incisors.

These structures were identified and traced for each PA cephalogram at each time point of all included subjects. Structures that were not clear on one cephalogram (such as maxillary and mandibular molars that were either not in occlusion or superimposed on other teeth), were identified by comparing a sequential radiograph(s) of the same subject and locating the same structure on each cephalogram.

Three fiducial markers were traced for each PA cephalogram: right and left ear rod metallic inserts, and the "R" or "L" lead indicator. These fiducials were used to accurately reposition the acetate tracing paper over the radiograph when verifying landmark identification.

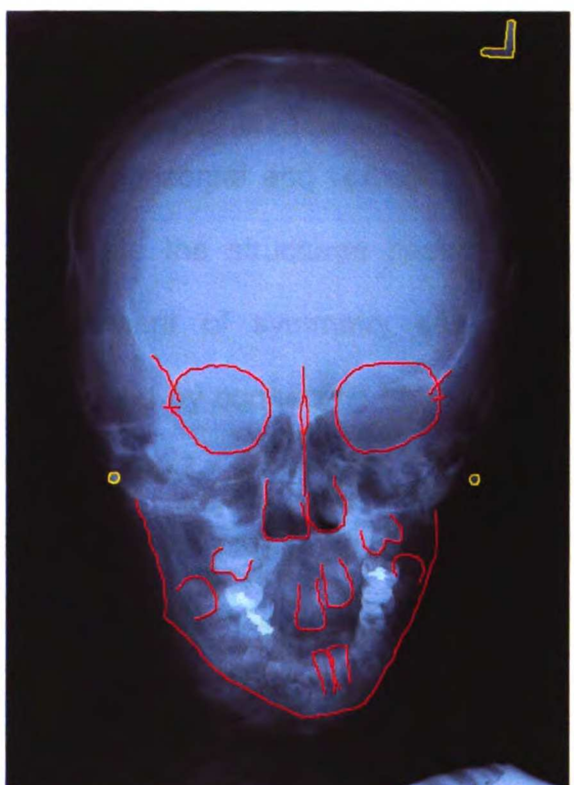

Figure 2: PA cephalogram and tracing overlay of 5y, 11m old male with Type III HFM

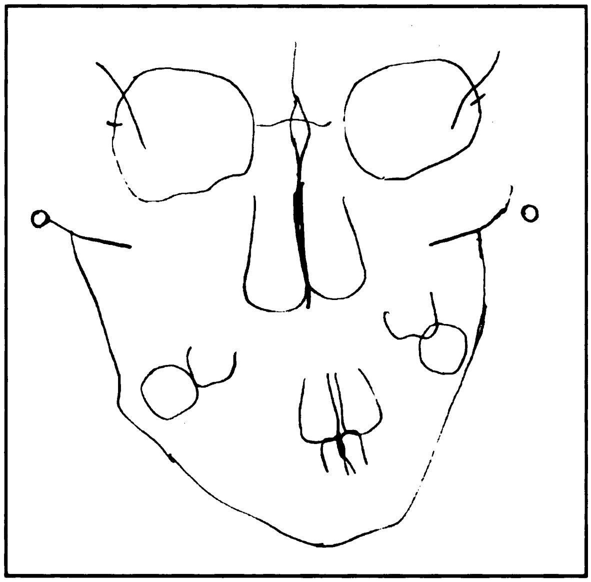

Figure 3: Tracing of PA cephalogram from subject in Fig 2

REFERENCE PLANE IDENTIFICATION IN THE PA CEPHALOGRAM

After reviewing previous studies that have analyzed PA cephalograms[58,59,61,62], the horizontal and vertical reference planes used in this study were chosen to divide the structures based on stable landmarks and enable accurate measurement of symmetry and spatial dimension. The reference planes were derived by connecting the medial points of the right and left zygomatico-frontal sutures (Z-r and Z-l) to form the horizontal plane (Z-Z), and drawing a perpendicular line from the tip of crista galli (Cg) to the horizontal plane to form the vertical plane (Cg⊥); (Figure 4). All linear and angular measurements were made using these reference planes.

IDENTIFICATION OF LANDMARKS

After the horizontal and vertical reference lines were established, the remaining landmarks were identified and planes formed accordingly. The piriform plane (P-P) was drawn tangent to the inferior borders of the right and left piriform apertures (P-r and P-l). The intergonial plane (Go-Go) was drawn between the right and left intergonial points (Go-r and Go-l); each point located at the intersection of lines tangent to the respective mandibular ramus and body. Using these derived gonial points, instead of an estimated gonial angle, allows repeatable and precise localization of the same structurally-based point at each radiographic time point even when the mandibular angle may be deformed and anomalous. The maxillary molar plane (MxMP) was drawn as a tangent to the most inferior cusps of the right and left maxillary first molar teeth (MxM-r and MxM-l), and the mandibular molar plane (MnMP) was formed by the superior borders of the right and left mandibular second molar buds or cusps (MnM-r and MnM-l). The mandibular midline plane (MMP) was formed by a line bisecting the right left mandibular incisor long axes, located between the mandibular central incisors and intersecting the chin. See Figure 4 and Table 2 for diagrams and definitions of these landmarks.

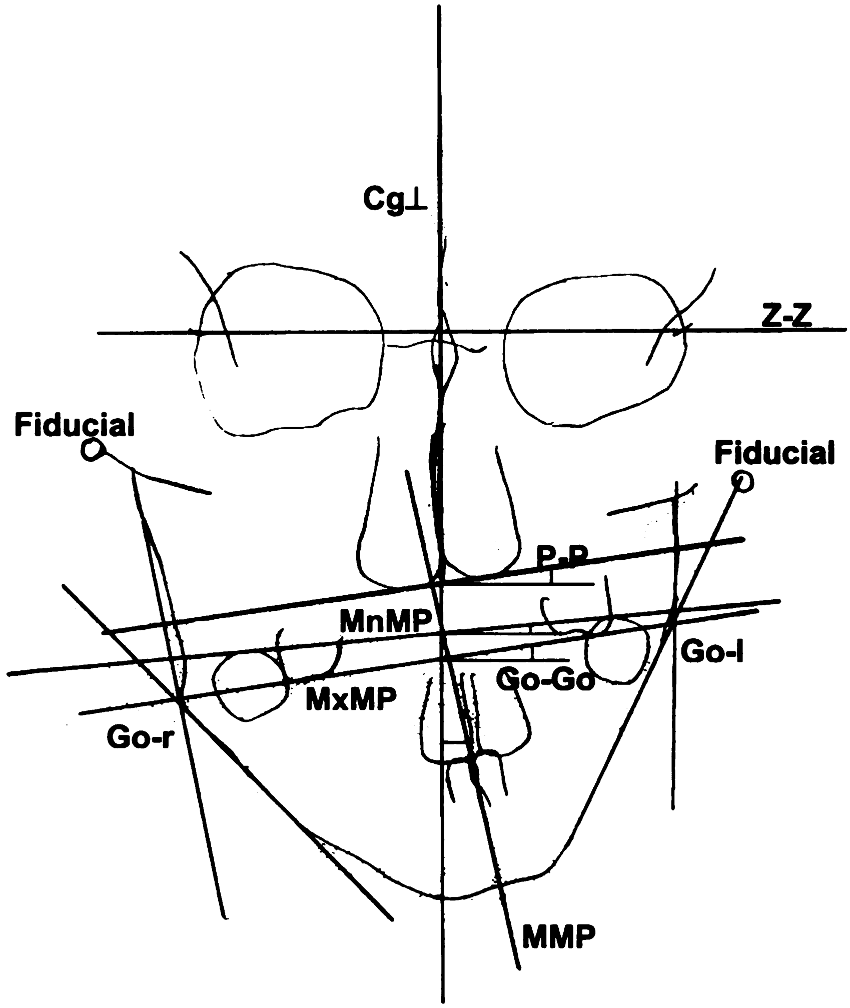

Figure 4: Cephalometric landmarks. In this PA tracing, MxMP and Go-Go are coincident. Angles measured indicated with red lines.

Table 2: Definition of Landmarks

	Landmark	Definition
1	Horizontal reference plane (Z-Z)	line connecting the medial points of the left and right zygomatico-frontal sutures
2	Vertical reference plane (Cg⊥)	line from the tip of crista galli perpendicular to the horizontal reference plane
3	Piriform Plane (P-P)	tangent to inferior borders of piriform apertures
4	Gonial angle points (Go-r and Go-l)	right and left points located at the intersection of lines tangent to the mandibular ramus and body; this method allows for repeatable identification on each radiographic time point when the gonial angle is often difficult to locate in a severely malformed mandible
5	Intergonial plane (Go-Go)	line connecting right and left gonial angle points
6	Maxillary molar plane (MxMP)	tangent to maxillary first molar cusps
7	Mandibular molar plane (MnMP)	tangent to superior borders of mandibular second molar buds or cusps
8	Mandibular midline plane (MMP)	line constructed along axis between mandibular incisors to the chin midpoint

MEASUREMENTS

Seven measurements, five angular and two linear, were made on each tracing to evaluate and characterize the growth and positional changes of the affected and contralateral (unaffected) sides of the mandible for all subjects at each time point. Angular deviations of P-P, MxMP, MnMP, and Go-Go from the true horizontal were measured (Figure 4). The MMP angle to the true vertical line was also recorded (Figure 4). The two linear measurements were from Go-r and Go-l to the true horizontal along a perpendicular, to evaluate the vertical displacement of the gonial points over time. After all measurements were taken, the affected and contralateral (unaffected) sides were identified by referring to the subject database.

Since this was a retrospective clinical study, precluding complete blinding of the examiner, care was taken to randomly order all tracings and hide all subject identifiers while measurements were taken. Random ordering of tracings was done using an internet-based random number generator (Research Randomizer, Wesleyan University, Middletown, CT).[73]

ERRORS OF METHOD

Errors of measurement are considered either systematic or random. Systematic error pertains to the error in radiographic machine set up, error in radiographic technique, varying head posture between different films, the factor of enlargement in cephalograms, and changing measurement techniques over time. Random error occurs by identification error, such as tracing error and measurement error.[74,75]

Frontal head films have inherent errors of projection. There are problems of rotation and of projection displacement (i.e., enlargement). In frontal cephalograms, downward rotation of the anterior part of the face is coupled with upward rotation of the posterior part. For this reason, PA films generated at different degrees of cranial rotation are not geometrically similar and not superimposable. The second problem is the change of enlargement factor by growth. As skull dimensions increase in a growing individual, the frontal facial plane moves closer to the film, and therefore the enlargement of orbital structures gets smaller.[58]

Several measures were taken to minimize the amount of systematic error. In this study, all radiographic films were taken using the same cephalostat machine and by the same radiology technician at the UCSF Craniofacial Center. In the case of some HFM patients who have missing external ear canals, difficulty in positioning the head in the cephalostat was encountered. In these instances, the ear rod on the affected side was placed where the condylar fossa would have been under normal conditions and not at the actual end of the mandible.[72] The average factor of enlargement (9.1%) is the same for all cephalograms used in this study; however the enlargement factor of the orbital structures did change due to growth. To account for this change in enlargement factor and varying head posture in serial films of the same subject, only angular measurements and ratio calculations were used for statistical analyses. Finally, in order to mitigate examiner bias, the principal examiner (PMG) was calibrated in the techniques of tracing and measuring by determining the most ideal methods of analysis in a pilot study on 19 subjects (54 headfilms). Also, all tracings and measurements were performed temporally close together, so that the examiner maintained the same concept of each landmark. Since serial records of each patient were traced sequentially on the same occasion, this reduced error variance within individuals, but may have increased risk of bias. However, all measurements were made on tracings that had all identifying information removed and their order randomly arranged.

Several steps were used to reduce random error in this cephalometric study. Some structures and landmarks are difficult to clearly identify due to either poor film quality or superimposition of other structures. If landmark visualization was impaired, cephalograms of the same subject from different time points were used to identify the structure in question by locating the same shape on all radiographs. In addition, repeatability of the methods of tracing and measuring was verified by performing a reliability analysis. Repeat tracing and measurements of 10 randomly selected radiographs were performed. Because this is a clinical study where the physical deformity of each subject is obvious to the investigator preventing complete blinding even if all classification information is hidden, there is no way to prevent the possibility of that bias.

RELIABILITY ANALYSIS

Ten PA cephalograms were randomly selected (Research Randomizer, Wesleyan University, Middletown, CT)[73] for repeat tracing and measurements. This repeat analysis was performed one month after the initial analysis. Comparison between the initial and repeat analysis was performed to determine the reliability and repeatability of the methods.

STATISTICAL ANALYSIS

The Lin's concordance correlation coefficient (ρ_c) was calculated to assess the agreement between two repeat tracing and measurement of 10 randomly selected PA cephalometric radiographs. The Lin's concordance coefficient (ρ_c) is robust on as few as 10 pairs of data. For continuous data, Lin suggested the following subjective categories to determine strength of agreement: "almost perfect" for $\rho_c > 0.99$, "substantial" for $0.95 < \rho_c < 0.99$, "moderate" for $0.90 < \rho_c < 0.95$, and "poor" for $\rho_c < 0.90$.[76]

The distribution of mandibular type was compared between genders with exact chi-square tests (including Cochran trend test considering type as ordinal). Age at first visit was compared among mandibular types with analysis of variance (ANOVA).

A mixed model regression analysis was used to analyze the longitudinal continuous data for each PA cephalometric measurement. Mixed models are a powerful class of models used for the analysis of correlated data. The key feature of mixed models is that, by introducing random effects in addition to fixed effects, they address multiple sources of variation. For example, in this longitudinal study they account for both within- and between-subject variation, since two visits from the same person will naturally be more correlated that two visits from two people. Subjects were assessed as random effects with a compound symmetric (exchangeable) correlation structure. Each PA cephalometric measurement was analyzed longitudinally by mandibular type using age as a covariate (both as fixed effects). Using mixed model regression allows for subjects to have unequal numbers of time points.

Analysis of the average rates of change of each PA cephalometric measurement was performed using ANOVA to evaluate for statistical significance between rates by mandibular types.

RESULTS

RELIABILITY ANALYSIS

Lin's concordance analysis demonstrated moderate to strong correlations (0.75 – 0.95) between the first and second measurements for 6 of the 7 measurements except affected gonial height. The summary of the Lin's concordance coefficients for all seven measurements is in Table 3. This repeatability analysis shows that the affected gonial height measurements are not very reliable. This further suggests that it is difficult to precisely and accurately identify the location of the affected gonial angle point. Therefore, the longitudinal analysis of growth and displacement in this sample of HFM patients will take into consideration the reliability strength of each measurement.

Table 3: Summary of concordance coefficients for repeatability analysis

Measurement	Lin's concordance coefficient (ρ_c)
Normal gonial height	0.78
Affected gonial height	0.36
Midline angle	0.95
Intergonial plane	0.75
Mandibular molar plane	0.94
Maxillary molar plane	0.90
Piriform plane	0.88

SUBJECTS

After reviewing the UCSF Craniofacial records approximately 150 patients were identified, and 47 subjects with varying types of HFM and at least 2 radiographic time points qualified for inclusion in this study. Of the 47 subjects, 26 had type I mandibular deformity, 9 had type IIa, 5 had type IIb, and 7 had type III (Figure 5). The subjects consisted of 24 males and 23 females, with no statistically significant difference in gender among types (Table 4). The subjects' race/ethnicity included 19 Whites, 15 Hispanics, 9 Asians, 3 African Americans, and 1 multiracial subject (White-Hispanic) (Figure 6). The average age of subjects at the included time points was 9.2 years, with a range from 5.0 to 17.0. The average age by mandibular type is shown in Table 5 and Figure 7, and the average age at the 1st time point by mandibular type is shown in Table 6 and Figure 8.

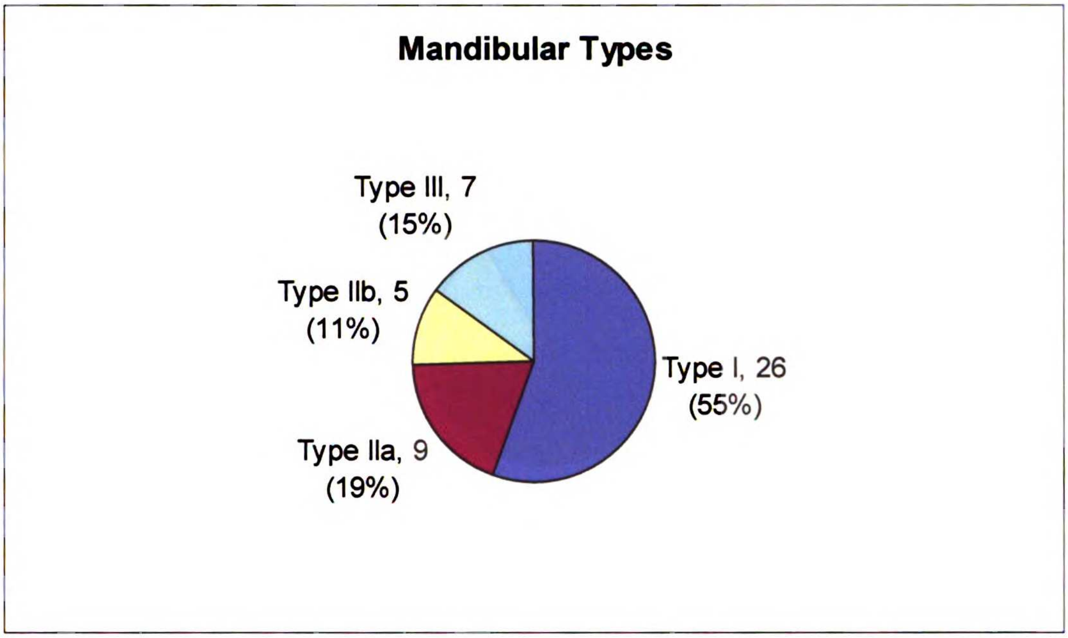

Figure 5: Distribution of mandibular types

Table 4: Gender of subjects by mandibular type, Cochran trend exact test 2 sided shows no statistically significant difference between types (p = 0.310)

Type	Males	Females	Total
I	12	14	26 (55%)
IIa	4	5	9 (19%)
IIb	3	2	5 (11%)
III	5	2	7 (15%)
TOTAL	24	23	47 (100%)

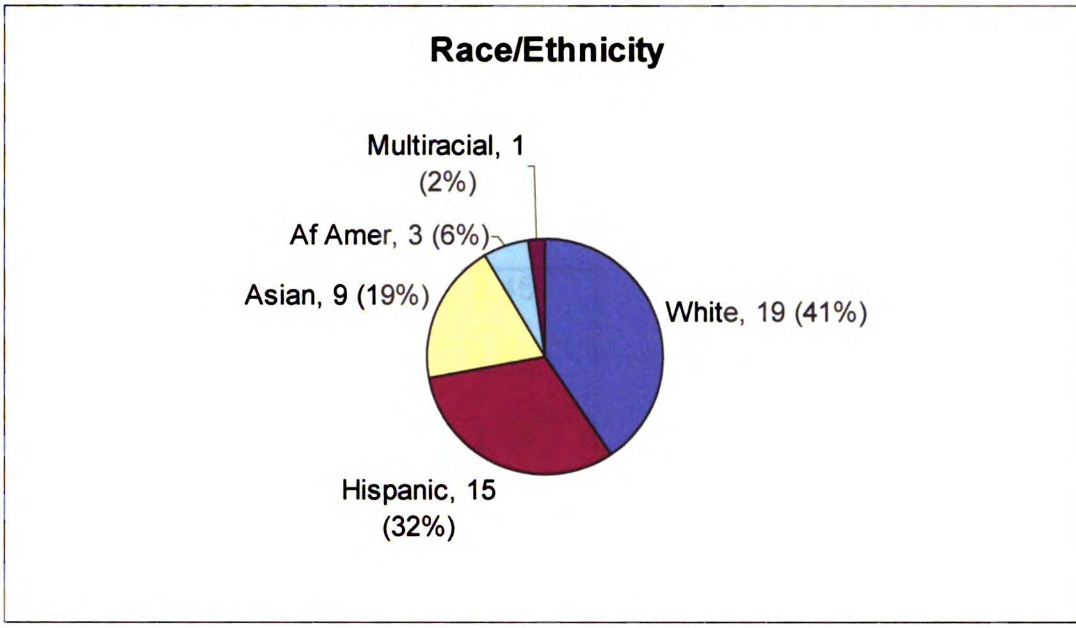

Figure 6: Race/Ethnicity of subjects

Table 5: Mean age of subjects by mandibular type; comparison of age among types with ANOVA shows no statistically significant difference (p = 0.192)

Type	Mean Age (years)	S.D.
I	9.3	2.71
IIa	10.3	2.45
IIb	7.4	1.53
III	8.6	2.04
Overall	9.2	2.54

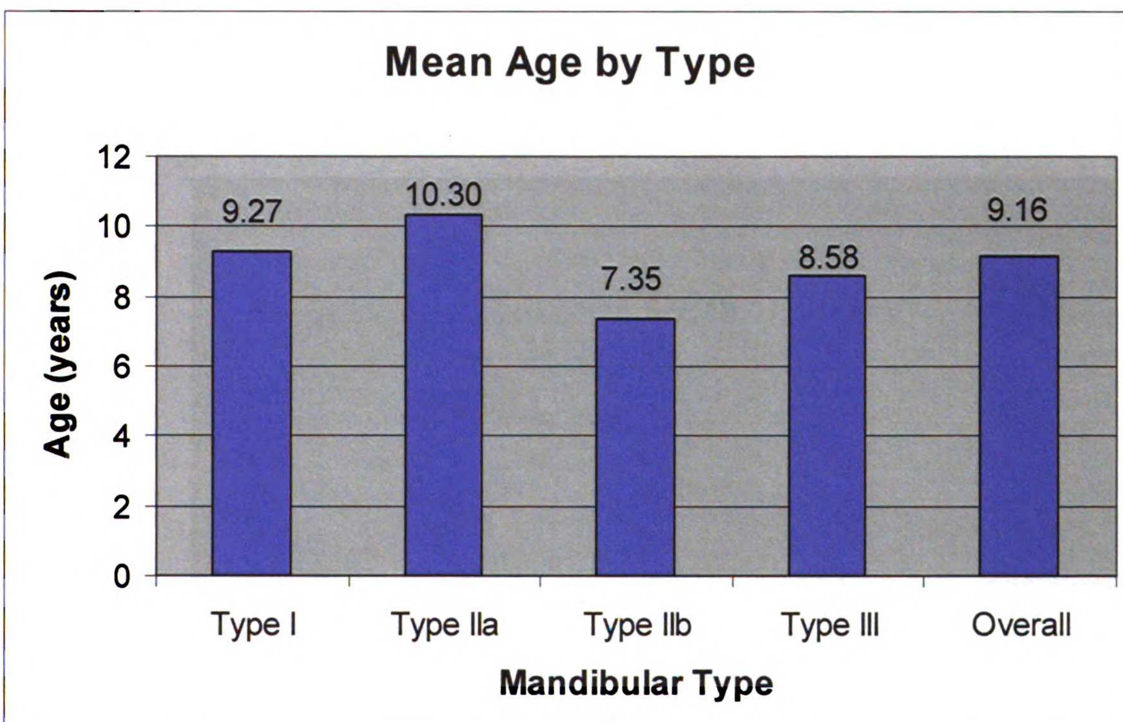

Figure 7: Mean age of subjects by mandibular type; comparison of age among types with ANOVA shows no statistically significant difference (p = 0.192)

Table 6: Mean age of subjects at 1st time point by mandibular type; comparison of age among types with ANOVA shows no statistically significant difference (p = 0.179)

Type	Mean Age (years)	S.D.
I	6.8	2.80
IIa	8.4	3.06
IIb	5.4	1.92
III	6.3	1.75
Overall	6.9	2.72

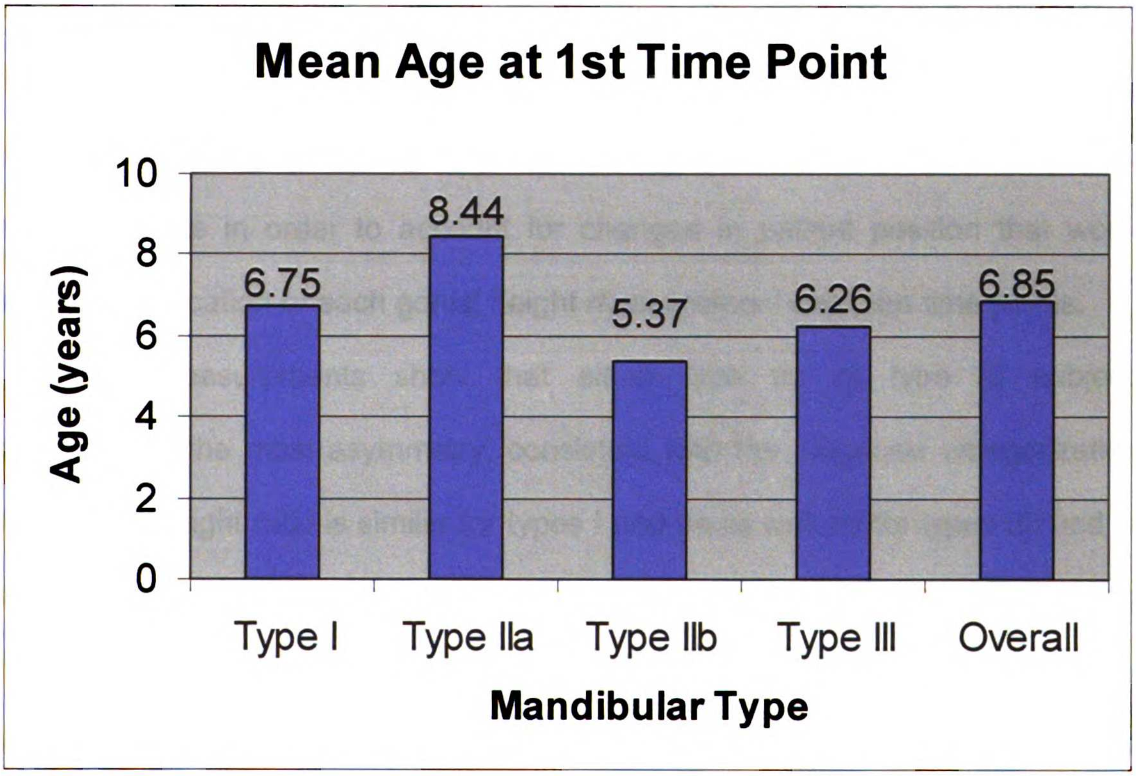

Figure 8: Mean age of subjects at 1st time point by mandibular type; comparison of age among types with ANOVA shows no statistically significant difference (p = 0.179)

MEASUREMENTS

The seven measurements, five angular and two linear, were recorded for each tracing to evaluate and characterize the growth and positional changes of the affected and contralateral (unaffected) sides of the mandible for all subjects at each time point. The means, standard deviations, and standard errors for the following six measurements averaged over all time points and separately averaged for the 1st time point are shown in Tables 7-18 and graphically displayed in Figures 9-20: gonial height ratio ([affected gonial height]/[unaffected gonial height]), mandibular midline plane (MMP) angle, intergonial plane (Go-Go) angle, mandibular molar plane (MnMP) angle, maxillary molar plane (MxMP) angle, and piriform plane (P-P) angle. The ratio of the affected gonial height to the unaffected gonial height was used instead of the individual linear measurements in order to account for changes in patient position that would affect magnification of each gonial height measurement between time points.

All measurements show that either type IIb or type III subjects demonstrate the most asymmetry, consistent with the diagnosis categorization. The gonial height ratio is similar for types I and IIa as well as for types IIb and III, demonstrating similar magnitudes of asymmetry between types I and IIa and also between types IIb and III. This same relationship exists when looking at the intergonial plane angle, which follows since the gonial height ratio and intergonial plane angle are based on the same anatomical landmarks. The mandibular midline plane angle, the mandibular molar plane angle, the maxillary molar plane angle, and the piriform plane angle all demonstrate that type IIb is the most asymmetric, since this type has the highest magnitude for these measurements. The mean values for all 6 measurements at the 1st time point demonstrate the same relationships as when averaged over all time points.

Table 7: Gonial height ratio ([affected gonial height]/[unaffected gonial height])

Mandibular Type	Mean	Std. Dev.	Std. Err. Of Mean
I	0.93	0.077	0.009
IIa	0.91	0.069	0.014
IIb	0.82	0.069	0.016
III	0.80	0.105	0.021
Overall	0.89	0.096	0.008

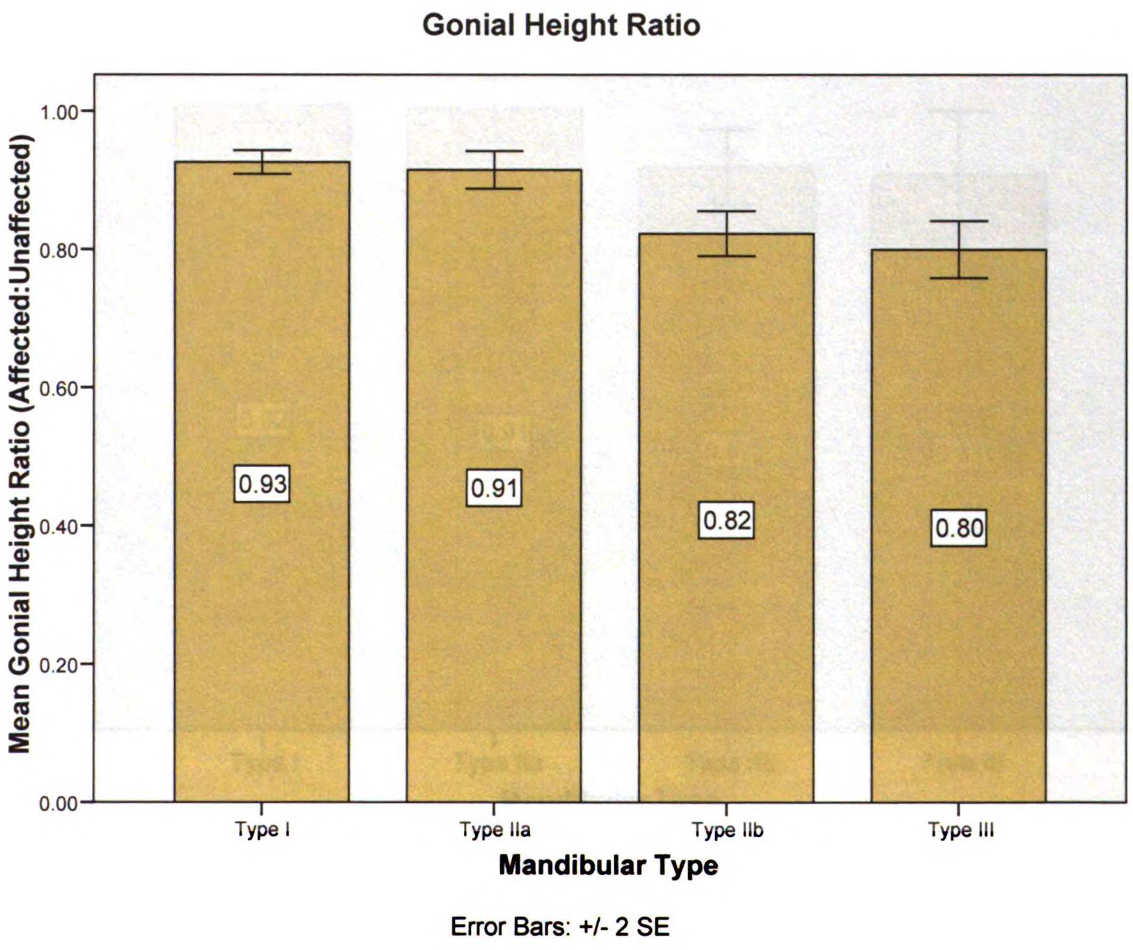

Figure 9: Gonial height ratio

Table 8: Gonial height ratio at 1st time point ([affected gonial height]/[unaffected gonial height])

Mandibular Type	Mean	Std. Dev.	Std. Err. Of Mean
I	0.92	0.063	0.012
IIa	0.91	0.074	0.025
IIb	0.82	0.062	0.028
III	0.81	0.124	0.047
Overall	0.89	0.085	0.012

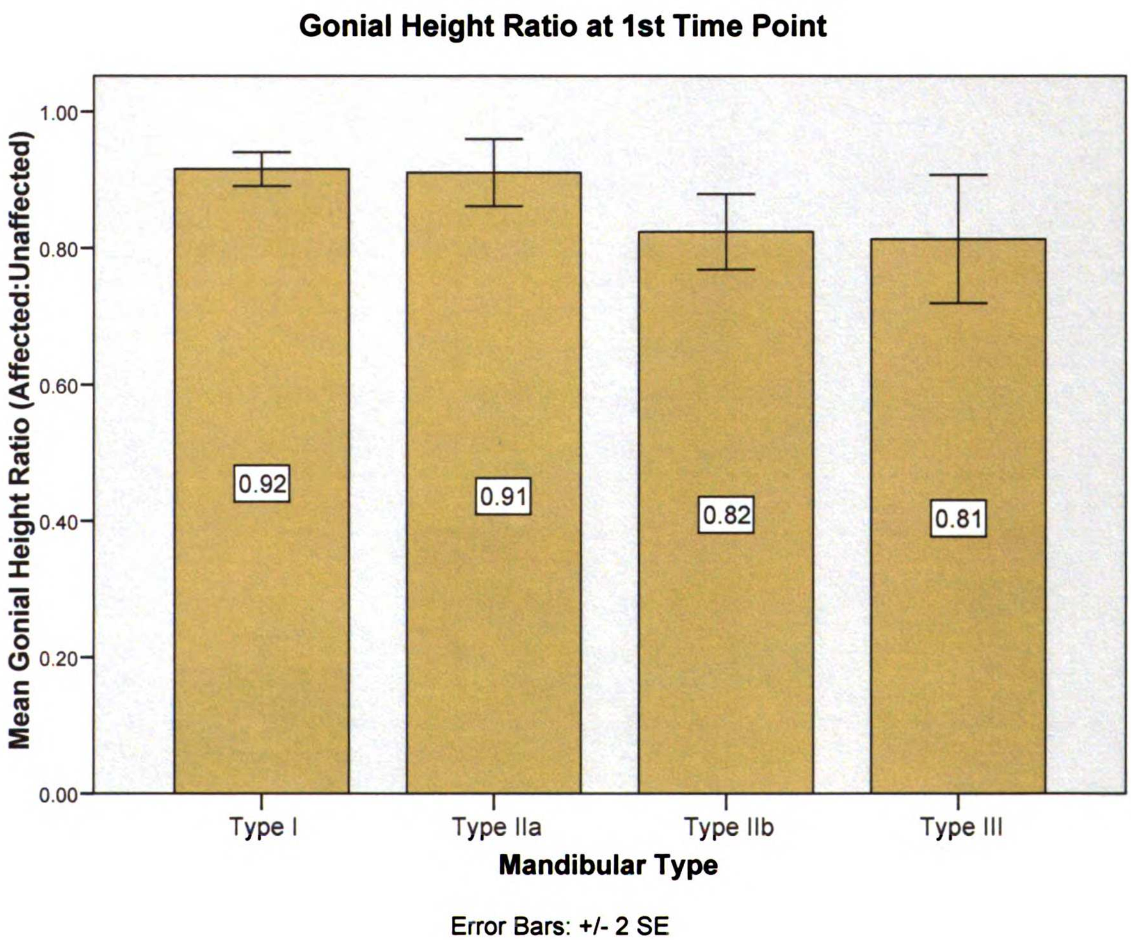

Figure 10: Gonial height ratio at 1st time point

Table 9: Mandibular midline plane angle

Mandibular Type	Mean (°)	Std. Dev.	Std. Err. Of Mean
I	5.5	6.30	0.70
IIa	11.6	6.53	1.31
IIb	23.7	7.88	1.86
III	11.5	5.44	1.07
Overall	9.7	8.66	0.71

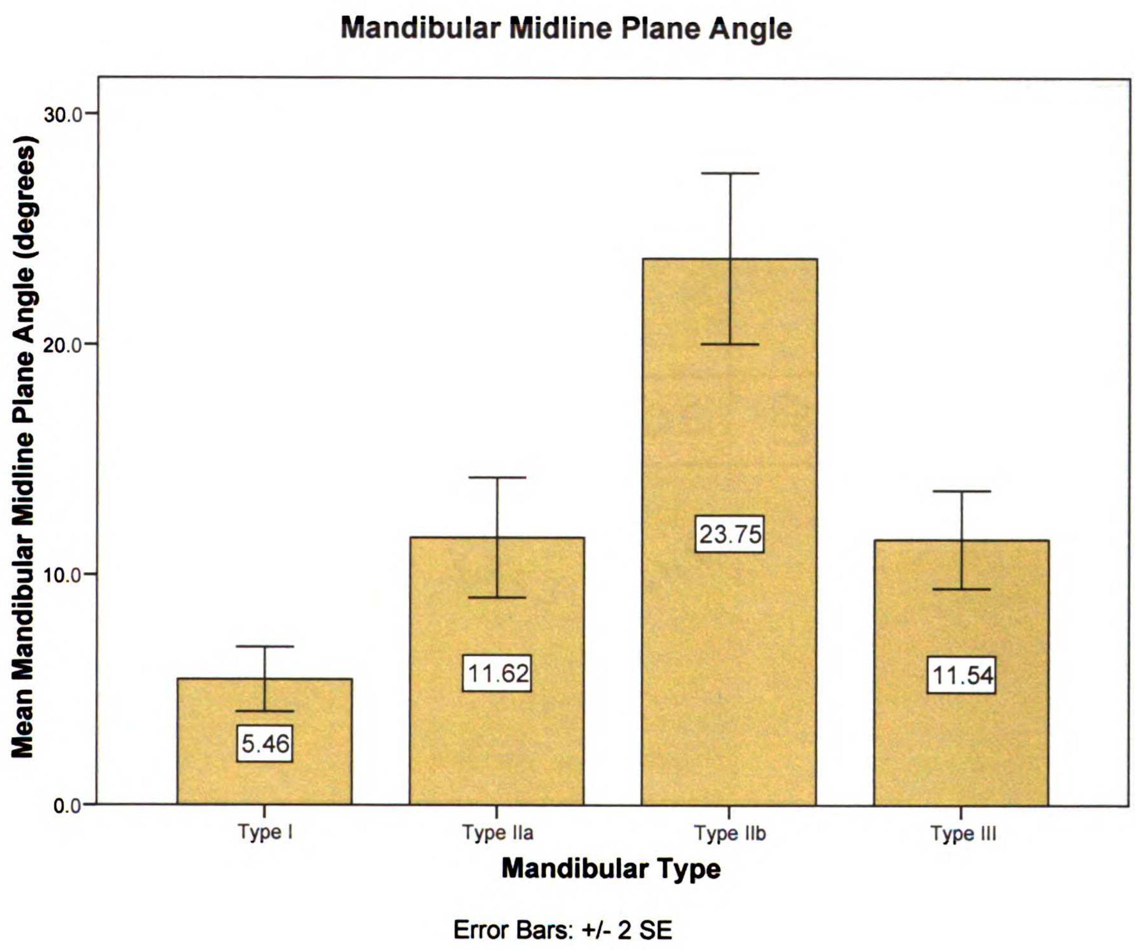

Figure 11: Mandibular midline plane angle

Table 10: Mandibular midline plane angle at 1st time point

Mandibular Type	Mean (°)	Std. Dev.	Std. Err. Of Mean
I	6.4	5.45	1.07
IIa	12.2	8.18	2.73
IIb	23.7	6.61	2.96
III	12.4	4.49	1.70
Overall	10.3	7.98	1.16

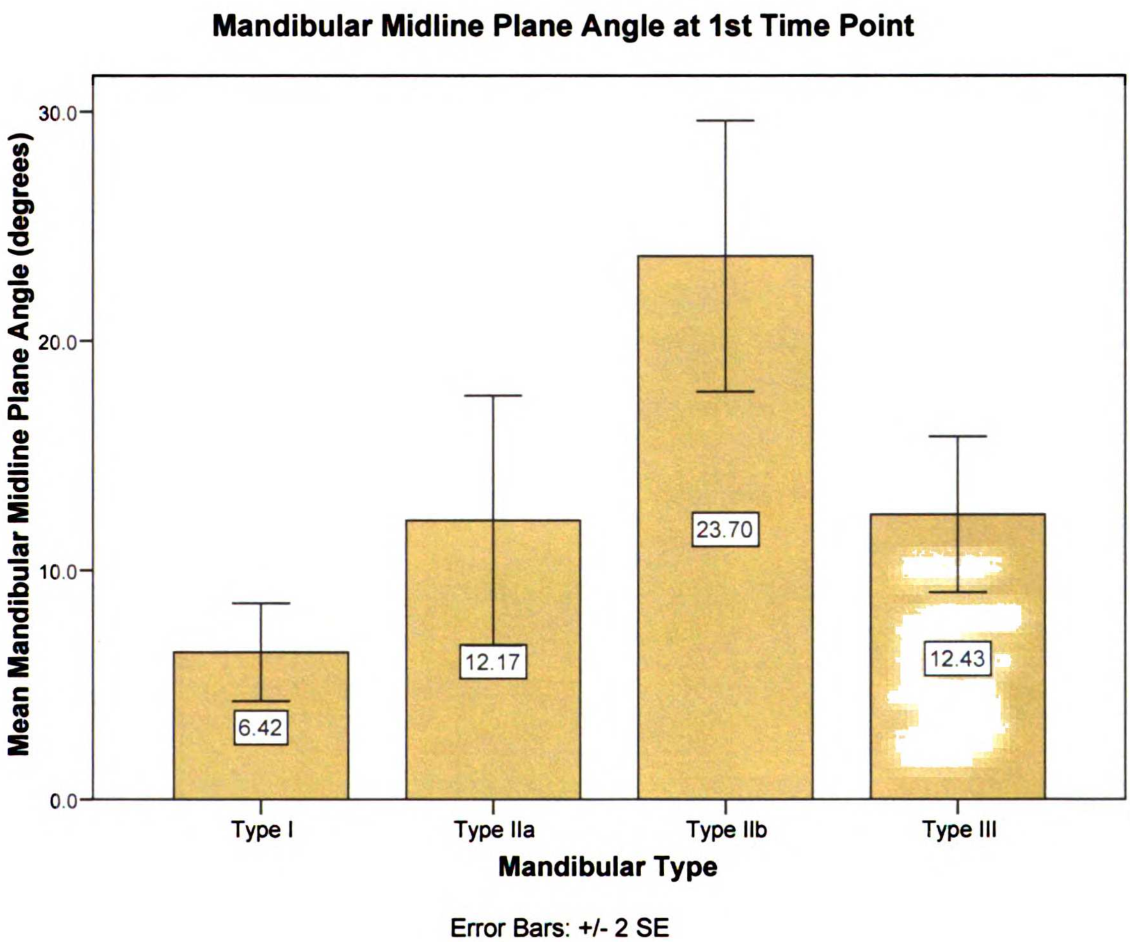

Figure 12: Mandibular midline plane angle at 1st time point

Table 11: Intergonial plane angle

Mandibular Type	Mean (°)	Std. Dev.	Std. Err. Of Mean
I	3.5	3.33	0.37
IIa	4.3	3.89	0.78
IIb	8.3	2.69	0.63
III	8.8	5.01	0.98
Overall	5.1	4.31	0.35

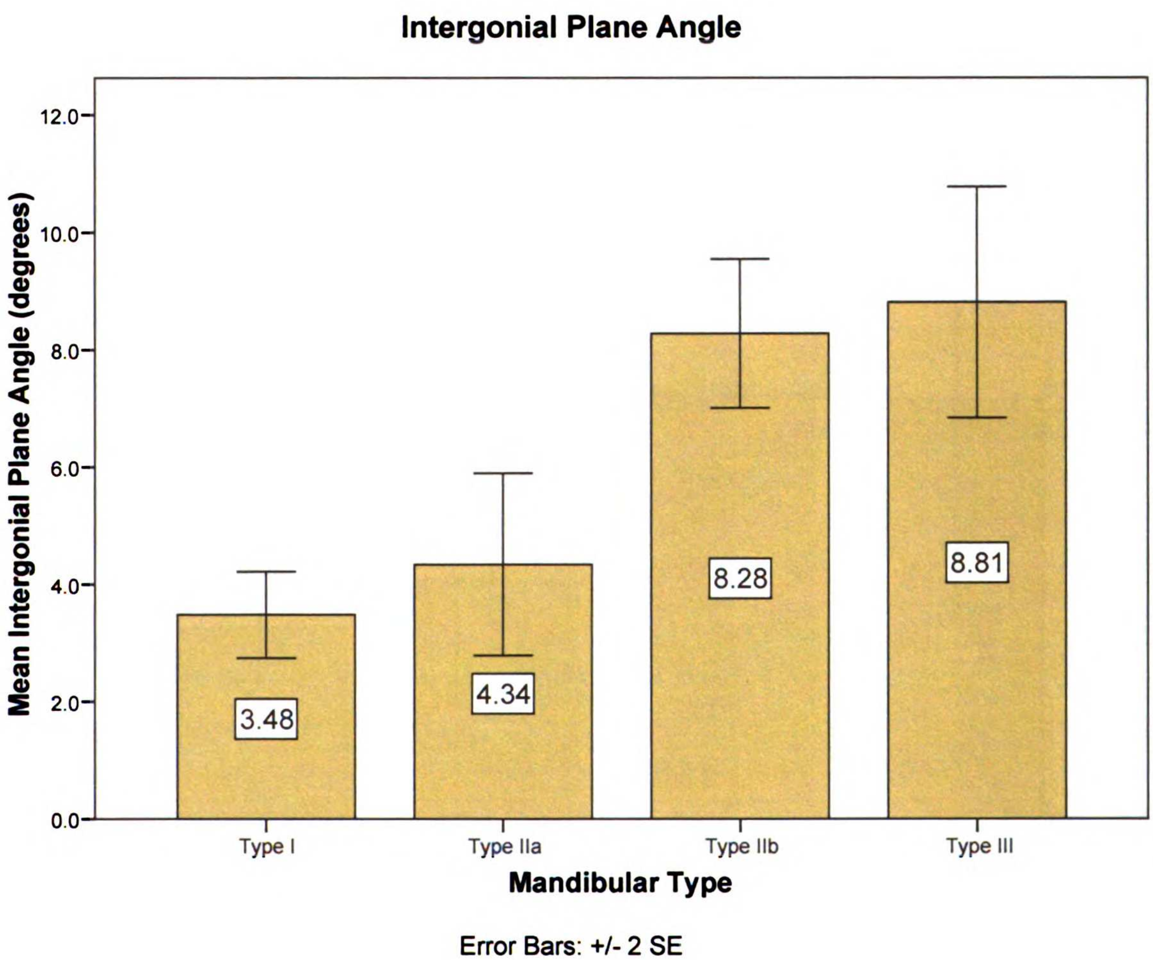

Figure 13: Intergonial plane angle

Table 12: Intergonial plane angle at 1st time point

Mandibular Type	Mean (°)	Std. Dev.	Std. Err. Of Mean
I	3.8	2.79	0.55
IIa	4.8	4.04	1.35
IIb	8.6	1.92	0.86
III	8.5	5.91	2.23
Overall	5.2	4.00	0.58

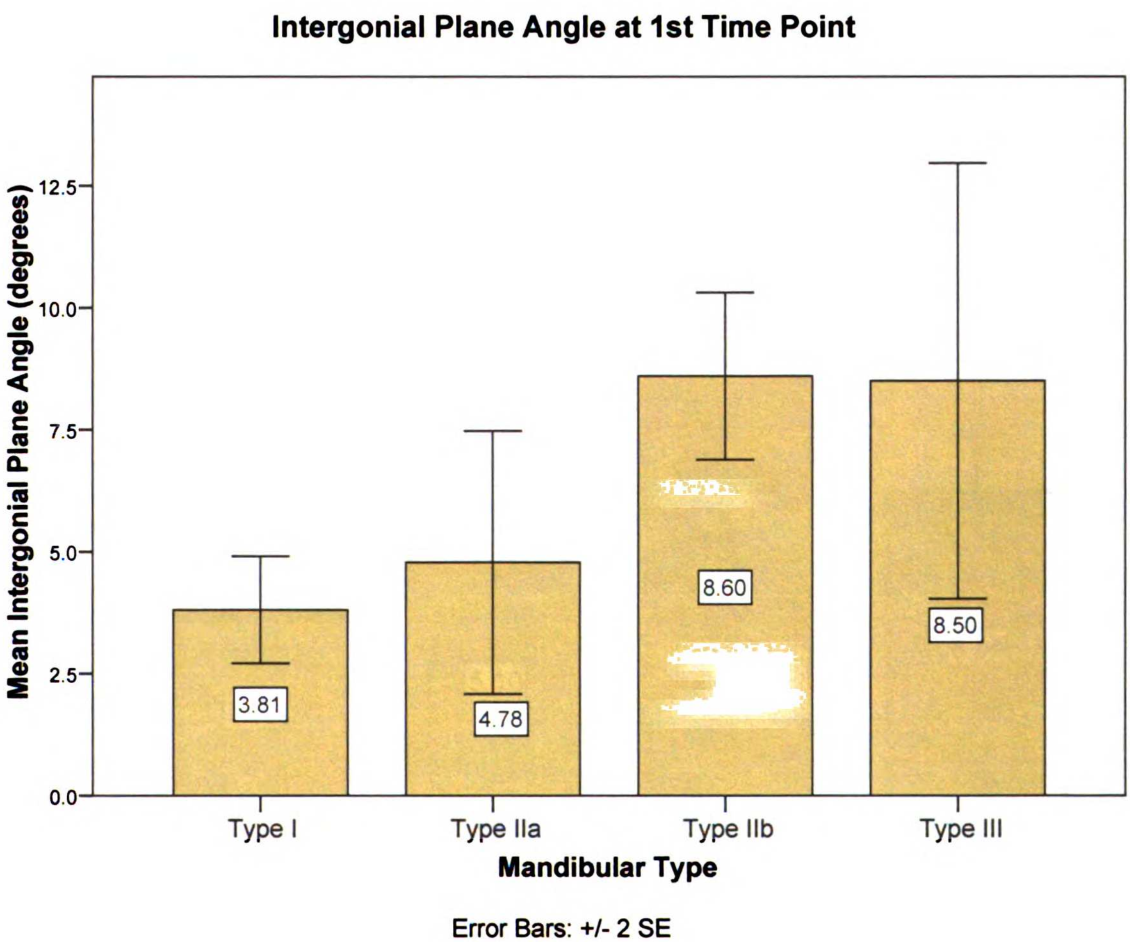

Figure 14: Intergonial plane angle at 1st time point

Table 13: Mandibular molar plane angle

Mandibular Type	Mean (°)	Std. Dev.	Std. Err. Of Mean
I	3.9	3.40	0.38
IIa	5.1	3.14	0.63
IIb	12.3	4.34	1.02
III	6.5	3.05	0.60
Overall	5.6	4.33	0.35

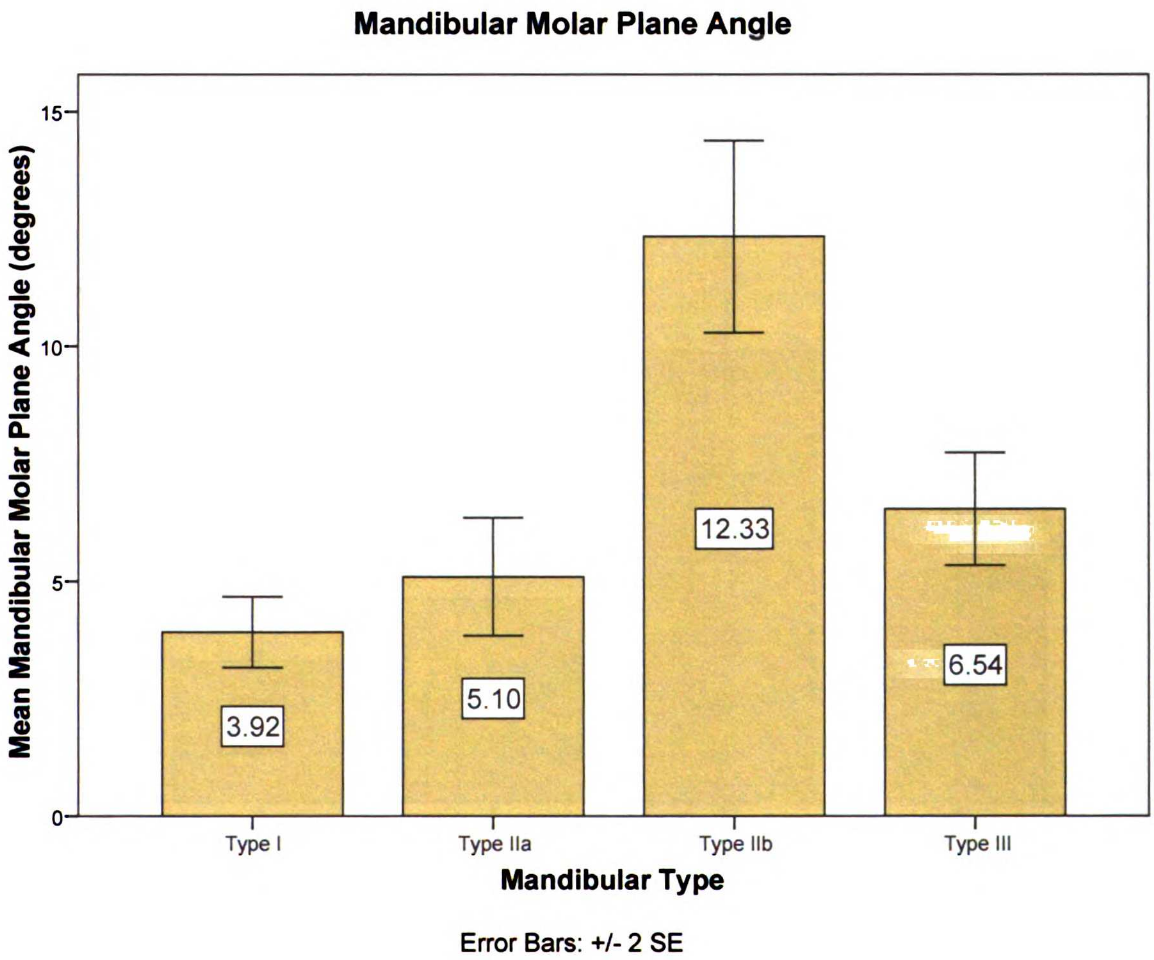

Figure 15: Mandibular molar plane angle

Table 14: Mandibular molar plane angle at 1st time point

Mandibular Type	Mean (°)	Std. Dev.	Std. Err. Of Mean
I	4.1	2.52	0.49
IIa	5.9	3.23	1.08
IIb	13.2	4.09	1.83
III	6.9	3.04	1.15
Overall	5.8	3.96	0.58

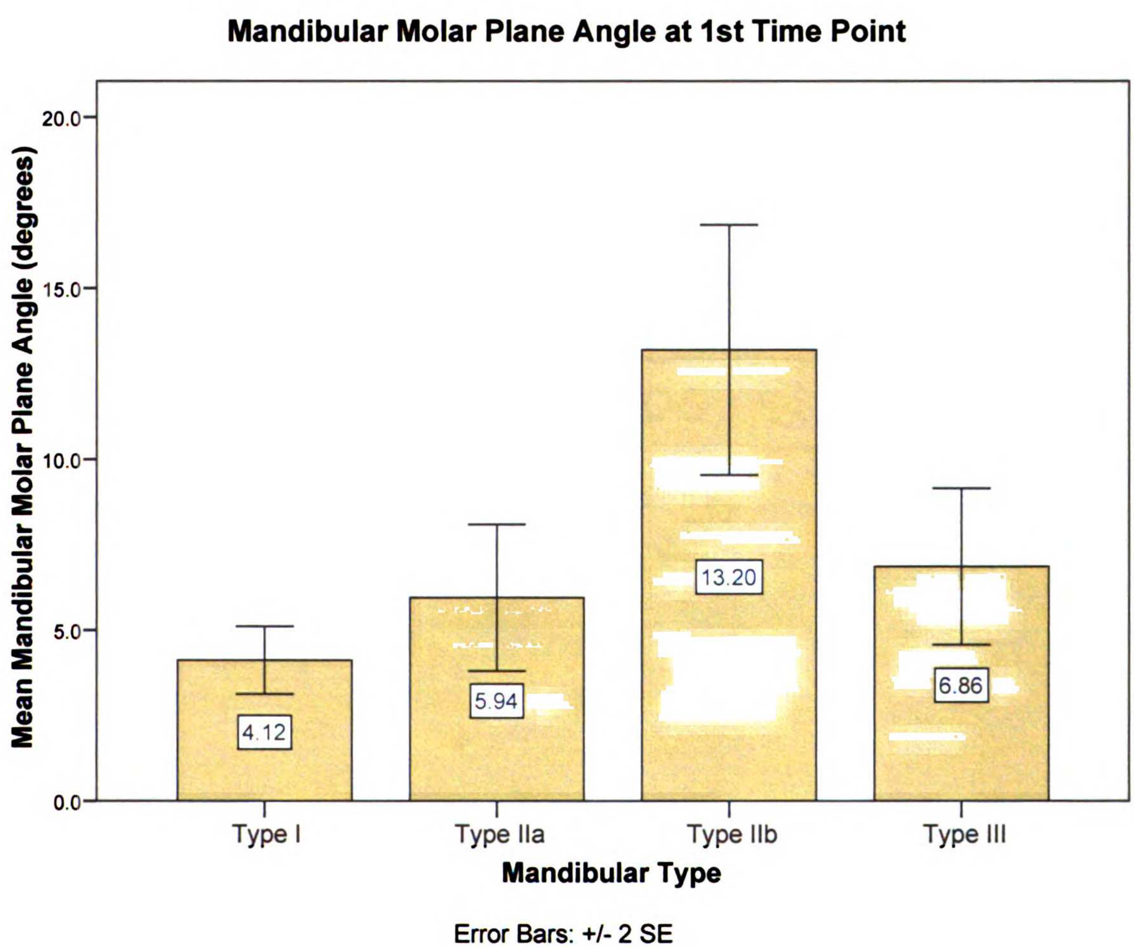

Figure 16: Mandibular molar plane angle at 1st time point

Table 15: Maxillary molar plane angle

Mandibular Type	Mean (°)	Std. Dev.	Std. Err. Of Mean
I	3.5	3.71	0.41
IIa	5.4	4.33	0.87
IIb	10.7	4.56	1.08
III	8.7	4.45	0.87
Overall	5.6	4.83	0.39

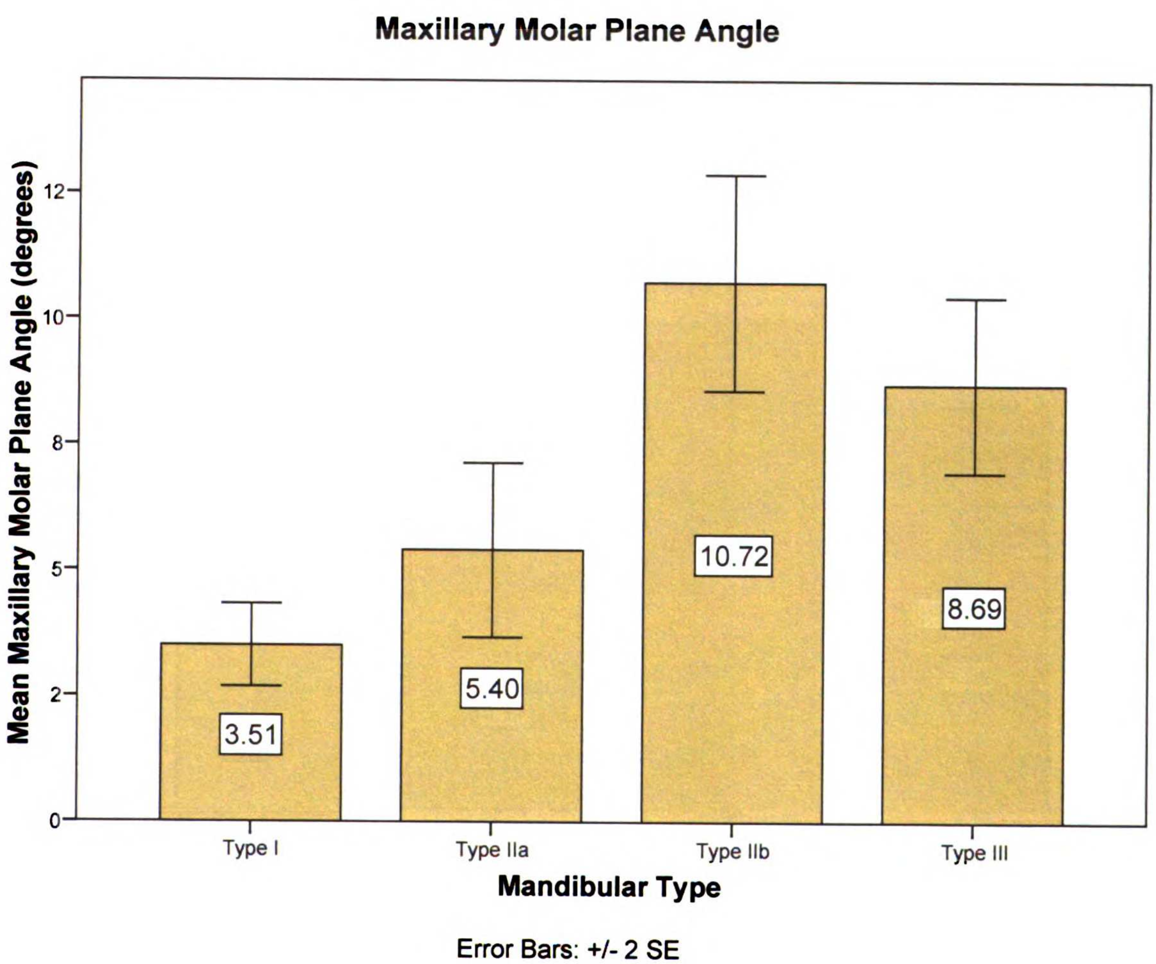

Figure 17: Maxillary molar plane angle

Table 16: Maxillary molar plane angle at 1st time point

Mandibular Type	Mean (°)	Std. Dev.	Std. Err. Of Mean
I	3.1	2.99	0.59
IIa	5.9	5.14	1.71
IIb	8.9	4.01	1.79
III	7.4	5.50	2.08
Overall	4.9	4.42	0.64

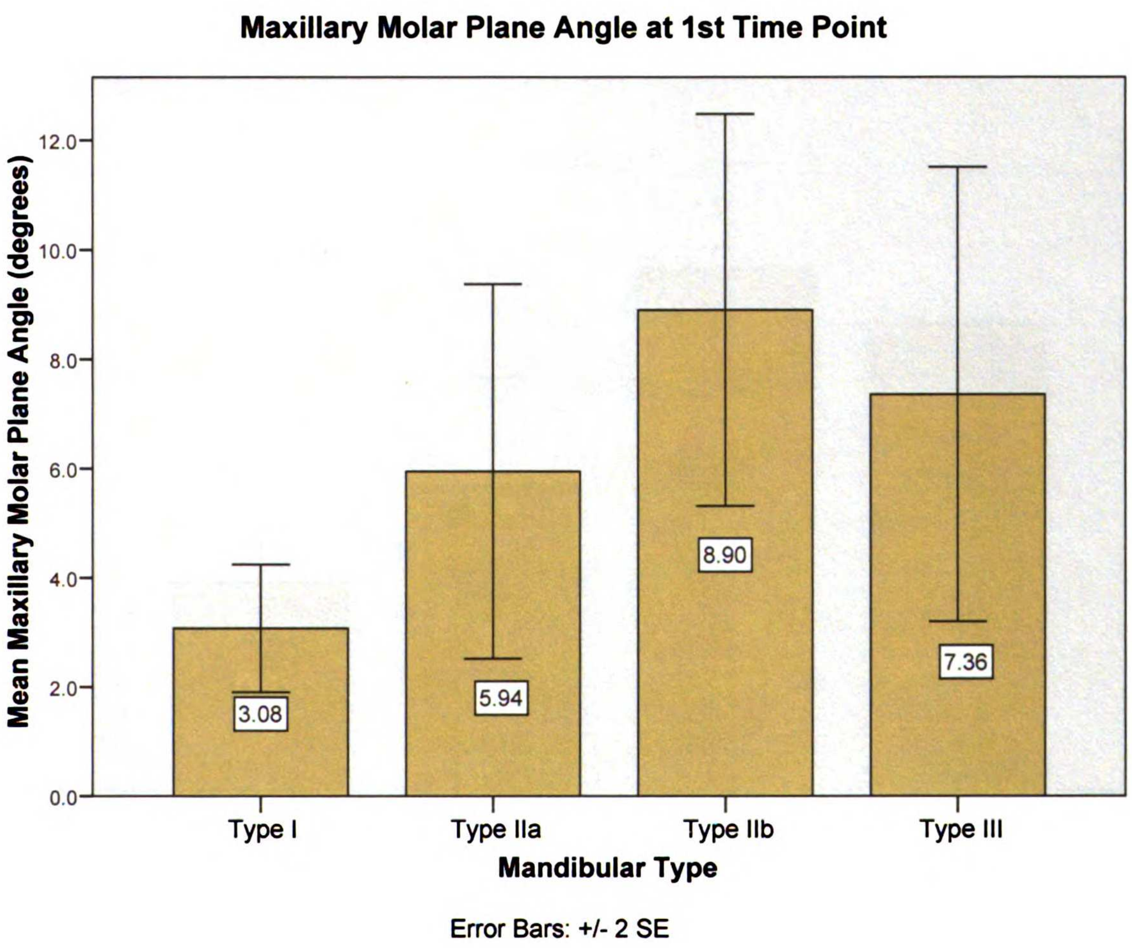

Figure 18: Maxillary molar plane angle at 1st time point

Table 17: Piriform plane angle

Mandibular Type	Mean (°)	Std. Dev.	Std. Err. Of Mean
I	4.2	5.42	0.60
IIa	6.2	5.56	1.11
IIb	10.6	4.58	1.08
III	9.5	7.84	1.54
Overall	6.2	6.31	0.52

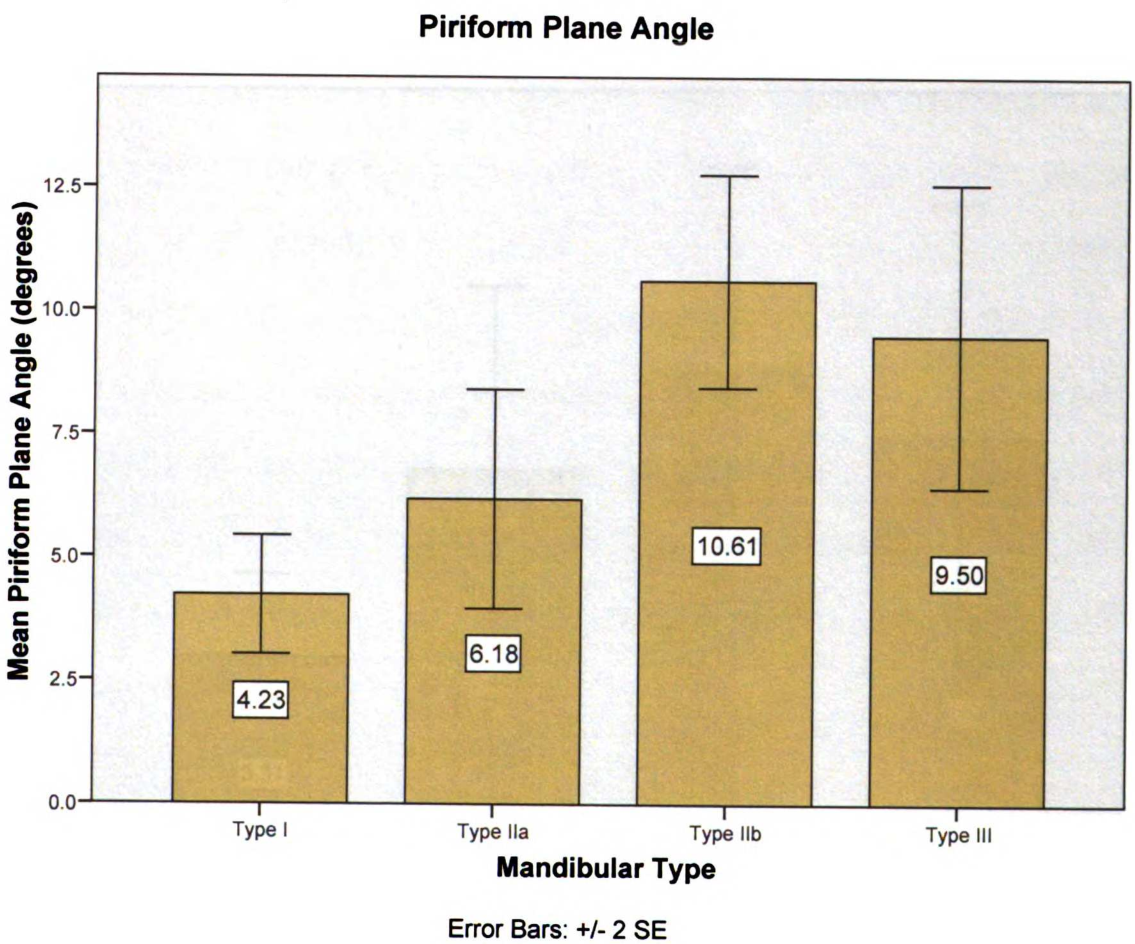

Figure 19: Piriform plane angle

Table 18: Piriform plane angle at 1st time point

Mandibular Type	Mean (°)	Std. Dev.	Std. Err. Of Mean
I	3.3	4.68	0.92
IIa	7.4	6.04	2.01
IIb	9.6	5.04	2.26
III	8.1	6.87	2.60
Overall	5.5	5.74	0.84

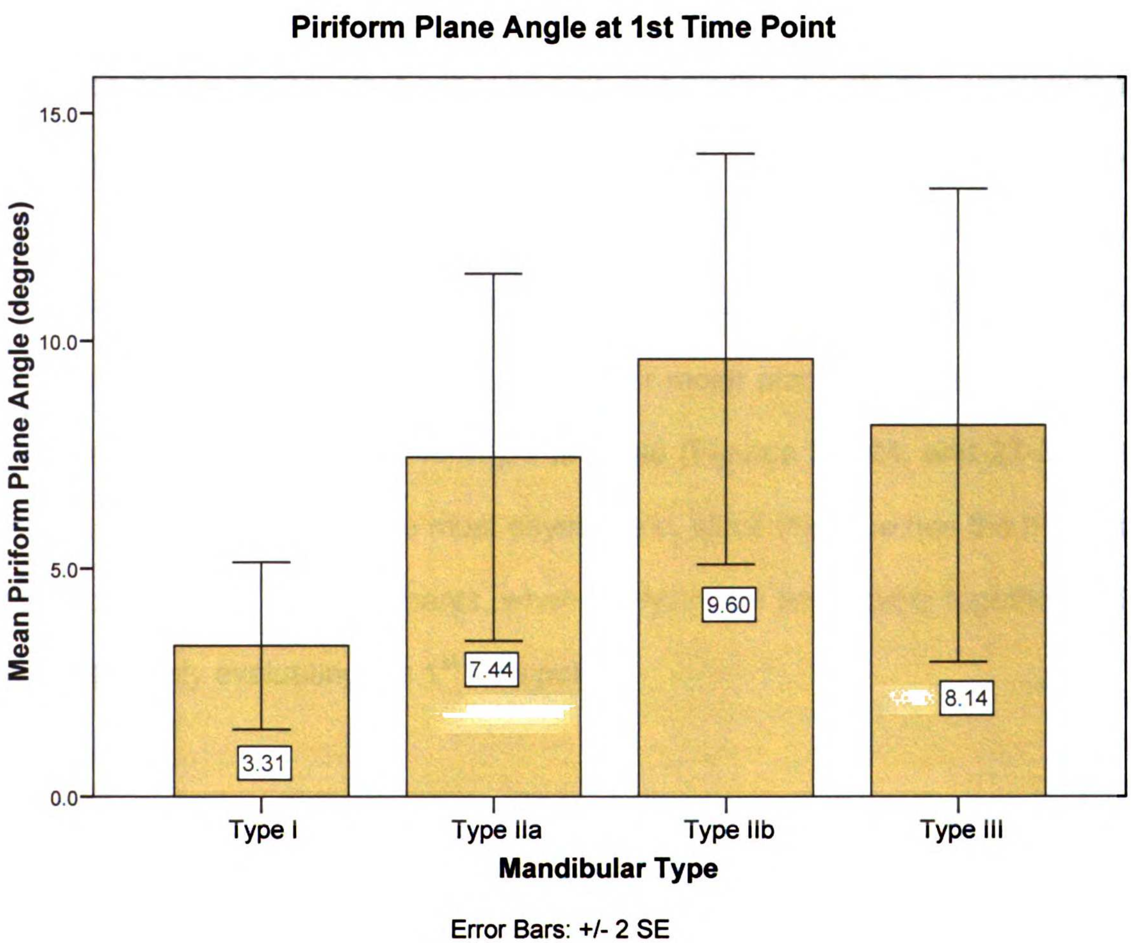

Figure 20: Piriform plane angle at 1st time point

REGRESSION ANALYSIS

The mixed model regression analysis, using age as the covariate, longitudinally analyzed each PA cephalometric measurement by mandibular type. This analysis accounted for both within- and between-subject variation, and allowed for unequal numbers of time points between subjects.

Figures 21-32 graphically display the estimated marginal means for each measurement by mandibular type at the mean age of 9.1 years, and separately at the mean age at the 1st time point of 6.8 years. These results are similar to the overall means of each measurement reported in the previous section. All regression analyses show that either type IIb or type III subjects demonstrate the most asymmetry. The gonial height ratio and intergonial plane angle graphs (Figures 21, 22, 25, and 26) show that subjects with type III mandibular deformity demonstrate the highest magnitude of asymmetry. On the other hand, the mandibular midline plane angle, the mandibular molar plane angle, the maxillary molar plane angle, and the piriform plane angle (Figures 23, 24, and 27-32) all demonstrate that type IIb is the most asymmetric, since this type has the highest magnitude for these measurements, when analyzing all time points together and when separately evaluating the 1st time points.

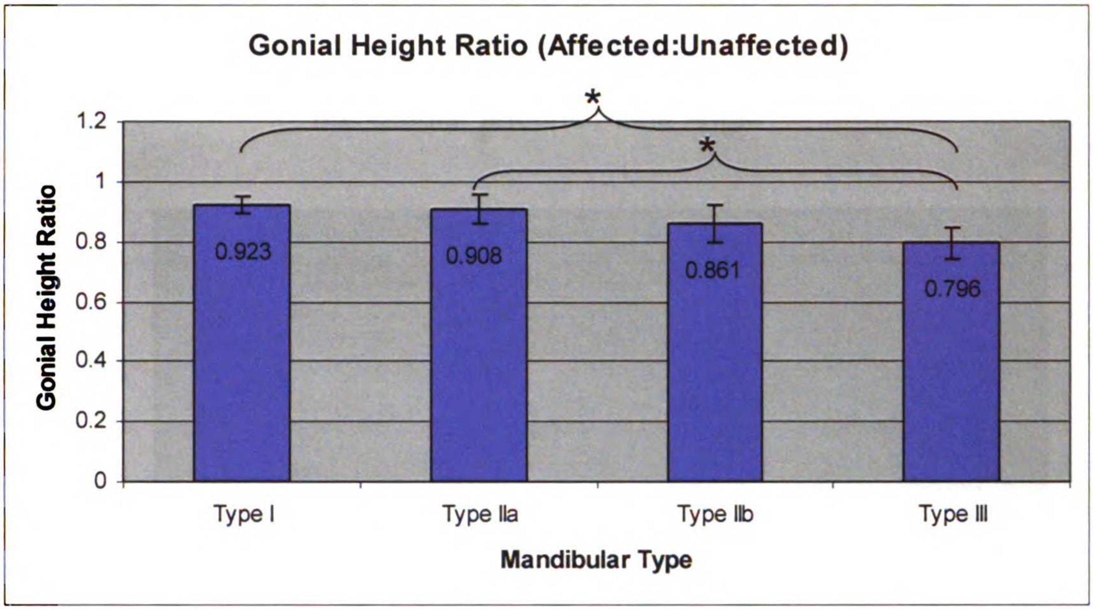

Figure 21: Regression analysis of mandibular height ratio (error bars are ± 2 S.E.). Statistically significant difference indicated by (*).

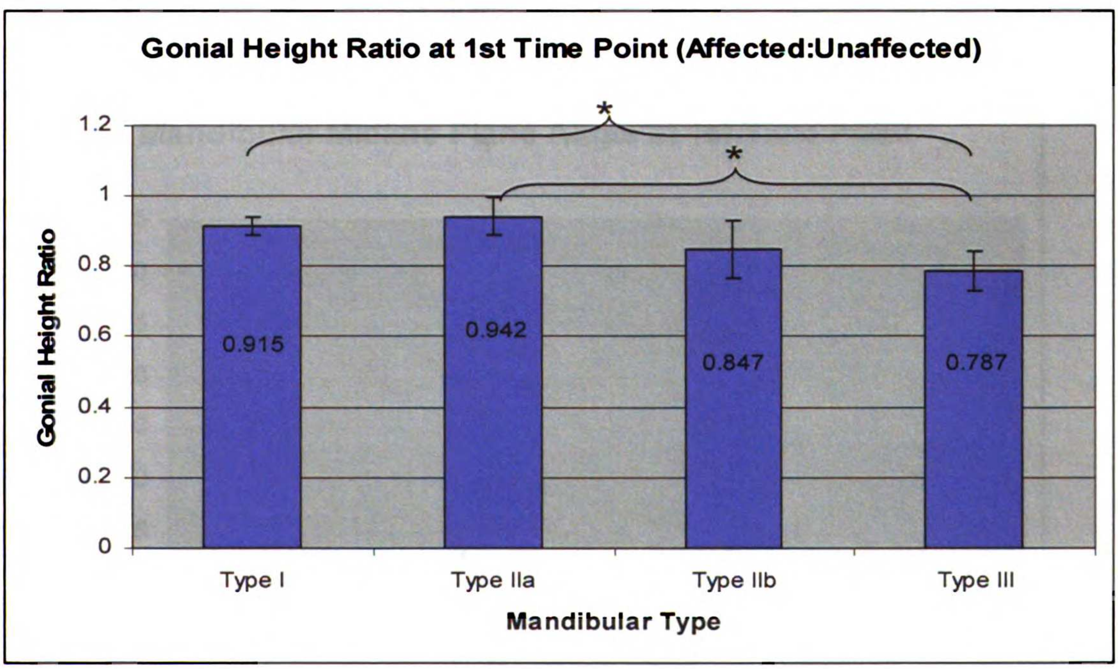

Figure 22: Regression analysis of mandibular height ratio at 1st time point (error bars are ± 2 S.E.). Statistically significant difference indicated by (*).

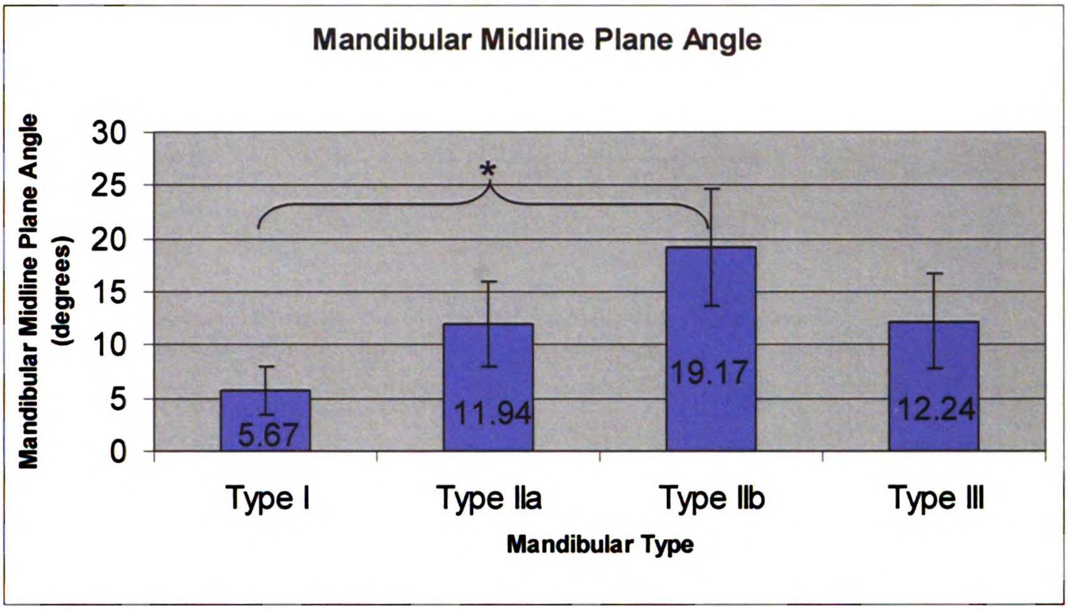

Figure 23: Regression analysis of mandibular midline plane angle (error bars are ± 2 S.E.). Statistically significant difference indicated by (*).

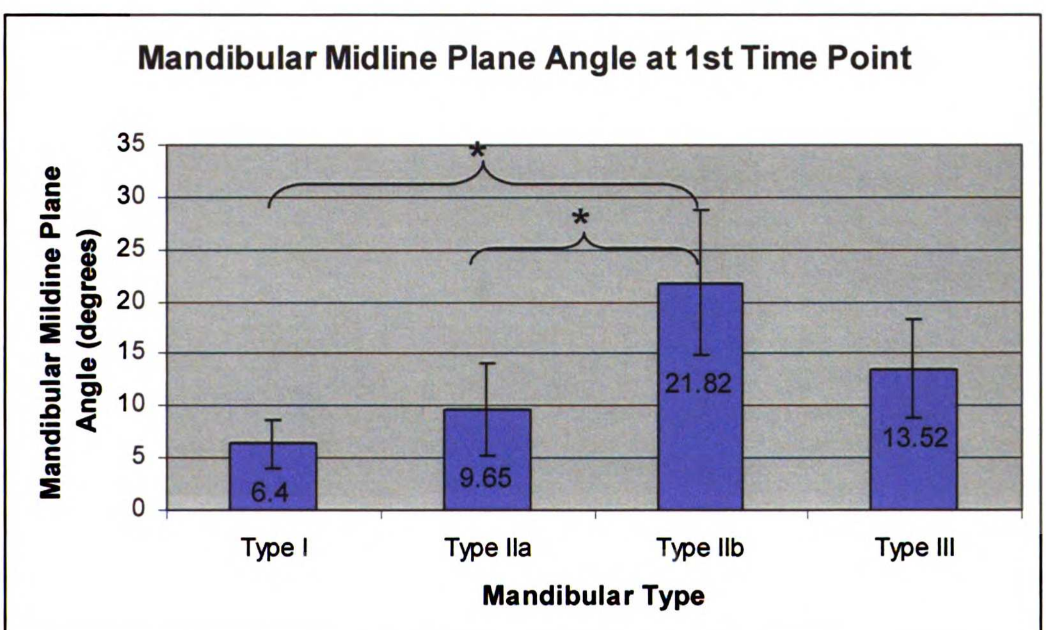

Figure 24: Regression analysis of mandibular midline plane angle at 1st time point (error bars are ± 2 S.E.). Statistically significant difference indicated by (*).

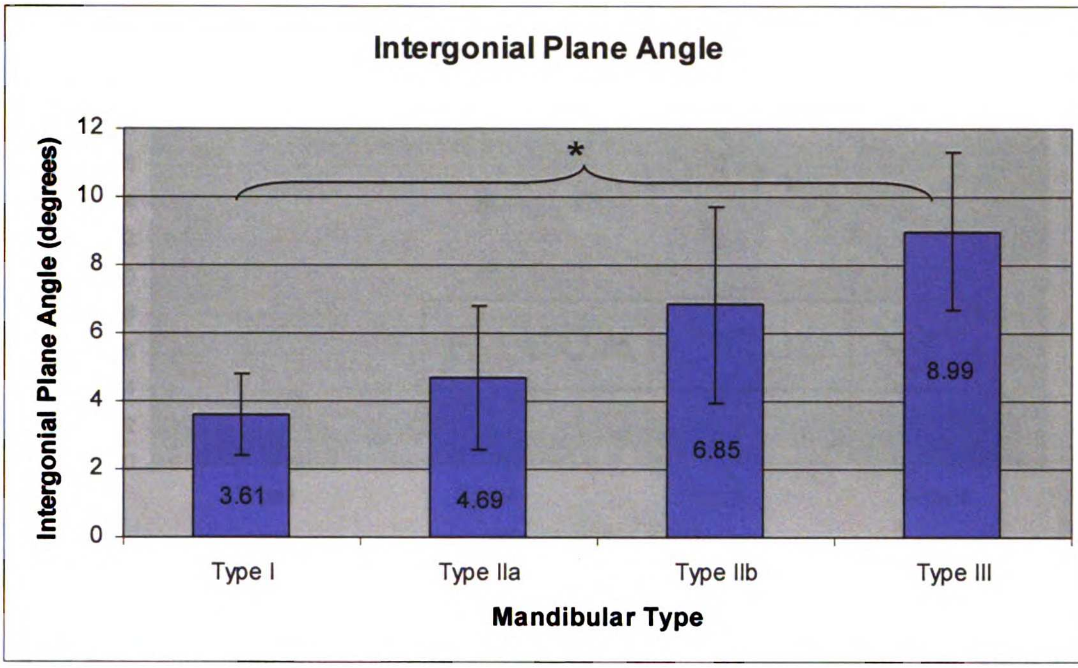

Figure 25: Regression analysis of intergonial plane angle (error bars are ± 2 S.E.). Statistically significant difference indicated by (*).

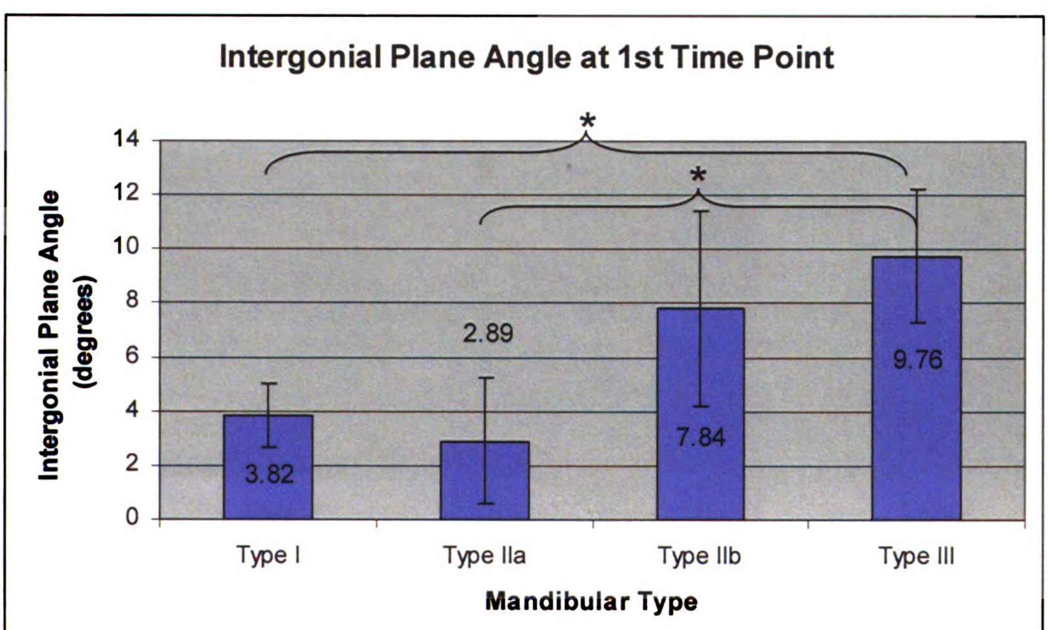

Figure 26: Regression analysis of intergonial plane angle at 1st time (error bars are ± 2 S.E.). Statistically significant difference indicated by (*).

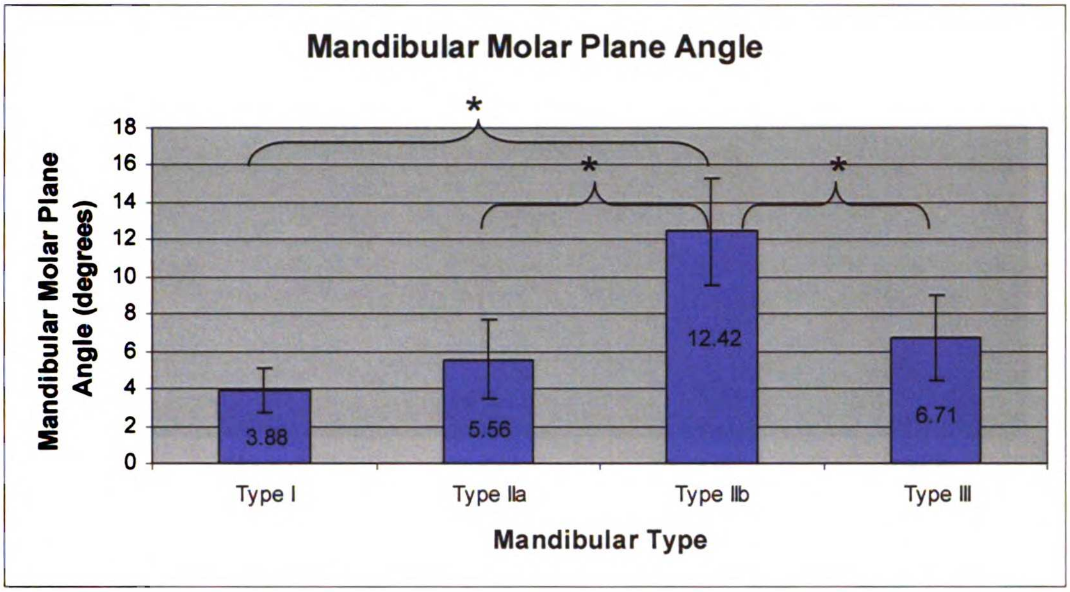

Figure 27: Regression analysis of mandibular molar plane angle (error bars are ± 2 S.E.). Statistically significant difference indicated by (*).

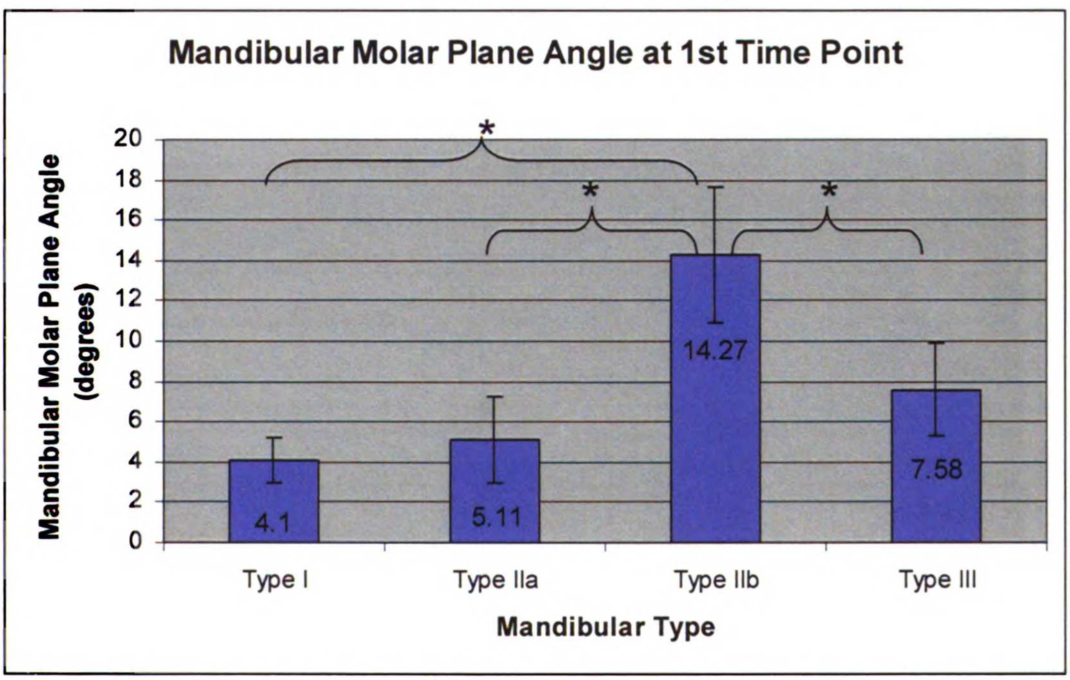

Figure 28: Regression analysis of mandibular molar plane angle at 1st time point (error bars are ± 2 S.E.). Statistically significant difference indicated by (*).

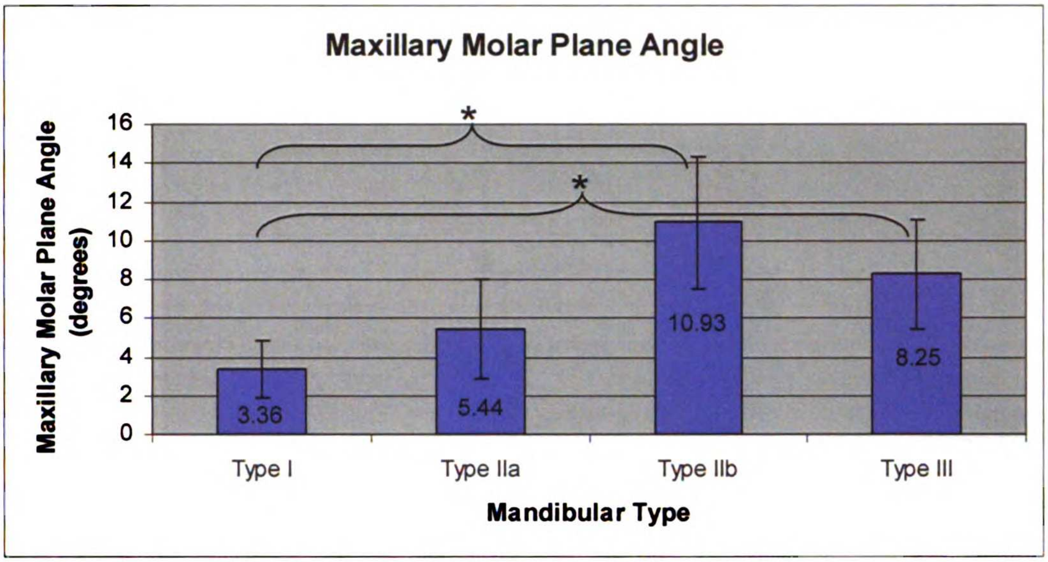

Figure 29: Regression analysis of maxillary molar plane angle (error bars are ± 2 S.E.). Statistically significant difference indicated by (*).

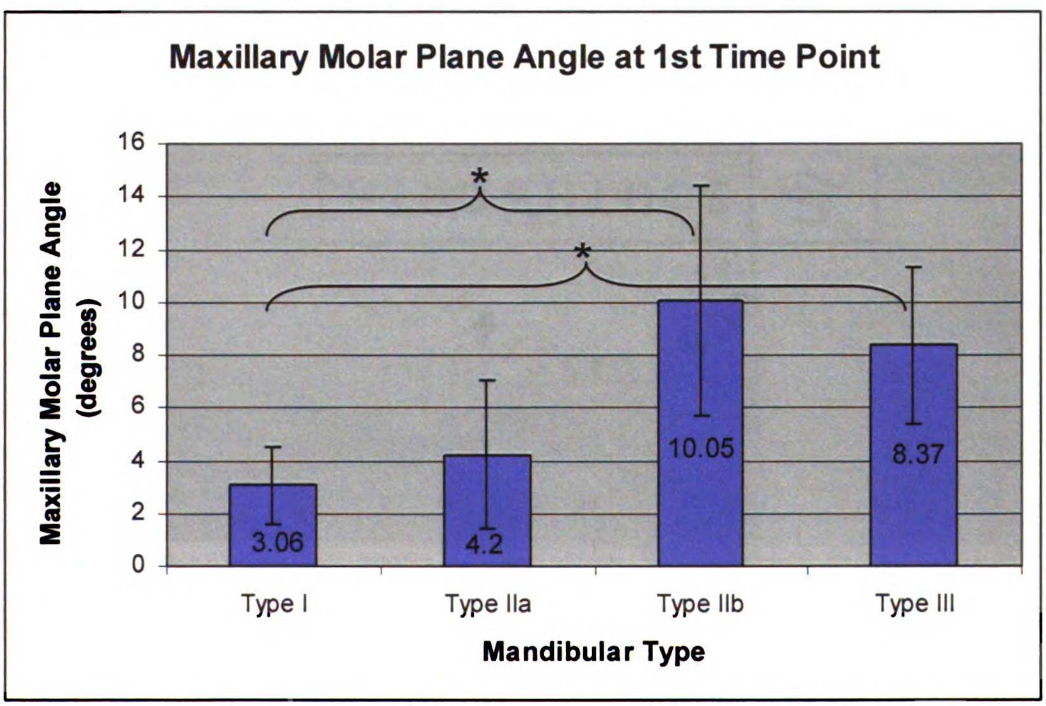

Figure 30: Regression analysis of maxillary molar plane angle at 1st time point (error bars are ± 2 S.E.). Statistically significant difference indicated by (*).

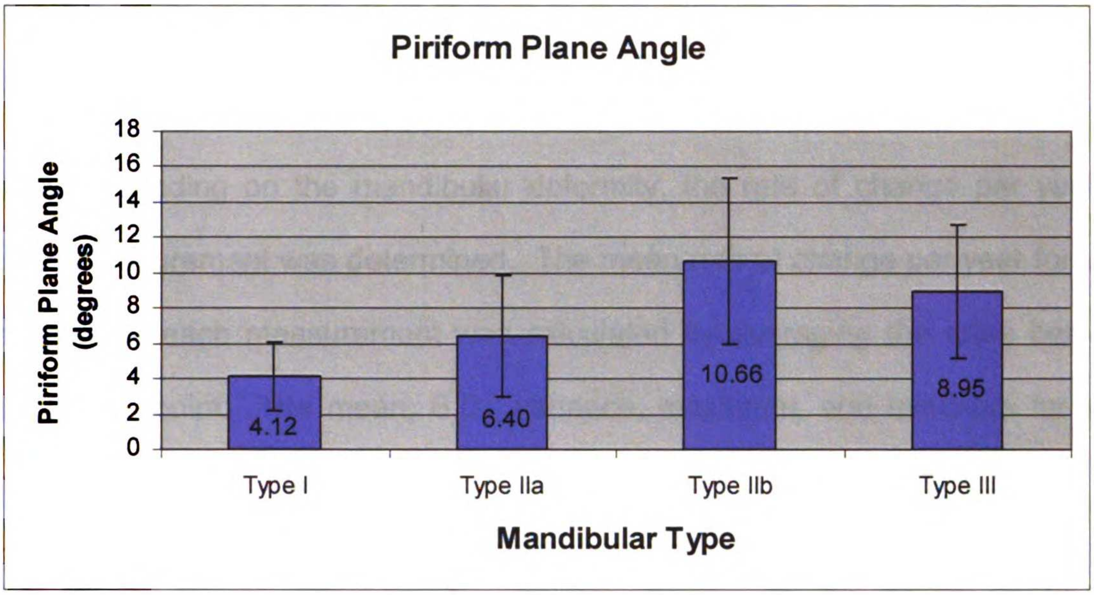

Figure 31: Regression analysis of piriform plane angle (error bars are ± 2 S.E.)

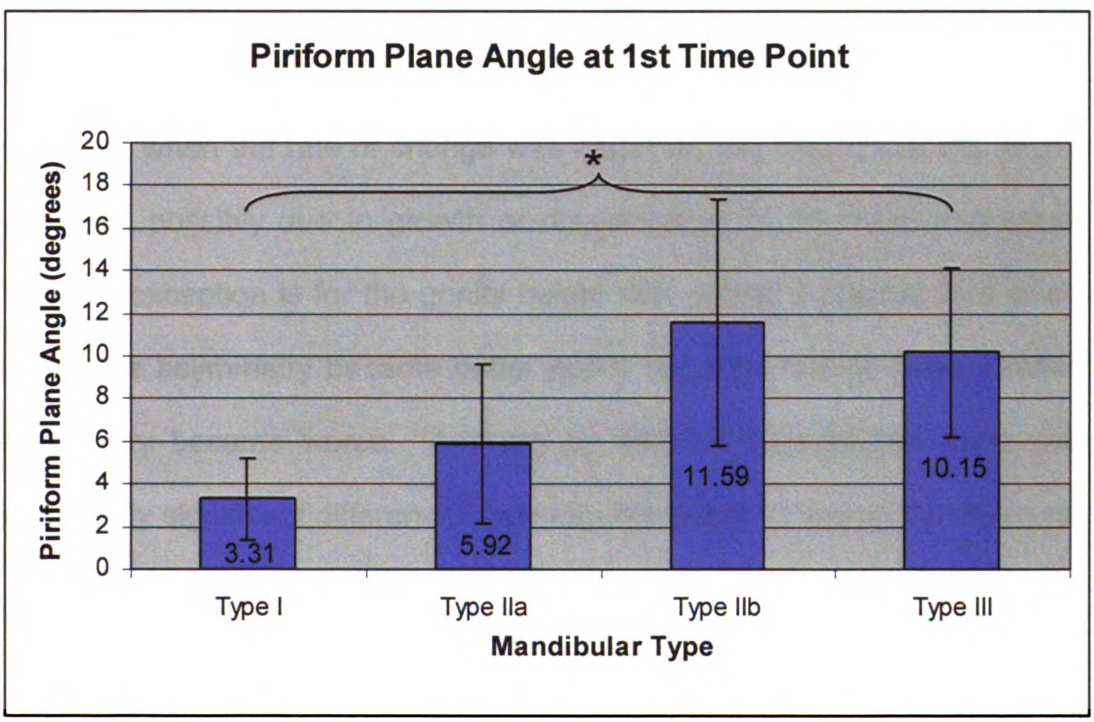

Figure 32: Regression analysis of piriform plane angle at 1st time point (error bars are ± 2 S.E.). Statistically significant difference indicated by (*).

MEAN RATE OF CHANGE

To determine if the asymmetry worsens, stays the same, or improves over time, depending on the mandibular deformity, the rate of change per year for each measurement was determined. The mean rate of change per year for each subject for each measurement was calculated by averaging the rates between each time point. The mean, S.D., variance, maximum, and minimum for each measurement by mandibular type are in Tables 19-24 and the means are graphically displayed in Figures 33-38.

This analysis demonstrated a wide range of rates for each measurement. While the average rates centered on zero, the maximum and minimum values varied from the mean and in one instance as much as ~14 degrees/year. When the rate of change was positive, this meant the asymmetry became worse. However, when the rate of change was negative, this meant that the asymmetry lessened, possibly due to growth or displacement of the measured structures. The one exception is for the gonial height ratio where a positive rate of change meant the asymmetry became better and a negative rate of change meant the asymmetry became worse. Analysis by ANOVA showed that there were no statistically significant differences between the types for any of the mean rates of change for each measurement.

Table 19: Mean rate of change of gonial height ratio (per year)

Type	Mean	S.D.	Variance	Minimum	Maximum	N
I	0.002	0.021	0	-0.049	0.050	26
IIa	-0.001	0.015	0	-0.031	0.024	9
IIb	0.013	0.017	0	-0.007	0.038	5
III	-0.006	0.036	0.001	-0.076	0.045	7

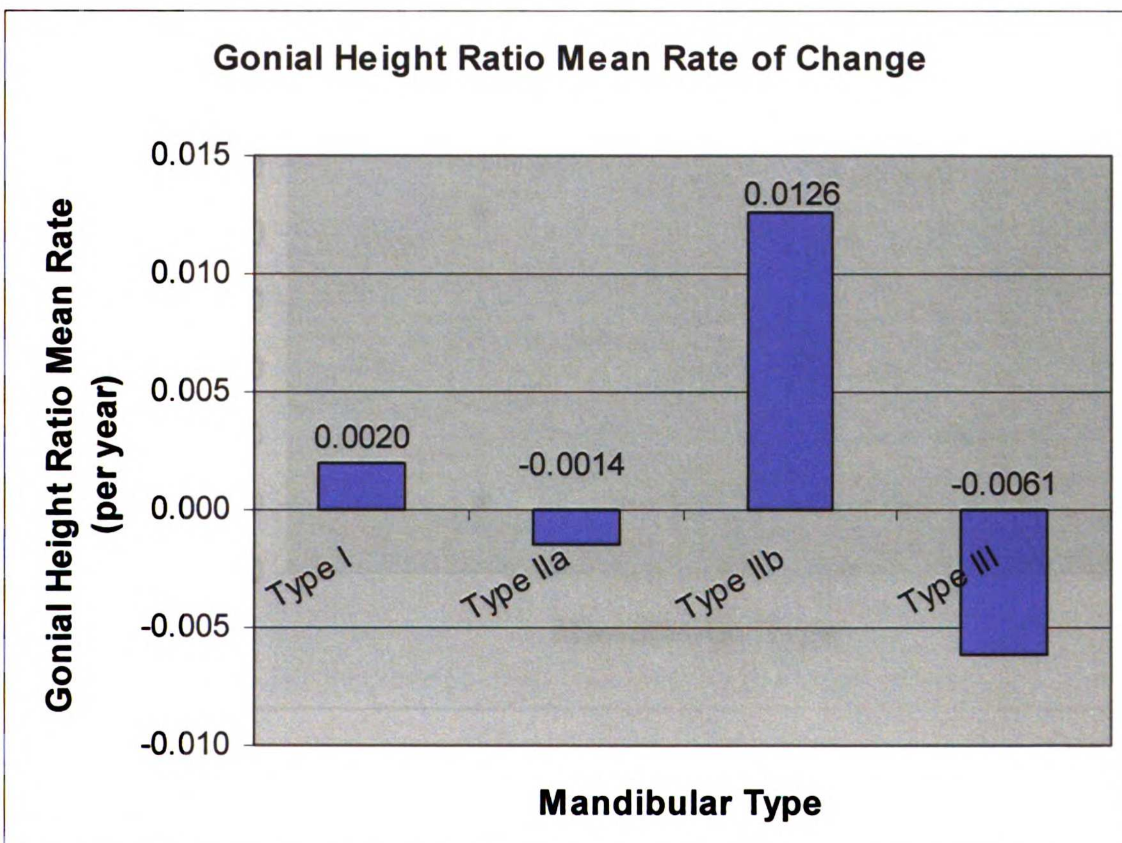

Figure 33: Mean rate of change of gonial height ratio

Table 20: Mean rate of change of mandibular midline plane angle (degrees/year)

Type	Mean	S.D.	Variance	Minimum	Maximum	N
I	-0.407	1.204	1.449	-2.609	2.571	26
IIa	-0.085	1.651	2.724	-3.210	2.254	9
IIb	-1.225	4.442	19.730	-6.792	5.625	5
III	-0.200	2.154	4.641	-3.612	1.674	7

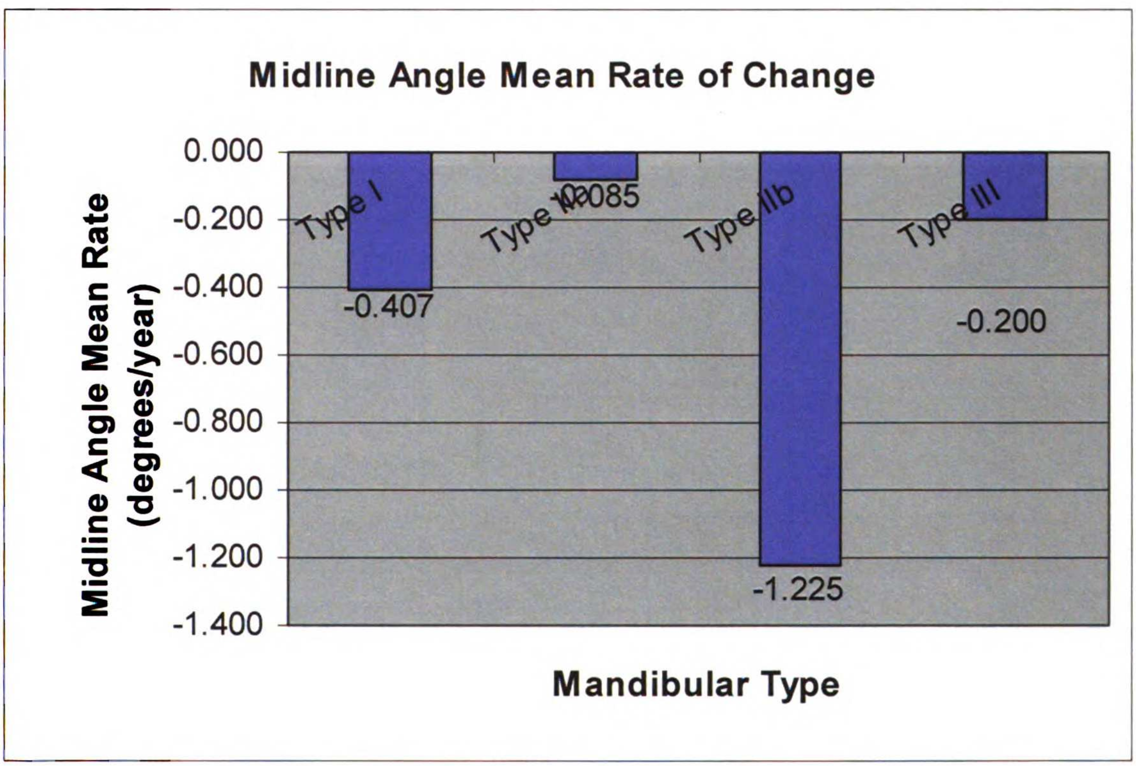

Figure 34: Mean rate of change of mandibular midline plane angle

Table 21: Mean rate of change of intergonial plane angle (degrees/year)

Type	Mean	S.D.	Variance	Minimum	Maximum	N
I	-0.212	1.030	1.062	-2.256	1.895	26
IIa	0.092	0.661	0.437	-0.918	1.408	9
IIb	-0.739	0.842	0.708	-1.989	0	5
III	0.109	1.575	2.480	-1.674	3.158	7

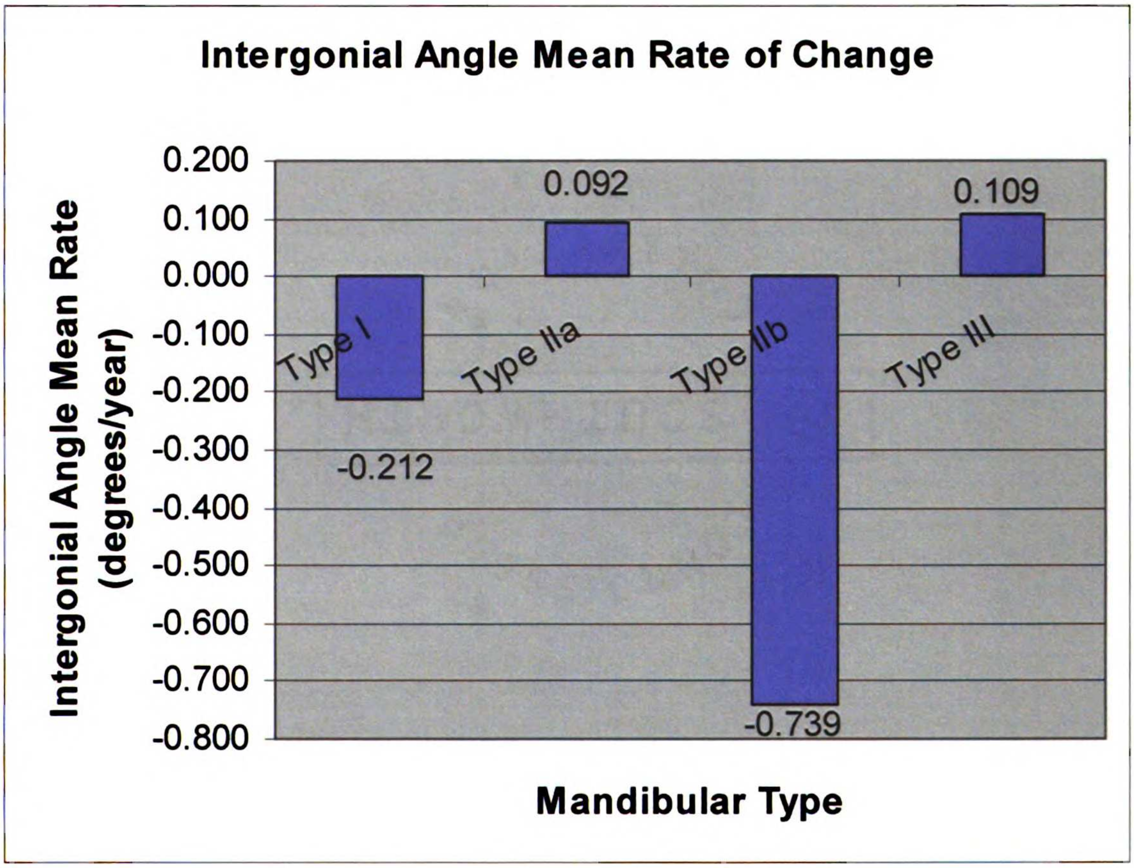

Figure 35: Mean rate of change of intergonial plane angle

Table 22: Mean rate of change of mandibular molar plane angle (degrees/year)

Type	Mean	S.D.	Variance	Minimum	Maximum	N
I	-0.073	1.549	2.401	-5.188	4.737	26
IIa	-0.184	1.232	1.518	-1.837	2.254	9
IIb	-0.111	0.153	0.023	-0.285	0	5
III	0.087	0.545	0.298	-0.789	0.673	7

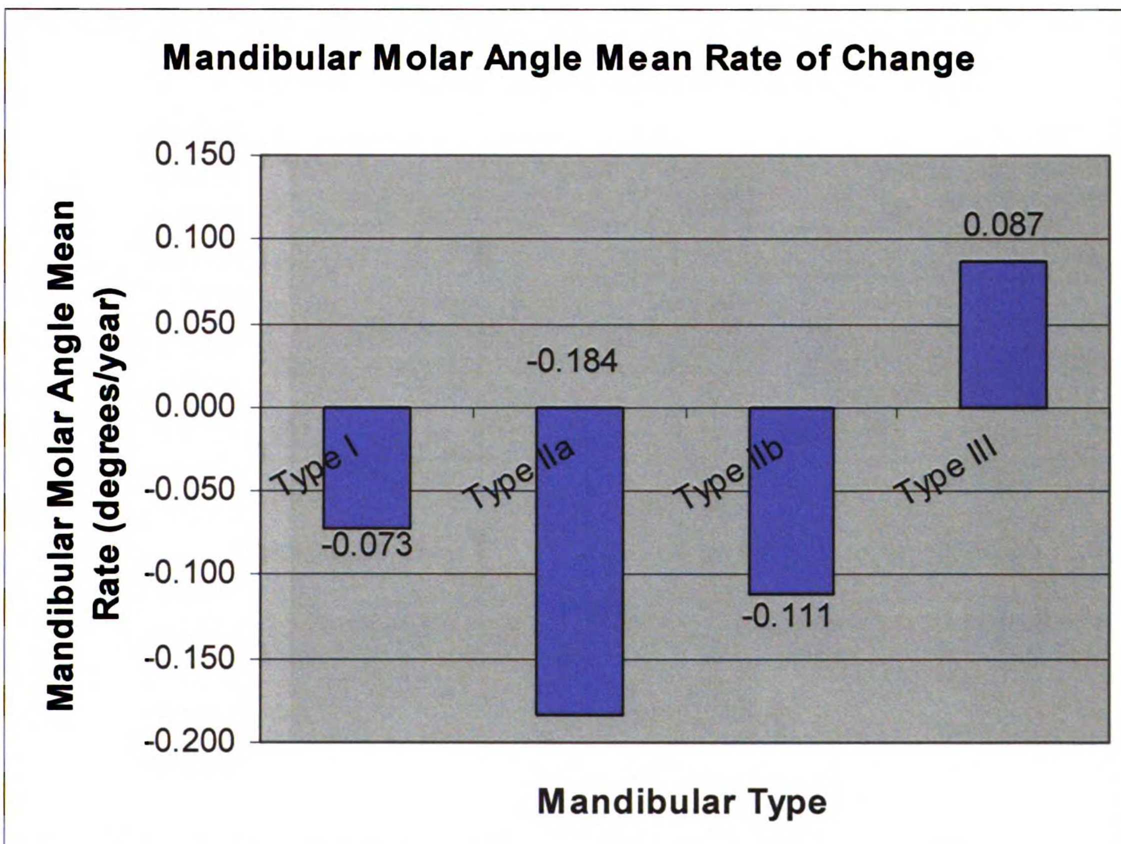

Figure 36: Mean rate of change of mandibular molar plane angle

Table 23: Mean rate of change of maxillary molar plane angle (degrees/year)

Type	Mean	S.D.	Variance	Minimum	Maximum	N
I	0.265	1.158	1.340	-2.932	3.750	26
IIa	-0.368	0.877	0.769	-1.739	0.715	9
IIb	1.923	3.351	11.232	-0.525	7.763	5
III	0.296	1.212	1.470	-1.674	2.007	7

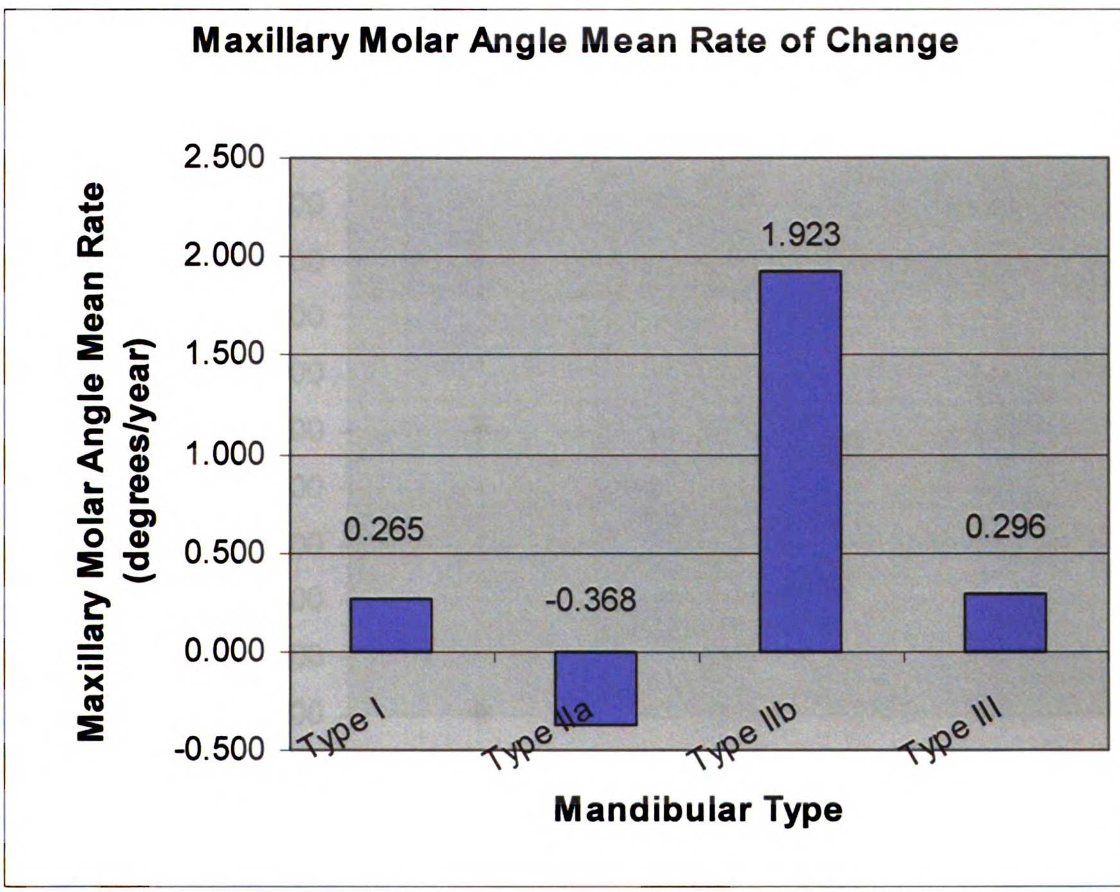

Figure 37: Mean rate of change of maxillary molar plane angle

Table 24: Mean rate of change of piriform plane angle (degrees/year)

Type	Mean	S.D.	Variance	Minimum	Maximum	N
I	0.701	2.115	4.475	-2.707	8.161	26
IIa	-1.034	3.868	14.962	-10.102	4.507	9
IIb	-0.605	0.640	0.410	-1.326	0.016	5
III	-0.766	6.180	38.187	-14.233	3.684	7

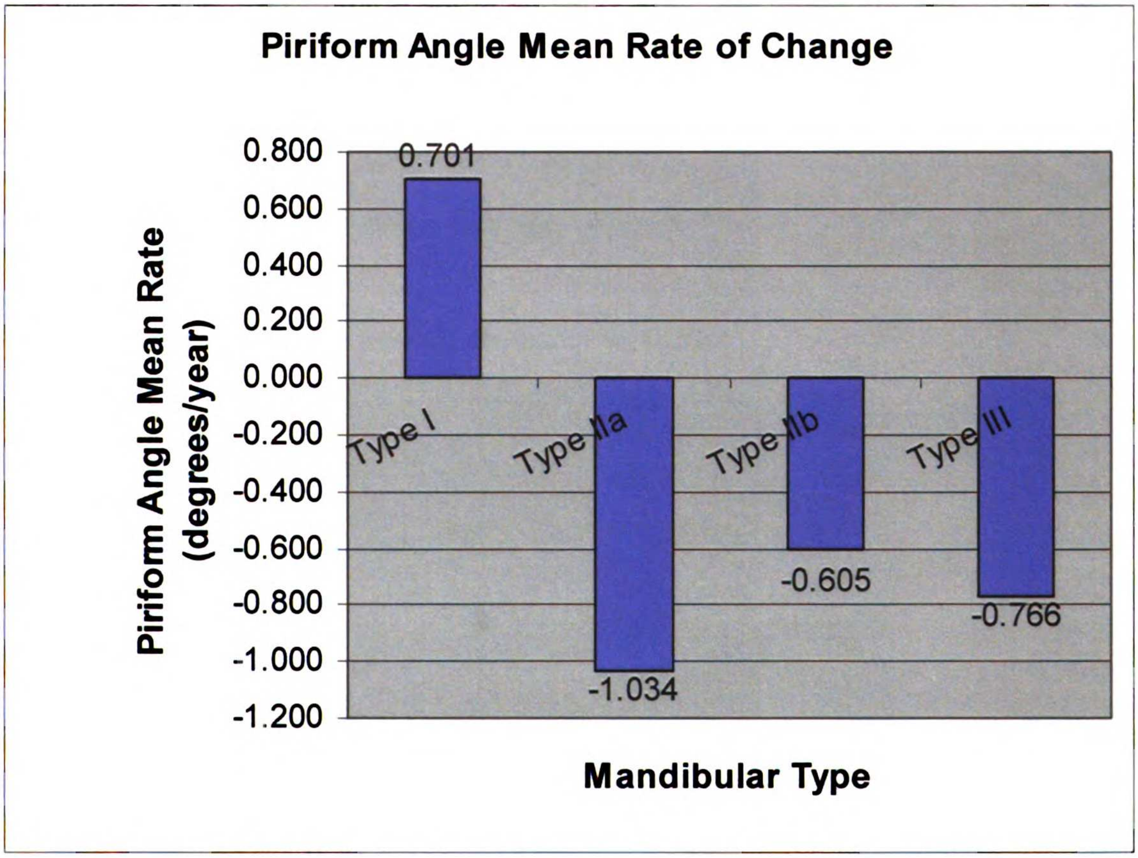

Figure 38: Mean rate of change of piriform plane angle

INDIVIDUAL RATE OF CHANGE BY TYPE

Figures 39-62 are histograms showing the individual mean rates of change for each subject for each measurement, split by mandibular type. These graphs demonstrate the range of values in rates within each type, such that most of the values are close to zero and then there are several outliers that deviate from zero either positively or negatively. Of note, the outliers within each mandibular type are often the same subjects from one measurement to the next.

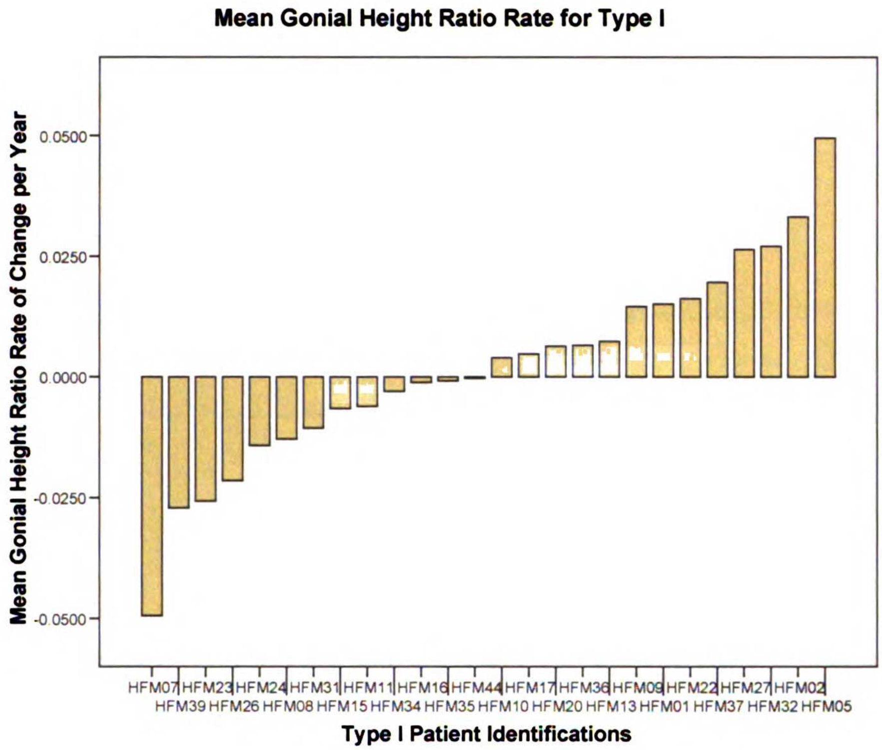

Figure 39: Mean gonial height ratio rate for type I subjects

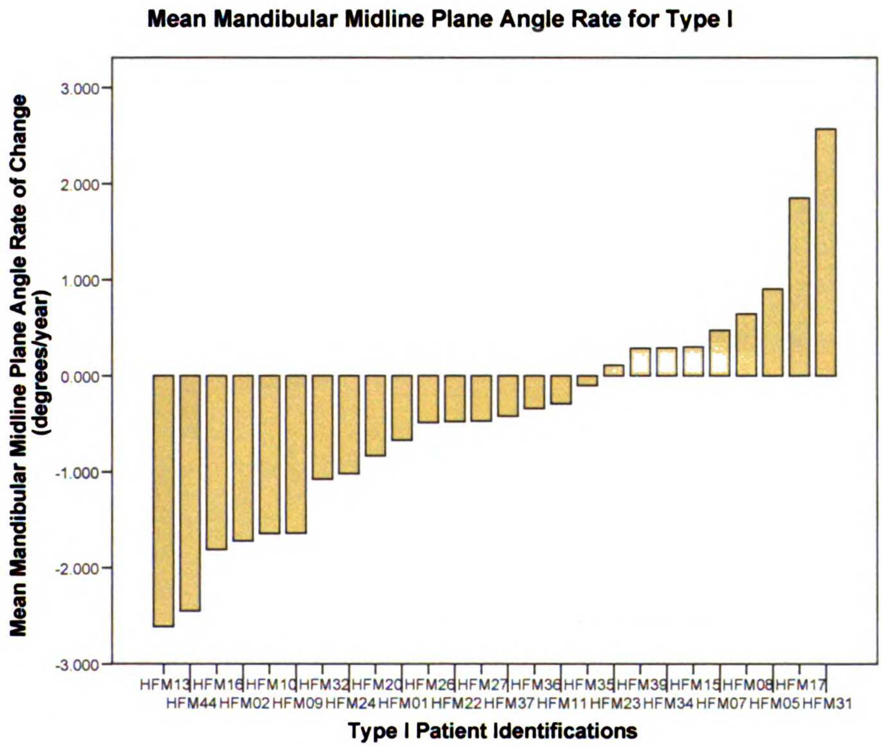

Figure 40: Mean mandibular midline plane angle rate for type I subjects

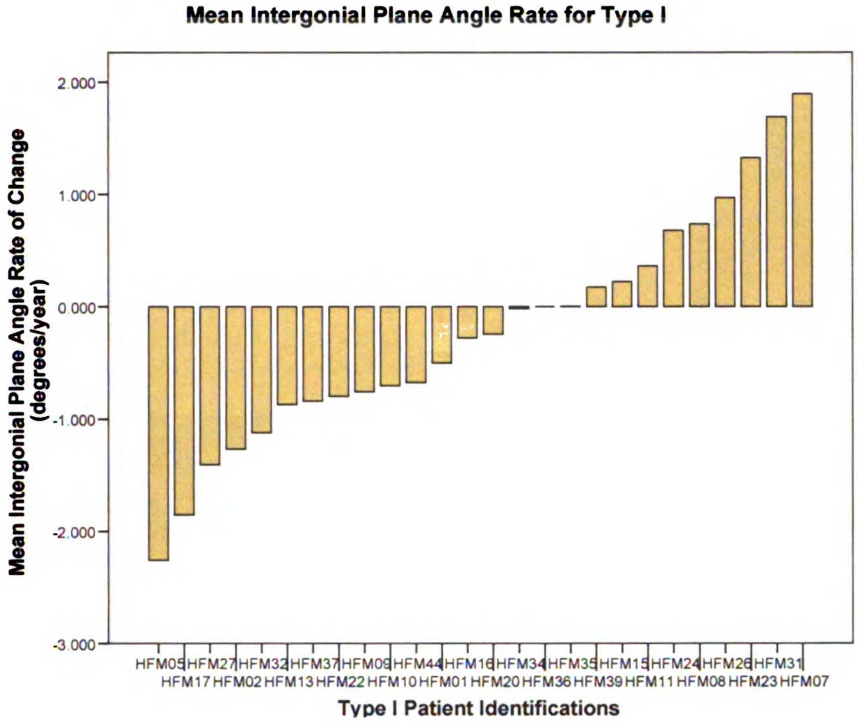

Figure 41: Mean intergonial plane angle rate for type I subjects

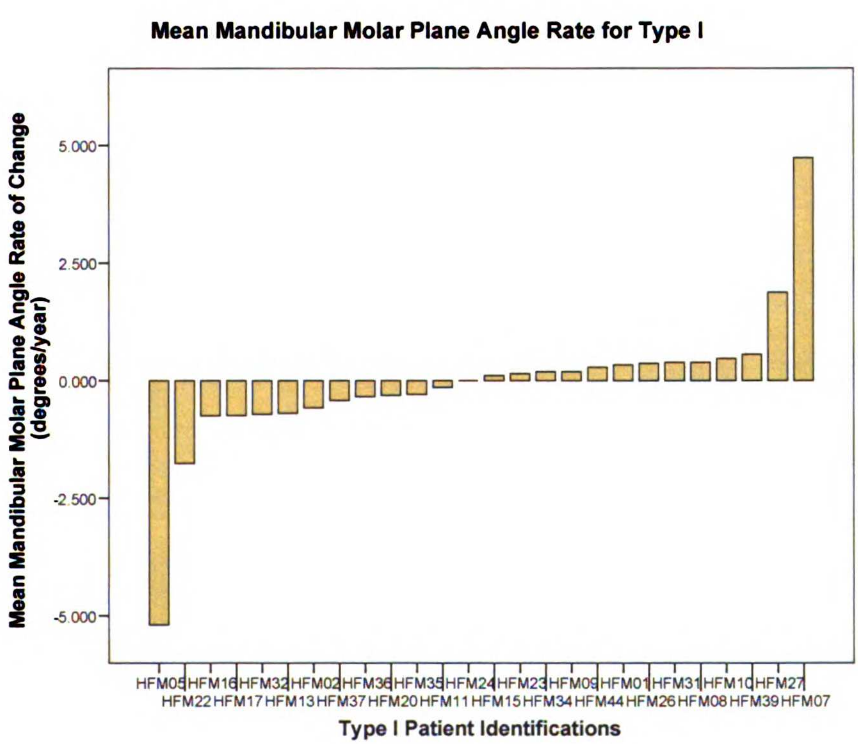

Figure 42: Mean mandibular molar plane angle rate for type I subjects

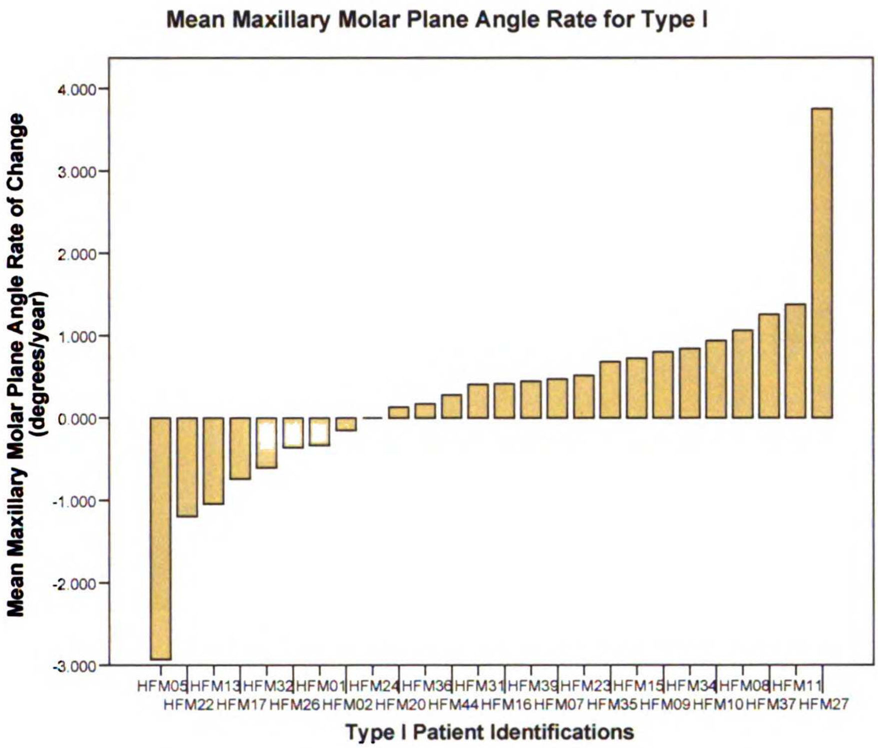

Figure 43: Mean maxillary molar plane angle rate for type I subjects

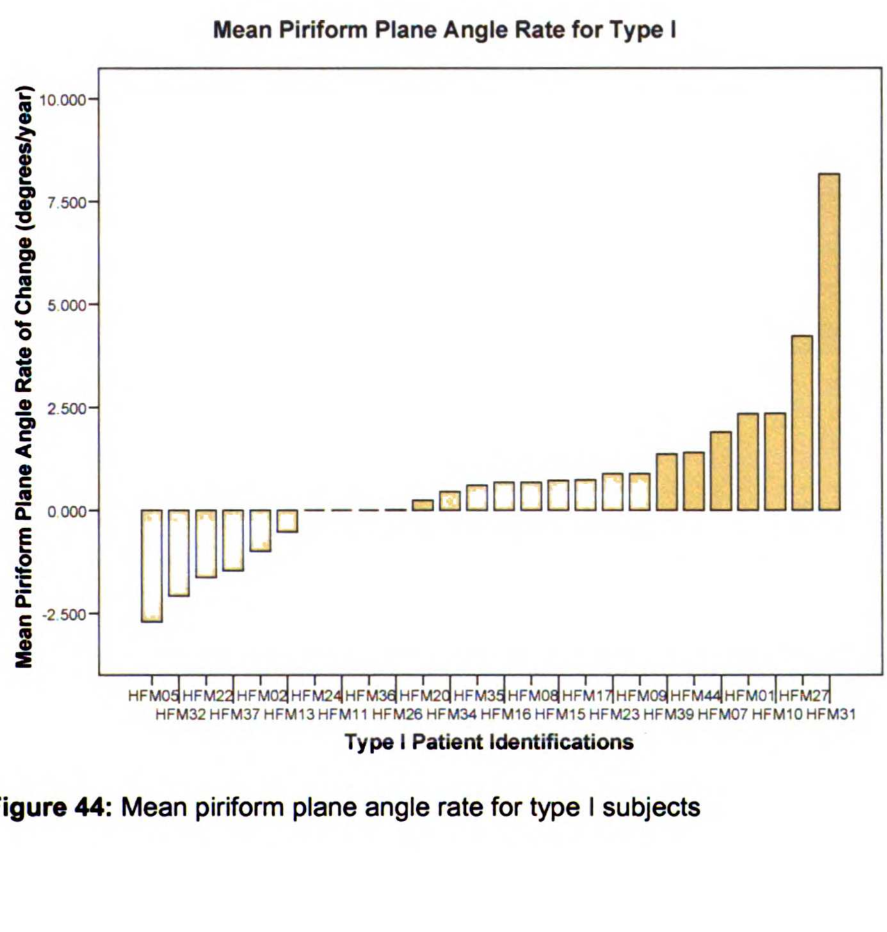

Figure 44: Mean piriform plane angle rate for type I subjects

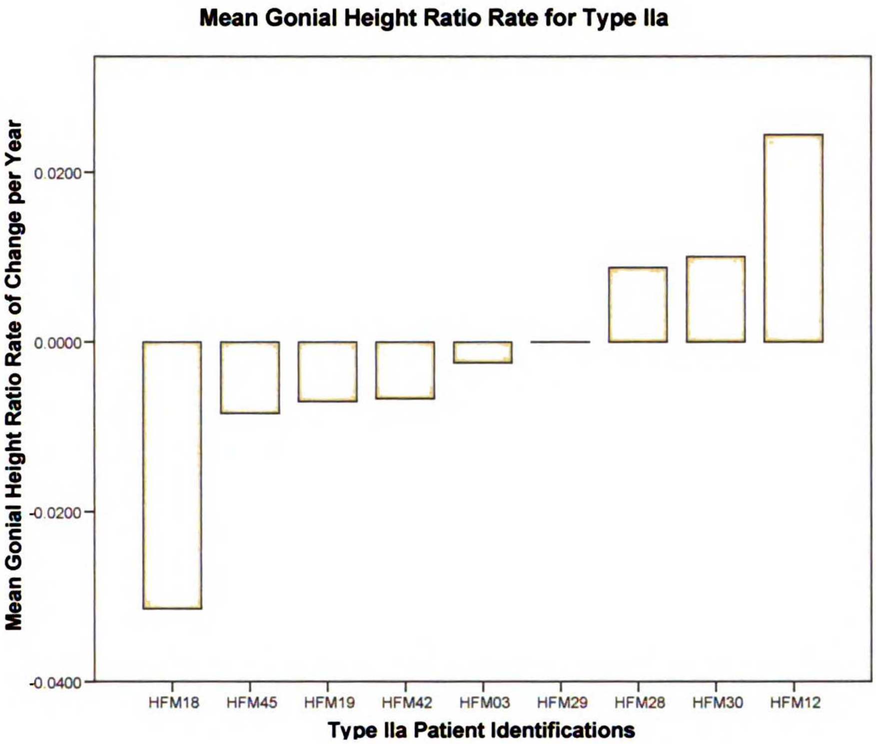

Figure 45: Mean gonial height ratio rate for type IIa subjects

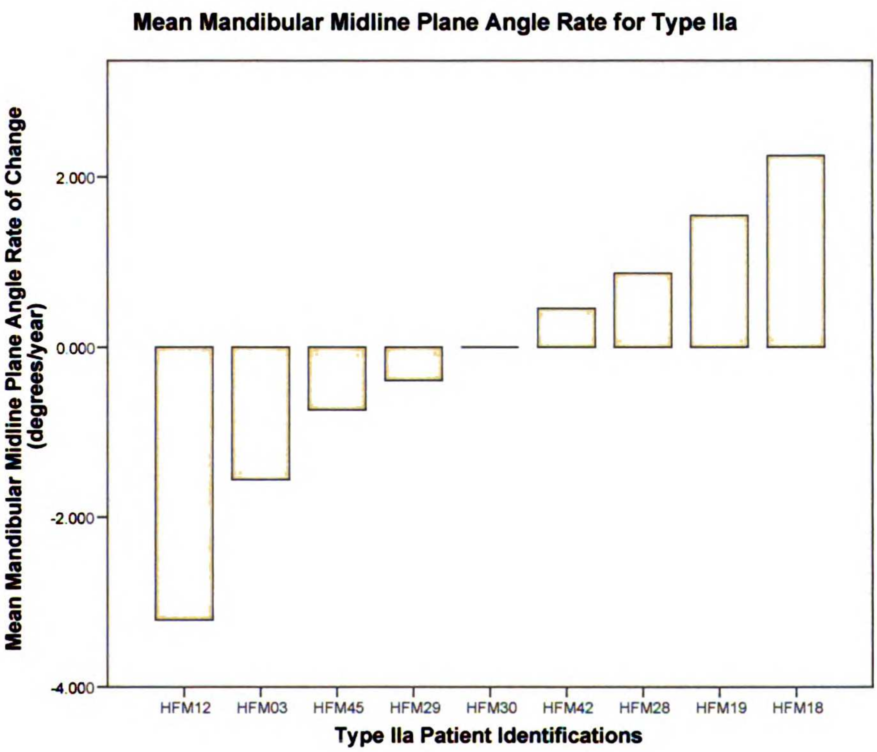

Figure 46: Mean mandibular molar plane angle rate for type IIa subjects

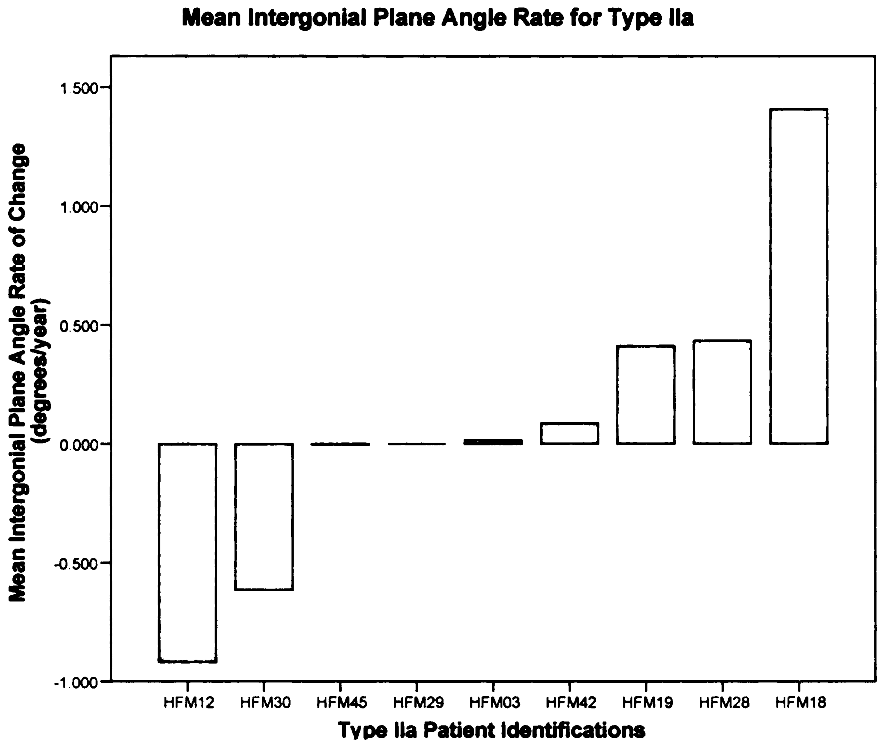

Figure 47: Mean intergonial plane angle rate for type IIa subjects

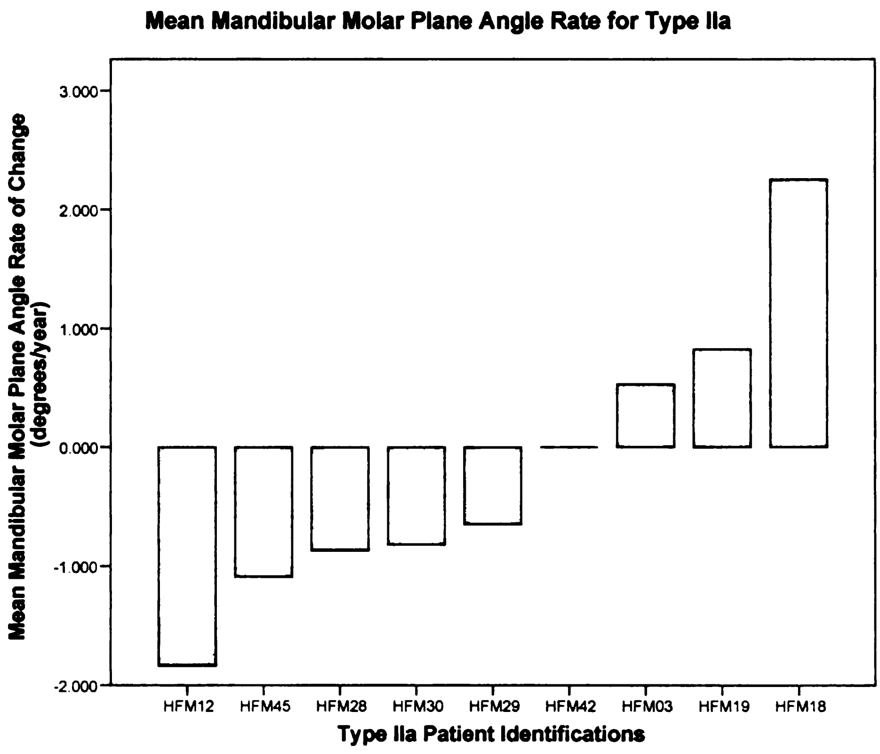

Figure 48: Mean mandibular molar plane angle rate for type IIa subjects

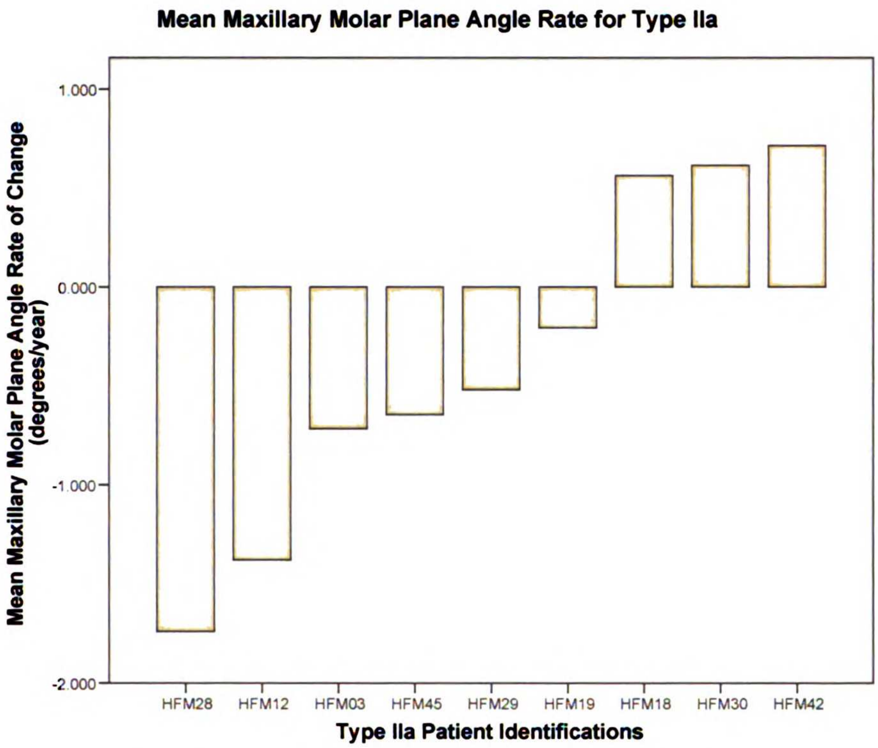

Figure 49: Mean maxillary molar plane angle rate for type IIa subjects

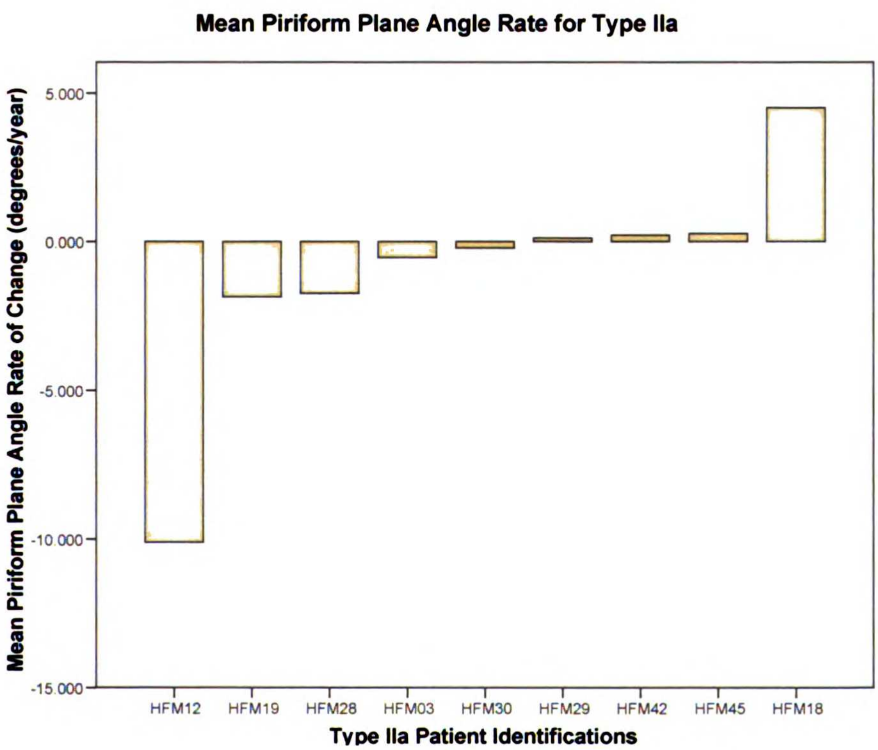

Figure 50: Mean piriform plane angle rate for type IIa subjects

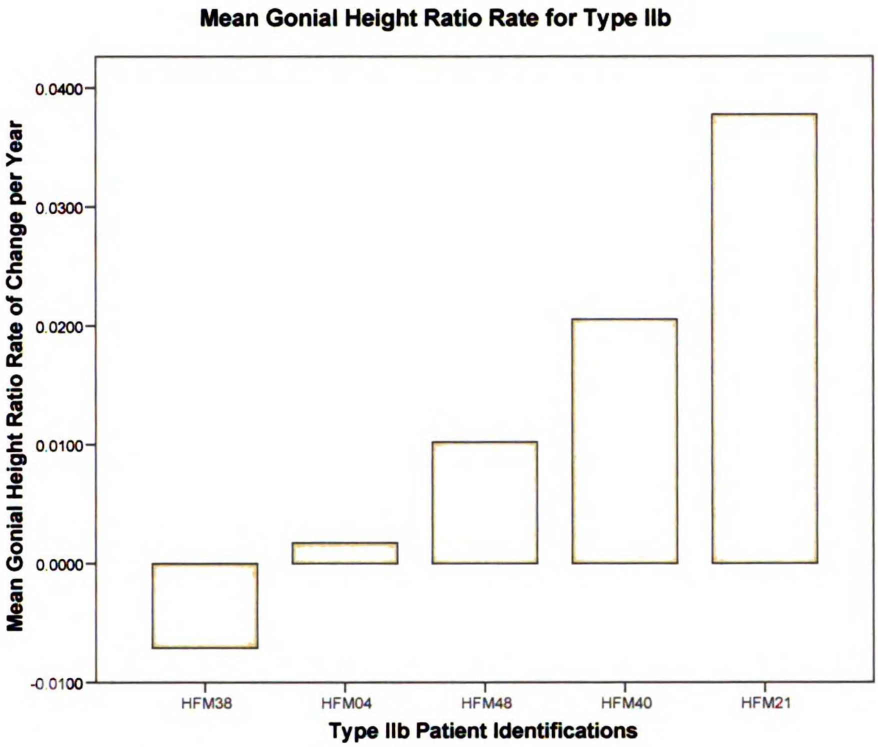

Figure 51: Mean gonial height ratio rate for type IIb subjects

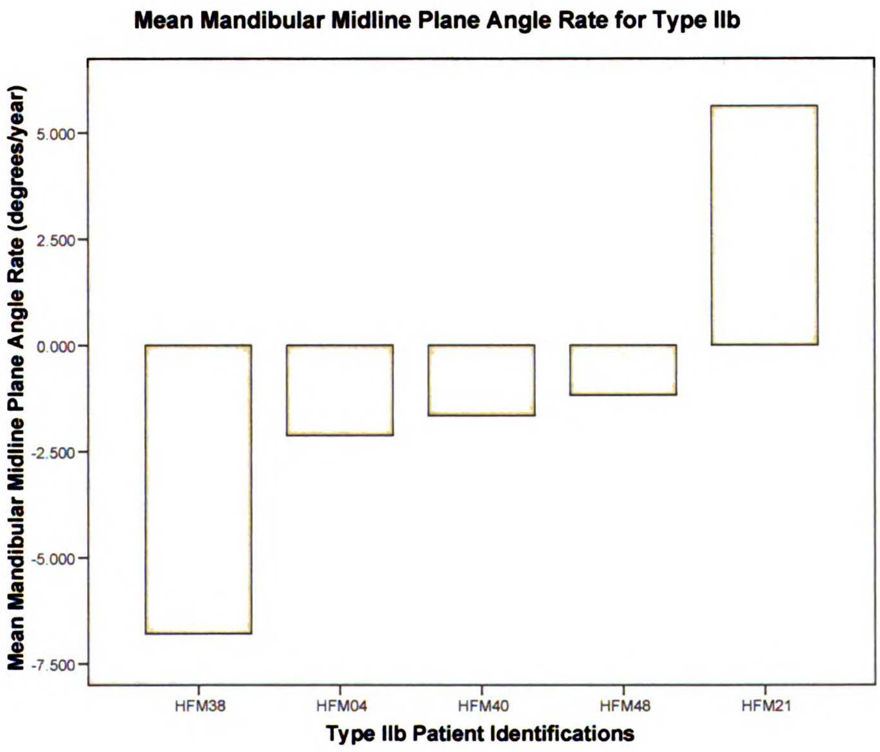

Figure 52: Mean mandibular midline plane angle rate for type IIb subjects

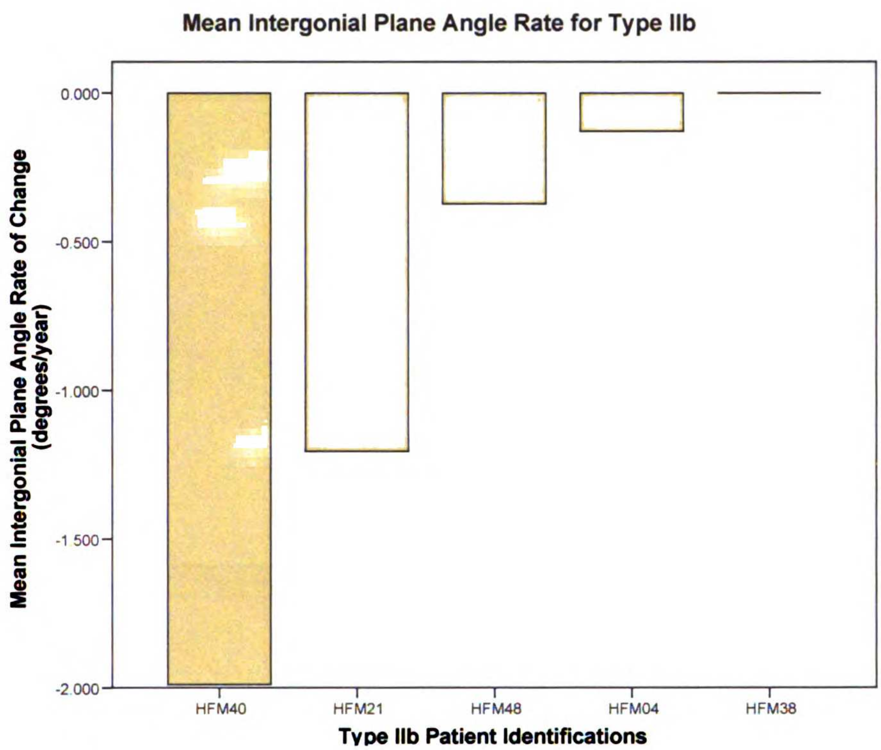

Figure 53: Mean intergonial plane angle rate for type IIb subjects

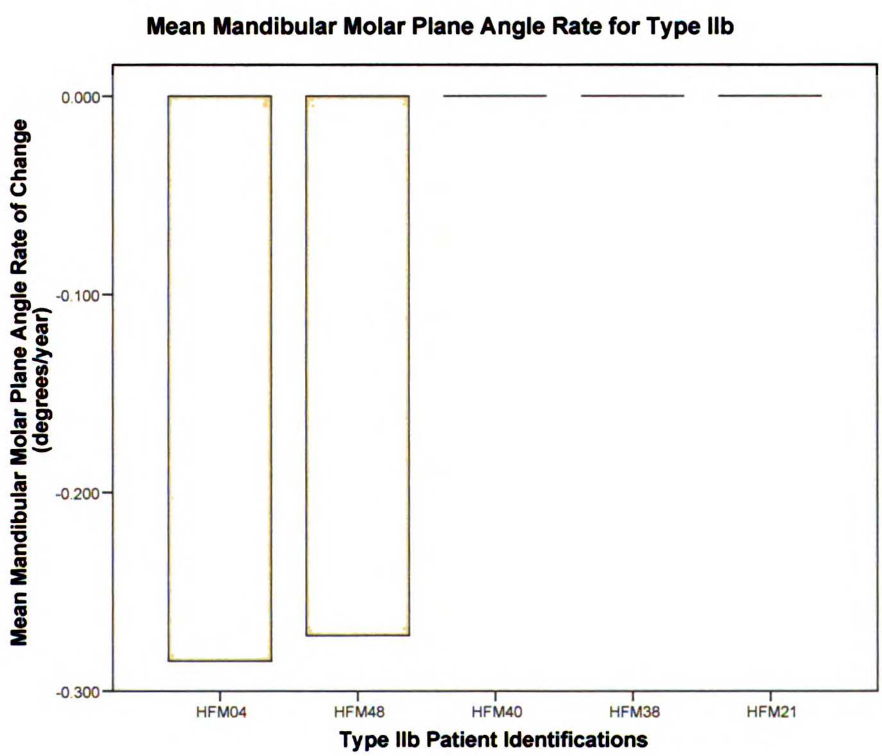

Figure 54: Mean mandibular molar plane angle rate for type IIb subjects

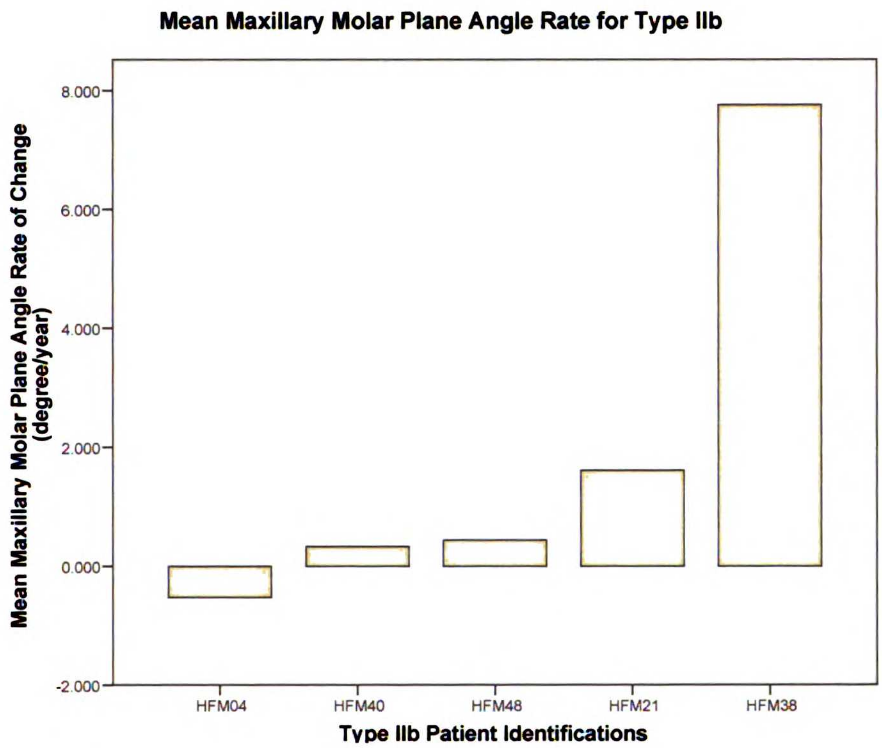

Figure 55: Mean maxillary molar plane angle rate for type IIb subjects

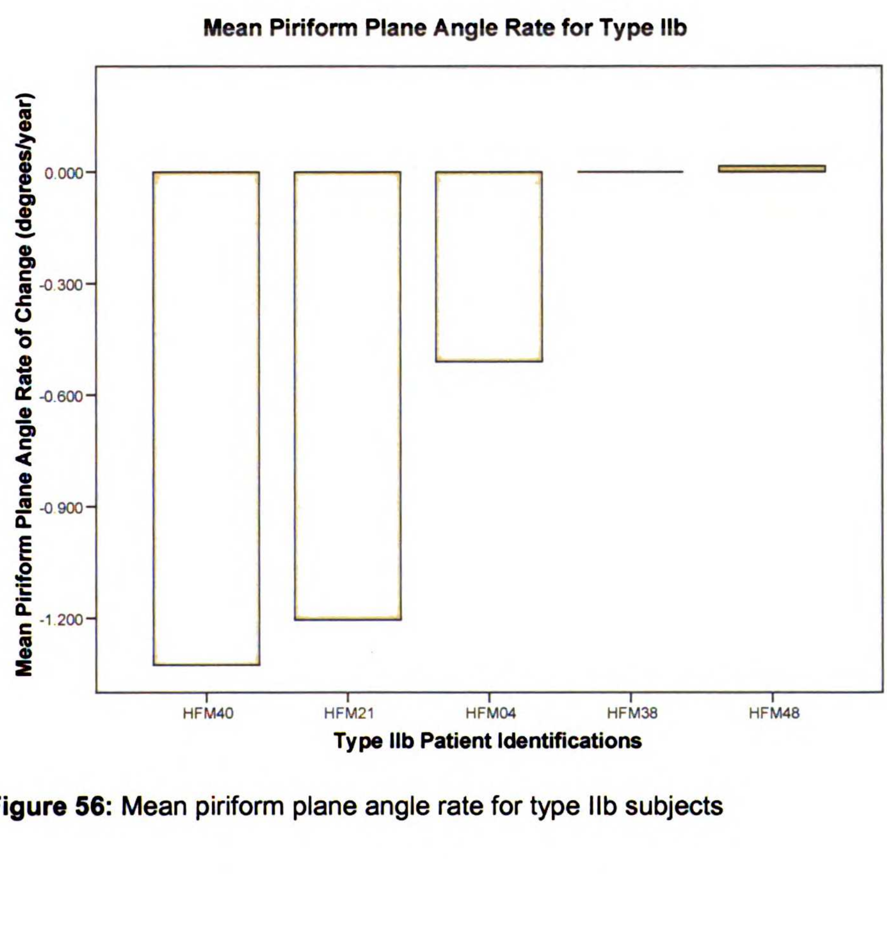

Figure 56: Mean piriform plane angle rate for type IIb subjects

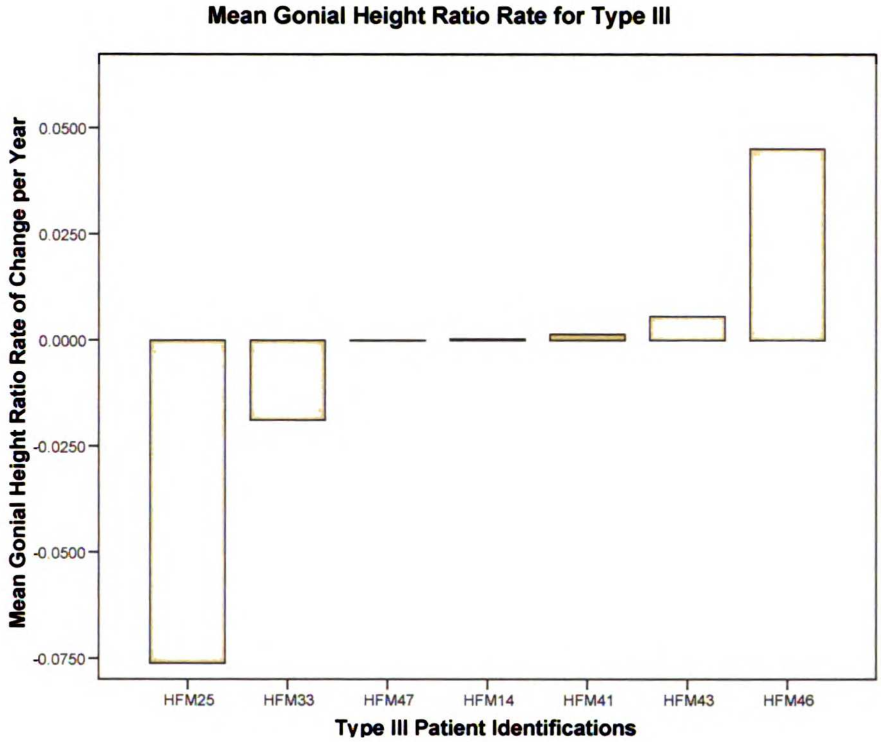

Figure 57: Mean gonial height ratio rate for type III subjects

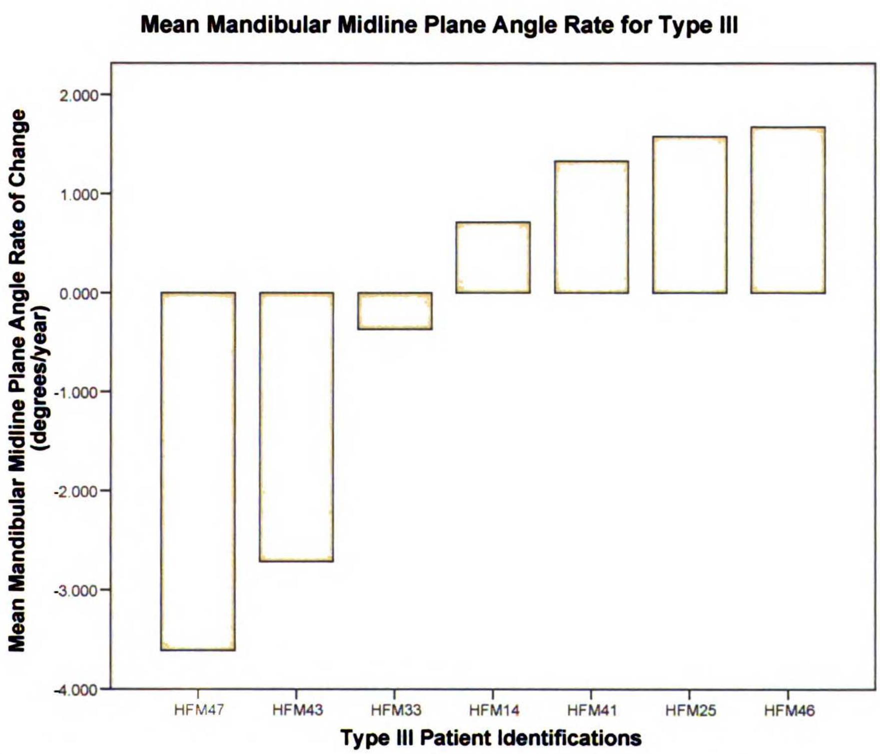

Figure 58: Mean mandibular midline plane angle rate for type III subjects

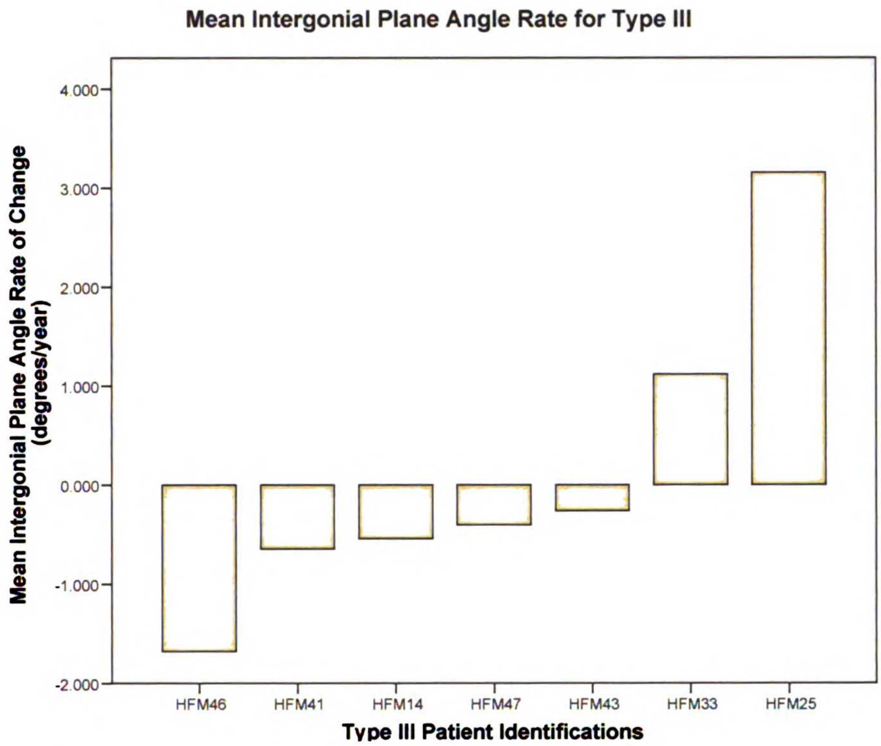

Figure 59: Mean intergonial plane angle rate for type III subjects

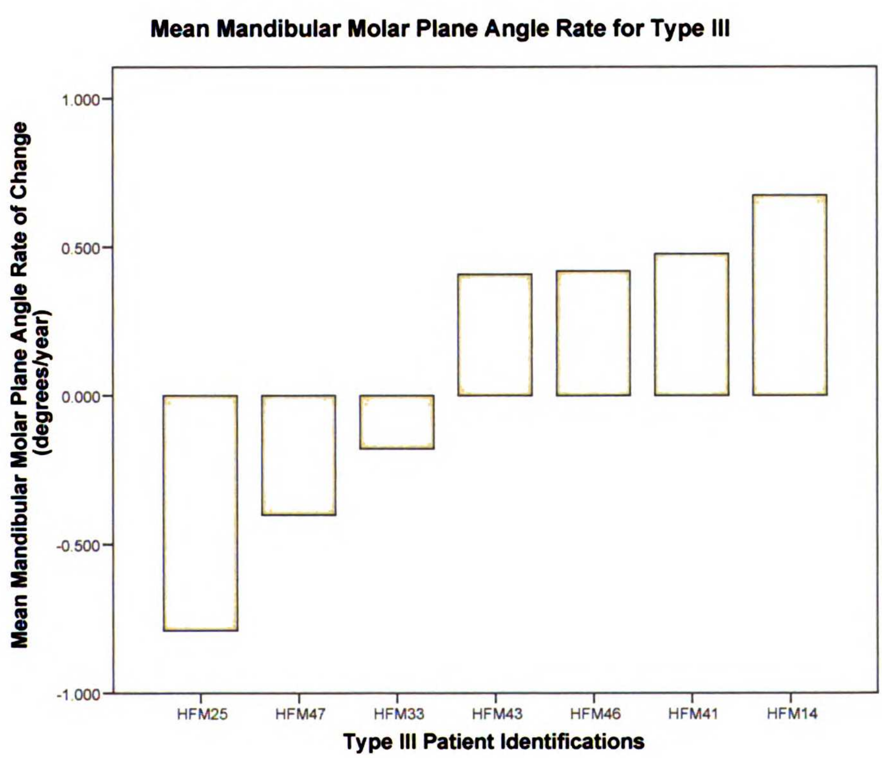

Figure 60: Mean mandibular molar plane angle rate for type III subjects

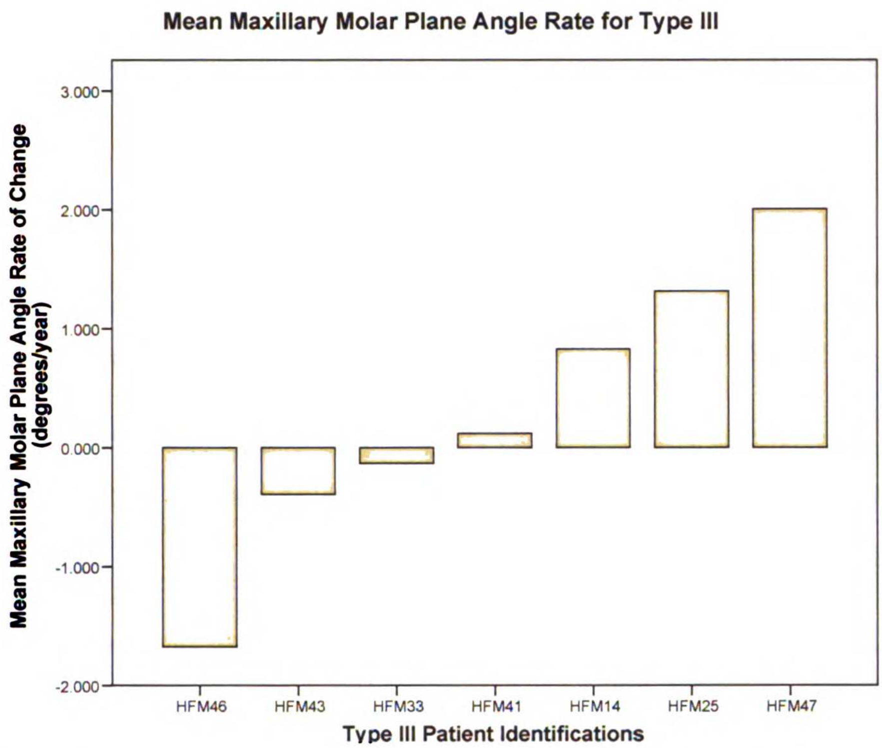

Figure 61: Mean maxillary molar plane angle rate for type III subjects

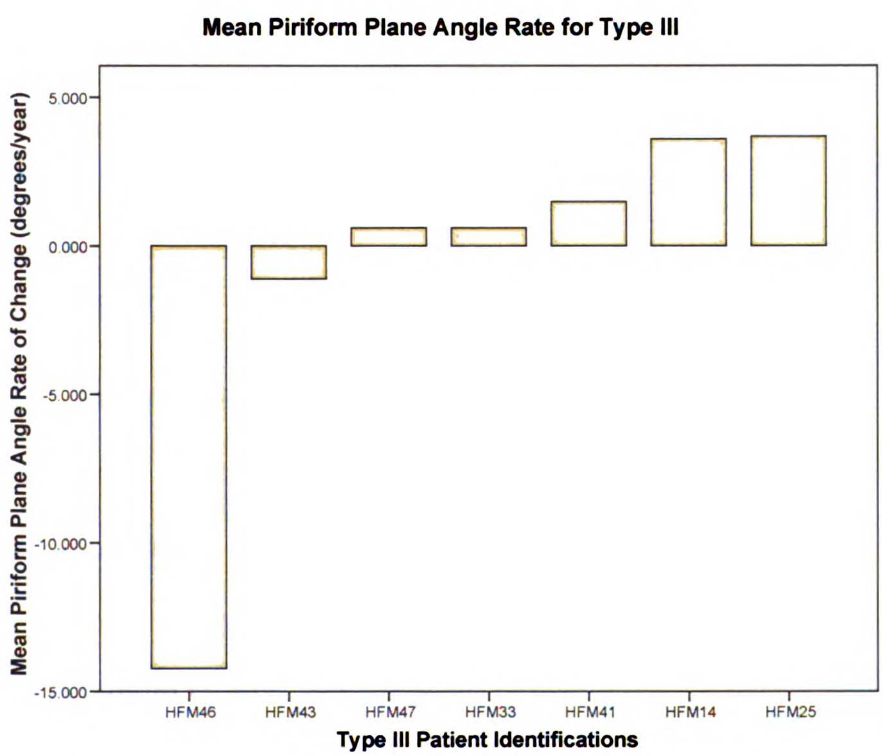

Figure 62: Mean piriform plane angle rate for type III subjects

DISCUSSION

REPEATABILITY ANALYSIS

The repeatability analysis demonstrated moderate to strong correlations ($0.75 < \rho_c < 0.95$) for all measurements except affected gonial height ($\rho_c = 0.36$). This suggests that it is difficult to precisely and accurately identify the location of the affected gonial angle point. The affected gonial angle point is based on the anomalous structure of the deformed mandibular side where the ramus condyle unit appears to join the mandibular body. In this study, the point is identified by the intersection of tangents along the mandibular ramus and body, and these tangents are often not perfectly repeatable due to the unusual contours of the affected skeletal structures. Therefore, the conclusions of this study will be based less on measurements that include the affected gonial point, including the gonial height ratio and the intergonial plane angle.

ASYMMETRY BY MANDIBULAR TYPE

Hemifacial microsomia is a complicated asymmetric deformity that has a wide range of skeletal and soft tissue involvement. Even within the same mandibular type, each patient can have a variable amount of deformity, such that no two patients look alike. Each group of mandibular deformity includes subjects with minimum to moderate amounts of asymmetry, and an angular measurement can deviate as much as 10 degrees from one subject to the next in the same group.

Both the overall averages and the regression analyses of each measurement for all time points and for just the 1st time points show that either type IIb or III had the most severe asymmetry, as expected by the diagnostic category. The measurements which demonstrated that type III was more asymmetric were the gonial height ratio and the intergonial angle, which were not as repeatable or reliable as the other measurements because they are based on the identification of the affected gonial angle point, the least reliable point. The group of subjects with mandibular type IIb demonstrated more asymmetry according to the measurements of midline mandibular plane angle, mandibular molar plane angle, maxillary molar plane angle, and piriform plane angle, which demonstrated more repeatable identification. There were statistically significant differences for several of the measurements between either type IIb or III and one or several of the other groups.

It may seem surprising that subjects with a type IIb mandibular deformity demonstrate more asymmetry than those with type III. One explanation for this is the difference in the freedom of movement of the affected mandibular side based on the structures that are present in each type. In individuals with type IIb deformity the presence of some bony and soft tissue structures that may have attachments to the skull base or surrounding tissues, can restrict growth of affected side. On the other hand, in type III subjects the entire mandibular structure is not inhibited by bony articulations and can be carried forward by the surrounding soft tissues and muscles, thus improving the asymmetry, not by mandibular growth but by mandibular positioning.

RATE OF CHANGE OF ASYMMETRY BY MANDIBULAR TYPE

Our results do not resolve the controversy over whether the asymmetry increases or improves during growth. The question: does the affected side grow at the same or decreased rate as the contralateral side is still unanswered. Previous studies have shown conflicting evidence on this issue.

In this study, the mean rates of change of each measurement were, in general, just above or just below zero. This implies that on average, there was no significant increase or improvement of the asymmetry over time. This does not agree with either of the previously reported theories that the asymmetry worsens[7-11] or stays the same[1-6] throughout growth. Evaluating subjects individually in each of the four groups shows that the rate and direction of change in asymmetry will vary among individuals in the same group so that in some the asymmetry can become more marked and in some decrease.

The results from this study support the statement made by Rune *et al.* that there is no interindividual pattern of displacement of the jaws, suggesting that the relevance of general statements about articular growth in HFM may be questioned.[3-5] It can also be argued that the measurements analyzed in this study are not appropriate for assessing growth, but measure a combination of growth and mandibular displacement. Since all of these measurements are based on 2-D radiographs in which the structures are superimposed it is not possible to quantify volume changes of the bony components. Additionally, the ratios and angles measured in this study are influenced by rotational changes of subjects from one radiographic time point to the next. Therefore, the rates of change may not only reflect growth and positional changes, but also error introduced by varying head positions. Although this rotational effect was minimized by using the same cephalostat and radiology technician, it is unlikely to replicate the exact head position between time points.

LIMITATIONS OF THE STUDY

As with many retrospective clinical studies, several limitations were encountered. These limitations exist because the analyses were based on available patient data and not on standardized and controlled laboratory generated information.

The lowest number of subjects (n = 5) was found in the type IIb mandibular deformity group. This could have caused selection bias, and therefore, the statistical results may be misleading since they are not based on the same number of subjects in each group.

The variable nature of the HFM deformity leads to a range of asymmetry within each mandibular type; that is that not all type I subjects look the same just as not all type III subjects look the same. Therefore, grouping subjects based on their type of mandibular deformity may not accurately represent the degree of asymmetry of each subject. However, at this time there is no better way to categorize individuals with HFM.

The potential for future development of categories will rely on providing more accurate information on the growth sites of both the maxilla and mandible as well as determining how function influences growth and modeling. Does a smaller condyle infer that it has less growth potential, or that its rate of growth is less? Does an anteriorly placed condyle suggest it is loaded differently during function and impair its potential for change in rate of growth? Does the asymmetry with accompanying changes in muscles indicate that subjects will always function on the intact side, so that the more impaired side does not experience loading which could affect remodeling of the bone? Studies on muscle function suggest that type I patients can recruit their temporalis and masseter muscles relatively normally.[53] Does the extended corpus of the type III subjects have any potential to grow based on apposition and resorption of bone, or only remodel its shape? More information is needed on understanding the endochondral growth potential in the HFM patient, and methods to affect intramembranous bone growth in other regions of the mandible. Much of the present molecular studies of the condyle and bone provide some exciting potential approaches to rehabilitation and enhancing growth of bone.

Finally, this study is analyzing a 3-D problem using 2-D radiographs. This presents the inherent difficulty of being able to take accurate and precise measurements from 2-D films in which structures are superimposed on each other and dimensions are affected by film magnification and the subject's rotational position. The use of 3-D data generated from CT images may provide more accurate and precise information regarding longitudinal shape and size changes of the facial structures in patients with HFM.

CONCLUSIONS

Longitudinal retrospective analysis of PA cephalograms of 47 subjects with untreated HFM was performed to characterize growth and displacement of the mandible. The findings include:

1. Subjects with type IIb mandibular deformity demonstrated the most asymmetry based on measurements that were highly repeatable. This group may demonstrate more asymmetry compared to type III subjects because of growth constraints imposed by limitations in movements not present in type III individuals.
2. The mean rates of change of the measurements analyzed in this study were inconclusive in determining whether or not the asymmetry in HFM individuals increases, improves, or stays the same during growth. There was a wide range of change in each of the four groups with some individuals becoming more asymmetrical and others becoming less. There was a wide spectrum of expression of how the mandible changed using these 2-dimensional measures from a frontal full head x-ray. Thus previous studies can not be supported or refuted. Therefore, timing of surgical treatment of the maxillo-mandibular deformities in HFM patients must be determined based on an individual patient's clinical presentation.
3. Using 2-D radiographs to evaluate changes in HFM patients may not be adequate to quantify longitudinal growth and positional changes. The use of 3-D images and methods of 3-D superimposition is needed

to more accurately measure structural and positional changes in HFM patients. Further investigation using 3-D technology should be undertaken.

REFERENCES

1. Polley JW, Figueroa AA, Liou EJ, Cohen M. Longitudinal analysis of mandibular asymmetry in hemifacial microsomia. Plast Reconstr Surg 1997;99:328-339.

2. Posnick JC. Surgical correction of mandibular hypoplasia in hemifacial microsomia: a personal perspective. J Oral Maxillofac Surg 1998;56:639-650.

3. Rune B, Sarnas KV, Selvik G, Jacobsson S. Roentgen stereometry with the aid of metallic implants in hemifacial microsomia. Am J Orthod 1983;84:231-247.

4. Rune B, Sarnas KV, Selvik G, Jacobsson S. Roentgen stereometry in the study of craniofacial anomalies--the state of the art in Sweden. Br J Orthod 1986;13:151-157.

5. Rune B, Selvik G, Sarnas KV, Jacobsson S. Growth in hemifacial microsomia studied with the aid of roentgen stereophotogrammetry and metallic implants. Cleft Palate J 1981;18:128-146.

6. Sarnas KV, Rune B, Aberg M. Maxillary and mandibular displacement in hemifacial microsomia: a longitudinal Roentgen stereometric study of 21 patients with the aid of metallic implants. Cleft Palate Craniofac J 2004;41:290-303.

7. Converse JM, Coccaro PJ, Wood-Smith D. Hemifacial microsomia (dysostosis otomandibularis). Fortschr Kiefer Gesichtschir 1974;18:53-63.

8. Kaban LB, Moses MH, Mulliken JB. Surgical correction of hemifacial microsomia in the growing child. Plast Reconstr Surg 1988;82:9-19.

9. Kearns GJ, Padwa BL, Mulliken JB, Kaban LB. Progression of facial asymmetry in hemifacial microsomia. Plast Reconstr Surg 2000;105:492-498.

10. Mulliken JB, Kaban LB. Analysis and treatment of hemifacial microsomia in childhood. Clin Plast Surg 1987;14:91-100.

11. Murray JE, Kaban LB, Mulliken JB. Analysis and treatment of hemifacial microsomia. Plast Reconstr Surg 1984;74:186-199.

12. Grabb WC. The first and second branchial arch syndrome. Plast Reconstr Surg 1965;36:485-508.

13. Poswillo D. The pathogenesis of the first and second branchial arch syndrome. Oral Surg Oral Med Oral Pathol 1973;35:302-328.

14. Horgan JE, Padwa BL, LaBrie RA, Mulliken JB. OMENS-Plus: analysis of craniofacial and extracraniofacial anomalies in hemifacial microsomia. Cleft Palate Craniofac J 1995;32:405-412.

15. Cousley RR, Calvert ML. Current concepts in the understanding and management of hemifacial microsomia. Br J Plast Surg 1997;50:536-551.

16. Cousley RR, Wilson DJ. Hemifacial microsomia: developmental consequence of perturbation of the auriculofacial cartilage model? Am J Med Genet 1992;42:461-466.

17. Soltan HC, Holmes LB. Familial occurrence of malformations possibly attributable to vascular abnormalities. J Pediatr 1986;108:112-114.

18. Johnston MC, Bronsky PT. Animal models for human craniofacial malformations. J Craniofac Genet Dev Biol 1991;11:277-291.

19. David DJ, Mahatumarat C, Cooter RD. Hemifacial microsomia: a multisystem classification. Plast Reconstr Surg 1987;80:525-535.

20. Vento AR, LaBrie RA, Mulliken JB. The O.M.E.N.S. classification of hemifacial microsomia. Cleft Palate Craniofac J 1991;28:68-76; discussion 77.

21. Pruzansky S. Not all dwarfed mandibles are alike. Birth Defects 1969;1:120.

22. Kaban LB, Mulliken JB, Murray JE. Three-dimensional approach to analysis and treatment of hemifacial microsomia. Cleft Palate J 1981;18:90-99.

23. Vargervik K, Kaban LB. Hemifacial microsomia - diagnosis and management. In: Bell W, editor. Modern practice in orthognathic and reconstructive surgery. Philadelphia: W.B. Saunders; 1992. p. 1533-1559.

24. Harvold EP, Vargervik K, Chierici G. Treatment of hemifacial microsomia. New York: A.R. Liss; 1983.

25. Vargervik K. Mandibular malformations: growth characteristics and management in hemifacial microsomia and Nager syndrome. Acta Odontol Scand 1998;56:331-338.

26. Kaban LB, Troulis MJ. Pediatric oral and maxillofacial surgery. Philadelphia: Saunders; 2004.

27. Hall BK, Herring SW. Paralysis and growth of the musculoskeletal system in the embryonic chick. J Morphol 1990;206:45-56.

28. Herring SW, Lakars TC. Craniofacial development in the absence of muscle contraction. J Craniofac Genet Dev Biol 1982;1:341-357.

29. Baume LJ. Embryogenesis of the human temporomandibular joint. Science 1962;138:904-905.

30. Baume LJ. Ontogenesis of the human temporomandibular joint. I. Development of the condyles. J Dent Res 1962;41:1327-1339.

31. Harvold EP. The theoretical basis for the treatment of hemifacial microsomia. In: Harvold EP, Vargervik K, Chierici G, editors. Treatment of hemifacial microsomia. New York: A.R. Liss; 1983. p. 1-37.

32. Hiraba K, Hibino K, Hiranuma K, Negoro T. EMG activities of two heads of the human lateral pterygoid muscle in relation to mandibular condyle movement and biting force. J Neurophysiol 2000;83:2120-2137.

33. Hylander WL, Bays R. An in vivo strain-gauge analysis of the squamosal-dentary joint reaction force during mastication and incisal biting in Macaca mulatta and Macaca fascicularis. Arch Oral Biol 1979;24:689-697.

34. Marks L, Teng S, Artun J, Herring S. Reaction strains on the condylar neck during mastication and maximum muscle stimulation in different condylar positions: an experimental study in the miniature pig. J Dent Res 1997;76:1412-1420.

35. Wood WW, Takada K, Hannam AG. The electromyographic activity of the inferior part of the human lateral pterygoid muscle during clenching and chewing. Arch Oral Biol 1986;31:245-253.

36. Storey A. Temporomandibular joint receptors. In: Anderson DJ, Matthews B, editors. Mastication : proceedings of a Symposium on the Clinical and Physiological Aspects of Mastication held at the Medical School, University of Bristol on 14-16 April 1975. Bristol: John Wright and Sons; 1976. p. 50.

37. Shen G, Darendeliler MA. The adaptive remodeling of condylar cartilage---a transition from chondrogenesis to osteogenesis. J Dent Res 2005;84:691-699.

38. Habib H, Hatta T, Udagawa J, Zhang L, Yoshimura Y, Otani H. Fetal jaw movement affects condylar cartilage development. J Dent Res 2005;84:474-479.

39. Bouvier M, Hylander WL. The effect of dietary consistency on morphology of the mandibular condylar cartilage in young Macaques (Macaca mulatta) Factors

and mechanisms influencing bone growth : proceedings of the international conference held at the University of California, Center for the Health Sciences, Los Angeles, California, January 5-7, 1982. New York: A.R. Liss; 1982. p. pp. 569-579.

40. Petrovic A, Stutzmann J, Oudet C. Control processes in postnatal growth of condylar cartilage of the mandible. In: McNamara JJ, editor. Monograph No. 4, Craniofacial Groth Series. Ann Arbor: University of Michigan; 1975. p. pp.101-153.

41. Copray JC, Jansen HW, Duterloo HS. Growth of the mandibular condylar cartilage of the rat in serum-free organ culture. Arch Oral Biol 1983;28:967-974.

42. Strauss PG, Closs EI, Schmidt J, Erfle V. Gene expression during osteogenic differentiation in mandibular condyles in vitro. J Cell Biol 1990;110:1369-1378.

43. Copray JC, Jansen HW, Duterloo HS. Growth and growth pressure of mandibular condylar and some primary cartilages of the rat in vitro. Am J Orthod Dentofacial Orthop 1986;90:19-28.

44. Pirttiniemi P, Kantomaa T. Electrical stimulation of masseter muscles maintains condylar cartilage in long-term organ culture. J Dent Res 1996;75:1365-1371.

45. Watahiki J, Yamaguchi T, Irie T, Nakano H, Maki K, Tachikawa T. Gene expression profiling of mouse condylar cartilage during mastication by means of laser microdissection and cDNA array. J Dent Res 2004;83:245-249.

46. Visnapuu V, Peltomaki T, Ronning O, Vahlberg T, Helenius H. Growth hormone and insulin-like growth factor I receptors in the temporomandibular joint of the rat. J Dent Res 2001;80:1903-1907.

47. Rabie AB, Tang GH, Xiong H, Hagg U. PTHrP regulates chondrocyte maturation in condylar cartilage. J Dent Res 2003;82:627-631.

48. Tang GH, Rabie AB. Runx2 regulates endochondral ossification in condyle during mandibular advancement. J Dent Res 2005;84:166-171.

49. Dohmoto A, Shimizu K, Asada Y, Maeda T. Quantitative trait loci on chromosomes 10 and 11 influencing mandible size of SMXA RI mouse strains. J Dent Res 2002;81:501-504.

50. Yamaguchi T, Maki K, Shibasaki Y. Growth hormone receptor gene variant and mandibular height in the normal Japanese population. Am J Orthod Dentofacial Orthop 2001;119:650-653.

51. Zhou J, Lu Y, Gao XH, Chen YC, Lu JJ, Bai YX et al. The growth hormone receptor gene is associated with mandibular height in a Chinese population. J Dent Res 2005;84:1052-1056.

52. Kaban LB, Padwa BL, Mulliken JB. Surgical correction of mandibular hypoplasia in hemifacial microsomia: the case for treatment in early childhood. J Oral Maxillofac Surg 1998;56:628-638.

53. Vargervik K, Miller AJ. Neuromuscular patterns in hemifacial microsomia. Am J Orthod 1984;86:33-42.

54. Teng S, Herring SW. Anatomic and directional variation in the mechanical properties of the mandibular condyle in pigs. J Dent Res 1996;75:1842-1850.

55. Lakars TC, Herring SW. Ontogeny of oral function in hamsters (Mesocricetus auratus). J Morphol 1980;165:237-254.

56. Herring S. Development of functional interactions between skeletal and muscular systems. In: Hall BK, editor. Differentiation and Morphogenesis of Bone. Boca Raton, FL: CRC Press; 1994. p. pp. 165-191.

57. Bishara SE, Burkey PS, Kharouf JG. Dental and facial asymmetries: a review. Angle Orthod 1994;64:89-98.

58. Lee Y-P. Postnatal development of the bony orbit: a study on PA cephalograms. Oral Biology. San Francisco: University of California San Francisco; 1997: p. 73.

59. Harvold EP. A roentgen study of the postnatal morphogenesis of the facial skeleton in cleft palate. Anatomical Institute. Oslo: University of Oslo; 1954.

60. Ishiguro K, Krogman WM, Mazaheri M, Harding RL. A longitudinal study of morphological craniofacial patterns via P-A x-ray headfilms in cleft patients from birth to six years of age. Cleft Palate J 1976;13:104-126.

61. Athanasiou A, Van der Meij A. Postero-anterior (frontal) cephalometry. In: Athanasiou A, editor. Orthodontic cephalometry. London: Mosby-Wolfe; 1995. p. 141-162.

62. Svanholt P, Solow B. Assessment of midline discrepancies on the posteroanterior cephalometric radiograph. Trans Eur Orthod Soc 1977;25:261-268.

63. Vargervik K, Ousterhout DK, Farias M. Factors affecting long-term results in hemifacial microsomia. Cleft Palate J 1986;23 Suppl 1:53-68.

64. Ousterhout DK, Vargervik K. Surgical treatment of the jaw deformities in hemifacial microsomia. Aust N Z J Surg 1987;57:77-87.

65. Ono I, Ohura T, Narumi E, Kawashima K, Matsuno I, Nakamura S et al. Three-dimensional analysis of craniofacial bones using three-dimensional computer tomography. J Craniomaxillofac Surg 1992;20:49-60.

66. Santos DT, Miyazaki O, Cavalcanti MG. Clinical-embryological and radiological correlations of oculo-auriculo-vertebral spectrum using 3D-CT. Dentomaxillofac Radiol 2003;32:8-14.

67. Troulis MJ, Everett P, Seldin EB, Kikinis R, Kaban LB. Development of a three-dimensional treatment planning system based on computed tomographic data. Int J Oral Maxillofac Surg 2002;31:349-357.

68. Whyte AM, Hourihan MD, Earley MJ, Sugar A. Radiological assessment of hemifacial microsomia by three-dimensional computed tomography. Dentomaxillofac Radiol 1990;19:119-125.

69. Maki K, Miller AJ, Okano T, Hatcher D, Yamaguchi T, Kobayashi H et al. Cortical bone mineral density in asymmetrical mandibles: a three-dimensional quantitative computed tomography study. Eur J Orthod 2001;23:217-232.

70. Vargervik K. Sequence and timing of treatment phases in hemifacial microsomia. In: Harvold EP, Vargervik K, Chierici G, editors. Treatment of hemifacial microsomia. New York: A.R. Liss; 1983. p. 133-137.

71. Converse JM, Coccaro PJ, Becker M, Wood-Smith D. On hemifacial microsomia. The first and second branchial arch syndrome. Plast Reconstr Surg 1973;51:268-279.

72. Chierici G. Radiologic assessment of facial asymmetry. In: Harvold EP, Vargervik K, Chierici G, editors. Treatment of hemifacial microsomia. New York: A.R. Liss, Inc; 1983. p. 57-87.

73. Urbaniak G, Plous S. Research randomizer [retrieved from randomizer.org]; 1997-2006.

74. Baumrind S, Moffitt F, Curry S. Three-dimensional x-ray stereometry from paired coplanar images: a progress report. Am J Orthod 1983;84:292-312.

75. Houston W. The analysis of errors in orthodontic measurements. Am J Orthod 1983;83:382-390.

76. Lin LI. A concordance correlation coefficient to evaluate reproducibility. Biometrics 1989;45:255-268.

APPENDICES

Appendix A: Data Collection Sheet

Name		Study ID #	CF Chart #	DOB	Sex	Race
Last	First					

OMENS	Mand Type	Fam Hx	Functional Appl

Xrays Dates					
Pan	Ceph	PA Ceph	R Oblique	L Oblique	3D CT

NOTES:

____

____

____

____

____

____